


12-2017

EVALUATING THE THERAPEUTIC EFFICACY OF RESTORING WILD-TYPE P53 ACTIVITY IN P53-MUTANT TUMORS

Connie A. Larsson

Follow this and additional works at: http://digitalcommons.library.tmc.edu/utgsbs_dissertations

 Part of the [Genetics and Genomics Commons](#), [Oncology Commons](#), and the [Therapeutics Commons](#)

Recommended Citation

Larsson, Connie A., "EVALUATING THE THERAPEUTIC EFFICACY OF RESTORING WILD-TYPE P53 ACTIVITY IN P53-MUTANT TUMORS" (2017). *UT GSBS Dissertations and Theses (Open Access)*. 815.
http://digitalcommons.library.tmc.edu/utgsbs_dissertations/815

This Dissertation (PhD) is brought to you for free and open access by the Graduate School of Biomedical Sciences at DigitalCommons@TMC. It has been accepted for inclusion in UT GSBS Dissertations and Theses (Open Access) by an authorized administrator of DigitalCommons@TMC. For more information, please contact laurel.sanders@library.tmc.edu.

**EVALUATING THE THERAPEUTIC EFFICACY OF RESTORING WILD-
TYPE P53 ACTIVITY IN P53-MUTANT TUMORS**

By

Connie Ann Larsson, B.S.

APPROVED:

Advisory Professor, Guillermina Lozano, Ph.D.

Richard R. Behringer, Ph.D.

Russell R. Broaddus, M.D.,Ph.D

Florian Muller, Ph.D.

Nicholas Navin, Ph.D.

APPROVED:

Dean, The University of Texas
MD Anderson Cancer Center UHealth Graduate School of Biomedical Sciences

**EVALUATING THE THERAPEUTIC EFFICACY OF RESTORING WILD-
TYPE P53 ACTIVITY IN P53-MUTANT TUMORS**

A

DISSERTATION

Presented to the Faculty of
The University of Texas
MD Anderson Cancer Center UTHealth
Graduate School of Biomedical Sciences
in Partial Fulfillment

of the Requirements

for the Degree of

DOCTOR OF PHILOSOPHY

by

Connie Ann Larsson, B.S.
Houston, Texas

December 2017

DEDICATION

To my loving mother, who loved boasting about me and was so proud of my pursuit to obtain a doctorate degree. I'm sorry I couldn't finish before you departed this world, but I know you are still here in spirit and watching over me from Heaven. Rest in peace mom. I love and miss you more than you could ever know.

ACKNOWLEDGEMENTS

The pursuit of science to better understand the unknown is an endeavor most successfully achieved through highly collaborative efforts, funding support, and the sharing of knowledge. Being said, I would first like to express my sincerest gratitude to my advisory mentor, Dr. Gigi Lozano, who started supporting me before I even began my training at the GSBS. Gigi, I will never forget the fact that you took a risk with me since I was conditionally accepted into the graduate school. Had it not been for your generosity and willingness to fund all three of my rotations I would not be defending this thesis project here at the GSBS. I cannot thank you enough for all your support and guidance throughout my graduate training. I would also like to extend my gratitude to the NIH, American Legion Auxiliary and Tzu Chi Foundation for their financial support in funding my research.

One of the best perks about working in the Lozano lab is that I met so many amazing people that are now some of my dearest friends. Therefore, I would like to give a special shout out to Dr. James G. Jackson, otherwise best known as “Coach”, for not only having ‘600 career wins’, but also for teaching me the four keys to success: Focus, Concentration, Preparation, and Execution. Over the years in lab I learned so much from you regarding all aspects of research and science and I watched how you struggled then conquer some very challenging hurdles. Your words of wisdom, sarcastic comments and derisive, yet constructive, criticisms has not only made my skin thicker, but pushed me to persevere through some of the most difficult times. Amanda and Sydney, I have become so close to the two of you over the years and I want to thank you both for always being there for me when I was going through the most difficult and trying times in my life. I can’t thank you enough for all that you’ve done, whether it be a shoulder to cry on when I was having a bad day, or taking care of a euthanasia notice on a moment’s notice. Amanda, you have also been so helpful throughout the years with my projects and I can’t thank you enough for

being so patient when it came to my incessant questions about certain experimental techniques. Sydney, you were naïve enough to volunteer with helping me when you first joined the lab, but you were instrumental when it came down to the last leg of my project. The combination therapy experiments would have been so daunting and difficult without all your help and assistance. Thank you both, for all that you've done. I know we will maintain a close friendship for many years to come.

I would also like to acknowledge my committee members, Dr. Richard Behringer, Dr. Russell Broadus, Dr. Florian Muller, and Dr. Nicholas Navin, for all your guidance and for always challenging me with insightful questions. Additionally, I want to give special thanks to Elisabeth Lindheim and all the administrators of the GSBS for their ceaseless efforts in assisting me every step of the way throughout my time in graduate school.

Of course, I could not have gotten to where I am right now without all the love and endless support from my family and friends. Poppa, you were the one that ignited my interest in science and you constantly pushed me to work harder so that I can amount to someone with purpose. Thank you for believing and teaching me that I am capable of achieving great things. Michele, my beautiful older sister, you nourished me from the moment I was born and provided me with everything and anything you could within your means. Thank you for being so selfless and for everything you have done throughout my entire life. Cat, my younger sister, you have given me the most beautiful and wonderful nieces that always puts a smile on my face and a warmth in my heart. There is no substitution or replacement for the sheer joy and happiness that you and your family have provided over the years. Maritza, my best friend, we did anything and everything together, from cocktail waitressing at Magic Island to teaching science at North Shore Senior High School. Your genuine interests in my research projects and the enthusiasm you exude while telling your friends about my research were always so uplifting. Thank you for maintaining a level of excitement and motivation with my research.

I could go on forever acknowledging everyone that played a substantial role throughout my time in graduate school and I apologize to those that I could not mention specifically.

EVALUATING THE THERAPEUTIC EFFICACY OF RESTORING WILD-TYPE P53 ACTIVITY IN P53-MUTANT TUMORS

Connie A. Larsson, B.S.

Advisor: Guillermina Lozano, Ph.D.

The p53 transcription factor is the most frequently altered in human cancers usually via missense mutations that undermine its transcriptional activity. Clinically, *TP53* mutations have been shown to be remarkably predictive of refractoriness to treatment, resulting in poor outcome. Consequently, the development of p53 pathway activating agents is rapidly evolving and gaining more attention in cancer therapeutics research, with several small molecule compounds currently in preclinical and clinical trials. However, it remains largely unknown what types or proportions of *p53*-mutant tumors will respond to p53 restoration-based therapies.

Using a mouse model of Li Fraumeni syndrome, we genetically restored wild-type *p53* in mice carrying a germline *p53*^{R172H} (corresponding to the *TP53*^{R175H} hotspot in humans) missense mutation and observed heterogeneous responses. We found that approximately 50% of tumors responded by regressing in volume whereas 50% of tumors failed to regress after p53 reinstatement. To gain insight into the molecular events underlying therapeutic response to p53 restoration, we sequenced the transcriptome of twelve p53-mutant thymic lymphomas that were sensitive (n=8) or resistant (n=4) to p53 restoration. Differential gene expression analyses suggested a critical role for the TNF pathway and RAR γ , an effector in the TNF pathway, in promoting response as they were up-regulated in tumors sensitive to p53 restoration. Furthermore, we demonstrate that pharmacological activation of RAR γ with the synthetic retinoid, CD437, sensitizes resistant tumors to p53 restoration while additively improving outcome and survival in tumors inherently sensitive to p53 restoration.

TABLE OF CONTENTS

APPROVAL PAGE	i
TITLE PAGE	ii
DEDICATION	iii
ACKNOWLEDGEMENTS	iv
ABSTRACT	vii
TABLE OF CONTENTS	viii
LIST OF ILLUSTRATIONS	x
LIST OF TABLES	xii
CHAPTER 1: INTRODUCTION	1
1.1 The discovery of p53, a bona-fide tumor suppressor.....	2
1.2 p53, guardian of the genome.....	2
1.3 Regulation of p53 activity.....	6
1.4 p53 mutations in cancer	8
1.5 Clinical significance of p53 mutations	8
1.6 Mouse models of p53 mutations.....	10
1.7 p53 and therapeutic approaches	11
1.8 Rationale and Aims.....	14
CHAPTER 2: EVALUATING THERAPEUTIC RESPONSE TO WILD-TYPE P53 RESTORATION IN TUMORS WITH A P53^{R172/H} MISSENSE MUTATION	15
2.1 Introduction.....	16
2.2 Methods	17
2.3 Results.....	20
2.4 Conclusion.....	33

CHAPTER 3: GLOBAL GENE EXPRESSION PROFILING TO IDENTIFY MOLECULAR SIGNATURES OF RESPONSE	34
3.1 Introduction	35
3.2 Methods	36
3.3 Results	37
3.4 Conclusion	46
CHAPTER 4: EXAMINING THE EFFECTS OF A COMBINATION THERAPY REGIMEN WITH A SYNTHETIC RETINOID	47
4.1 Introduction	48
4.2 Methods	52
4.3 Results	55
4.4 Conclusion	79
CHAPTER 5: DISCUSSION	80
Summary	81
Clinical implications	83
Advantages of our model	85
Significance	86
Future directions	87
APPENDIX	88
BIBLIOGRAPHY	89
VITA	107

LIST OF ILLUSTRATIONS

Figure 1	Schematic of the p53 protein along with hotspot mutations.....	5
Figure 2	Top 10 most recurrently mutated genes in human tumors.....	9
Figure 3	Genetic restoration of p53 <i>in vivo</i>	22
Figure 4	Survival and tumor spectrum of untreated $p53^{neo/R172H}$ mice.....	23
Figure 5	Tumor spectrum diversity of $p53^{neo/R172H}$ mice.....	24
Figure 6	Restoring p53 in p53-mutant tumors significantly prolongs survival.....	27
Figure 7	Tumor regression not required for prolonged survival.....	28
Figure 8	Variations in response to p53 restoration MRIs.....	30
Figure 9	Summary of response waterfall plot.....	31
Figure 10	Heatmap of the significantly differentially expressed genes.....	38
Figure 11	Ingenuity pathway upstream regulator analysis.....	40
Figure 12	GSEA of inflammatory response.....	41
Figure 13	Identifying druggable targets in TNF pathway.....	44
Figure 14	DESeq gene expression analyses of RARs.....	45
Figure 15	Overlapping roles of p53 and RAR in activating cell death.....	49
Figure 16	Syngeneic tumor transplant model & results of baseline experiment.....	50
Figure 17	Treatment regimen for combination therapy drug studies.....	56
Figure 18	Tumor growth curves of single agent-treated p53-resistant tumors	58
Figure 19	Survival of single-agent treated mice with p53-resistant tumors	59
Figure 20	Combotherapy tumor growth curve & survival in p53-resistant mice.....	60
Figure 21	Survival summary & tumor volume at day 12 in p53-resistant mice.....	61
Figure 22	Tumor growth curve & survival of tam-treated p53-sensitive tumors	63
Figure 23	Tumor growth curve & survival of CD437-treated p53-sensitive tumors.....	64
Figure 24	Tumor growth curve & survival of combo-treated p53-sensitive tumors.....	65

Figure 25	Survival summary & tumor volume at day 12 in sensitive line.....	66
Figure 26	Histological differences between sensitive & resistant lymphomas.....	68
Figure 27	Activation of p53 and RAR target genes in resistant syngeneic tumors.....	70
Figure 28	Evaluation of apoptosis in treated p53-resistant syngeneic tumors.....	72
Figure 29	H&E of treated syngeneic resistant T-cell lymphomas.....	74
Figure 30	H&E of treated syngeneic sensitive T-cell lymphomas.....	75
Figure 31	Immunophenotypic analyses of p53-resistant lymphoma.....	77
Figure 32	Immunophenotypic analyses of p53-sensitive lymphoma.....	78

LIST OF TABLES

Table 1	DNA primers for genotyping & recombination.....	19
Table 2	Detailed log of treated autochthonous tumors from the MRI cohort	32
Table 3	Top 10 most differentially expressed TNF downstream molecules	43

CHAPTER 1

INTRODUCTION

1.1 The discovery of p53, a bona fide tumor suppressor

In 1979 several groups identified a cellular protein of approximately 53 kilodaltons (kD) that co-precipitated with SV40 large T-antigen in rodent cell lines transformed by simian virus SV40 (1, 2). Subsequently, the same 53 kD protein was found in stable complexes with the E1B-55kd oncoprotein in adenovirus transformed cells (3). These findings led to the hypothesis that the 53 kD protein, appropriately named p53, was a cellular oncoprotein. This hypothesis was further supported by observations that transformed cell lines had exponentially higher levels of p53 protein compared to non-transformed cells and must therefore, be associated with cellular transformation (4).

However, confounding data demonstrating viral-induced murine erythroleukemias had inactivated p53 due to rearrangement at the *p53* locus emerged (5-7), suggesting that inactivation of p53 may provide a selective advantage for cellular transformation. This notion was further substantiated by human data where a large proportion of osteosarcomas had rearrangement in the *p53* gene that correlated with absence of p53 expression (8). The confusion surrounding the contradictory data implicating p53 as either a protooncogene or tumor suppressor was attributed to the existence of independently derived p53 cDNAs possessing mutations that impaired p53 function and promoted accumulation of mutant p53 proteins (9). A decade after its initial discovery, the paradoxical role of p53 was finally resolved and p53 was established as a bona fide tumor suppressor (8, 9).

1.2 p53, guardian of the genome

Encoded by the *TP53* gene, the p53 tumor suppressor protein is a transcription factor with the capacity to activate and/or repress the expression of hundreds of genes involved in a wide range of cellular processes that include, but are not limited to development, fertility, metabolism, DNA repair, survival, and stem cell homeostasis (10, 11). More importantly, p53 plays a pivotal role in maintaining genomic stability by initiating cellular programs that eliminate

or prevent the proliferation of damaged or transformed cells (12-14). Genotoxic conditions that cause damage to the DNA activates p53. There are a number of external stimuli that can activate p53 such as cellular exposure to ultra-violet (UV) radiation, ionizing radiation (IR), mutagens, and carcinogens, including chemotherapeutic agents (15, 16). Endogenous stress signals that promote the activation of p53 including hypoxia, oncogene activation, reactive oxygen species (ROS), and telomere attrition, to name a few (17).

Upon sensing these stress signals, p53 will transactivate target genes to initiate apoptosis, cell cycle arrest and senescence. These responses have been clearly shown, in both human and murine systems, to be crucial in suppressing cellular transformation, tumor progression, and mediating response to multiple cancer therapies (18-20). Pro-apoptotic genes induced by p53 include *p53- upregulated-modulator-of-apoptosis (Puma/Bbc3)* (21), *BCL2-associated-X- protein (Bax)* (22), *phorbol-12-myristate- 13-acetate-induced-protein-1 (PMAIP1/Noxa)* (23), *TP53 apoptosis effector (Perp)* (24), and *p53-regulated Apoptosis-Inducing Protein 1 (p53AIP1)* (25); whereas *cyclin-dependent-kinase-inhibitor-1A (Cdkn1a/p21)* (26), *cyclin G1 (Ccng1)* (27), and *growth arrest and DNA-damage-inducible 45 alpha (Gadd45a)* (28) are some of the p53 targets important for cell cycle arrest. However, this is not a complete list of all the p53 target genes and while apoptosis and cell cycle arrest are important tumor suppressive programs. Emerging data demonstrates that p53 can exert tumor suppressive activity through other mechanisms such as metabolic reprogramming (29), autophagy (10), and ferroptosis (30, 31). It is also worthy to note that although p53 has been implicated in the activation of over 400 genes (10), only 129 of them, thus far, have been experimentally validated as direct p53 transcriptional targets genes (11).

The p53 protein contains two acidic N-terminal transactivation domains (TAD), a proline-rich (Pr) domain, a sequence-specific DNA binding domain (DBD) that is centrally located, followed by a nuclear export signal (NLS), the tetramerization (TET) domain and a

basic C-terminal regulatory domain, which is important for regulating the stability and function of p53 activity (Figure 1) (32). In order for p53 to carry out its transcriptional activity, it must first form a homotetramer, and the TET domain (also referred to as the oligomerization domain) is critical for not only the oligomerization of p53 proteins, but for proper binding to DNA. The DBD of p53 is also crucial for DNA binding at p53 response elements (RE) of its target genes. Not surprisingly, the DBD is the target of approximately 90% of p53 mutations found in human cancers. Among them, six residues are considered 'hot spots' as they tend to be targeted for mutations more frequently than other residues (Figure 1) (33, 34). Moreover, many of these mutants have dominant-negative effects on WT p53 protein whereby the mutant protein can form a stable a complex with WT p53, thus abolishing its transcriptional activity (35). More details about the different types of p53 mutations and its effect on protein function are described in section 1.4.

Since p53 is capable of initiating cellular death programs, balancing p53 activity is critical and there is a fine threshold between having excessive or insufficient activity. On one hand, attenuating p53 allows for the survival and proliferation of mutated or transformed cells, thus leading to spontaneous tumorigenesis (36). Yet, unrestricted p53 activity can be deleterious and depending on the level of activation, can lead to organismal death (37). Therefore, the transcriptional activity of p53 is tightly regulated and described in the following section.

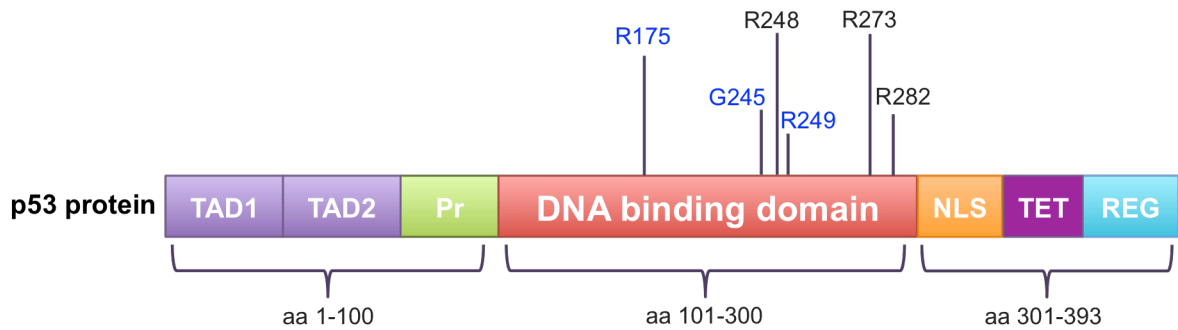


Figure 1: Schematic of the p53 protein along with the top six “hotspot” mutations

The p53 protein contains two N-terminal transactivation domains (TAD) followed by a proline-rich domain (Pr). The DNA binding domain (DBD) is critical for the transcriptional function of p53. Notably, all hotspot mutations fall within the DNA-binding domain of the p53 protein. Residues denoted with blue text are conformational mutants while residues denoted in black text are DNA contact mutants. The C-terminus of p53 contains the nuclear localization signal (NLS), the tetramerization (TET) domain, and the (REG) domain (residues 363-393), which is important for the negative regulation of p53.

1.3 Regulation of p53 activity

Considering the anti-proliferative and cell lethal effects of p53, it is not surprising that p53 protein has a very short half-life of less than 20 minutes in unstressed cells (4, 38). The protein turnover of p53 is a rather complex process that is governed by a milieu of post-translational modifications at different target residues impacting the stability and function of p53. These modifications include ubiquitination, phosphorylation, acetylation, sumoylation, neddylation, methylation, and glycosylation (4, 38, 39). The outcome of these modifications can vary and is dependent on the type and residue modified. This complexity is compounded by the fact that many of these post-translation modifications can converge on the same target residue or juxtapose to another modified residue, which in turn can either enhance or antagonize the effects of other modifications (39, 40). Protein ubiquitination is a cascading sequential process that requires three different classes of enzymes: E1-activating enzymes, E2-conjugating enzymes, and E3 ubiquitin ligases. Additionally, ubiquitination is a critical process for the regulation of p53 function and activity and the most critical regulator of p53 is an E3 ligase of the murine double minute (Mdm) family of proteins.

Mdm2 and its homologue, Mdm4 (AKA MdmX) are arguably the two most important negative regulators of p53 (41-45). Both Mdm2 and Mdm4 contain RING finger domains but they differ in that the RING domain of Mdm2 has E3 ligase activity whereas the RING domain of Mdm4 lacks enzymatic activity (45, 46). Additionally, Mdm2 interacts with Mdm4 via its RING domain. Inhibition of p53 by the Mdm proteins occurs via two mechanisms: 1) the RING domain of Mdm2 ubiquitinates p53 at key lysine residues that target p53 for proteasomal degradation (47) and 2) Mdm2/4 heterodimer directly binds to the N-terminal TAD domain of p53 to abolish its ability to transactivate its target genes (48-50). Keeping p53 levels under tight control is critical to maintain tissue and organismal homeostasis, as unrestricted p53 activity is cell lethal. This is highlighted by studies showing homozygous deletion of either *Mdm2* or *Mdm4* from the germline leads to early embryonic lethality in mice, and this lethal

phenotype can be rescued by concomitant deletion of *p53* (42, 43, 51). Additionally, abolishing the E3 ligase activity of Mdm2 or disrupting or the Mdm2-Mdm4 interaction via RING domain deletions or mutations results in embryonic lethality in mice that is p53-dependent (44, 48, 49), underscoring the critical role of the Mdm proteins in suppressing p53 activity.

In addition to the Mdm proteins, a number of other RING domain-containing proteins have been reported to negatively regulate p53 (40). These include, but are not limited to, Tripartite-motif protein 24 (*Trim24*) (52, 53), constitutively photomorphogenic 1 (*Cop1/Rfd2*) (54), and p53-induced protein with a RING-H2 domain (*Pirh2*) (55). Interestingly, mice with homozygous deletion of *Trim24* or *Pirh2* are viable and develop normally, suggesting that inhibition of p53 by *Trim24* or *Pirh2* is not as potent compared to the Mdm proteins (56, 57). In contrast, *Cop1* deficiency results in embryonic lethality at day E15.5 due to cardiovascular defects in mice (58, 59). However, this lethal phenotype was not attributed to unrestricted p53 since *Cop1*-deficient tissues did not exhibit elevated levels of p53 protein or upregulation of p53 target gene expression (58).

Activation of p53 upon DNA damage is critical to maintain genomic stability. However, it is just as critical that p53 becomes destabilized once the cell has recovered to ensure survival. Mdm2 regulates this transition by two different mechanisms. One involves Mdm2-mediated ubiquitination of key lysine residues that target p53 for proteasomal degradation (40). But the primary mechanism for down-regulating p53 activity is through an auto-regulatory negative feedback loop between p53 and Mdm2. Mdm2 is a transcriptional target of p53 and upon DNA damage p53 binds to the p53 response element (RE) in the P2 promoter of *Mdm2* to induce *Mdm2* expression, which in turn leads to the down-regulation of p53 activity and protein levels. Perturbing this feedback loop by mutating the RE in the *Mdm2* P2 promoter leads to hematopoietic defects and subsequent death in mice exposed to low dose ionizing radiation (60). Taken together, these findings further substantiate the notion that Mdm2 and Mdm4 are the most essential regulators of p53.

1.4 p53 mutations in cancer

Recent advancements in the era of genomics reveal that the p53 pathway is perturbed or attenuated in the majority of human cancers. Additionally, unbiased sequencing approaches carried out by the AACR Project Genie Consortium identified *TP53* as the most frequently mutated gene in all human cancers (Figure 2) (61), while a large subset of tumors without *p53* mutations inhibit p53 function by altering other central genes in the pathway by amplifying the *MDM2* or *MDM4* locus (62). Moreover, certain cancer types, such as ovarian serous cystadenocarcinoma, have near complete penetrance of p53 mutations (63). The p53 pathway can also be attenuated through inactivating mutations or deletions at the *CDNK2A* locus, which encodes two different tumor suppressor proteins, p16 and p14Arf (p19Arf in mouse) (33, 64). The critical role of the p53 pathway in preventing tumorigenesis is further highlighted by the observation that *TP53* mutations and *MDM2* or *MDM4* amplification are mutually exclusive events in human tumors (65). In addition, Li-Fraumeni Syndrome (LFS), an autosomal dominant hereditary disorder that is characterized by a predisposition to an early onset of cancer, is directly linked to germline *TP53* mutations (66).

1.5 Clinical significance of p53 mutations

Typically, *p53* mutation confers poor prognosis and chemoresistance (33), but our lab has shown in a mouse model of breast cancer that retention of wild-type p53 results in an inferior response to chemotherapy compared to tumors with complete loss of p53 function (67). This confounding observation challenged the dogma of p53 biology and was followed by the emergence of corroborating clinical data indicating the negative impact of p53 on treatment response. A clinical study on patients with muscle-invasive bladder carcinoma found resistance to frontline chemotherapy was associated with a wild-type p53 gene expression signature (68). Therefore, it must be taken into account how p53 mutation status will affect therapeutic response to anticancer therapies.

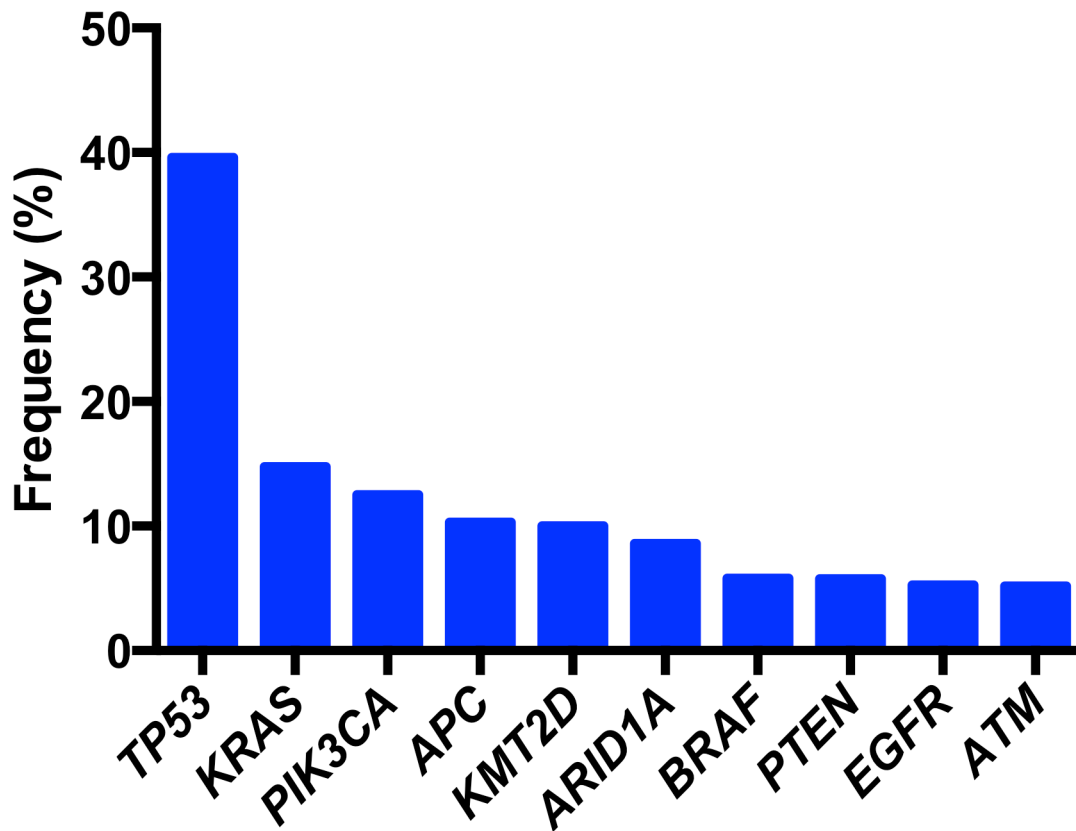


Figure 2. Top 10 most recurrently mutated genes in human tumors.

A graphical representation of data generated from the AACR Project Genie Consortium showing the top 10 most recurrently mutated genes in over 18,804 human tumor samples (61).

TP53 is the most frequently mutated gene, nearly 3-fold higher than the second most frequently mutated gene, *KRAS*.

With permission from: AACR Project GENIE Consortium. AACR Project GENIE: Powering Precision Medicine Through an International Consortium, *Cancer Discov.* 2017 Aug;7(8):818-831

C. Larsson would like to acknowledge the American Association for Cancer Research and its financial and material support in the development of the AACR Project GENIE registry, as well as members of the consortium for their commitment to data sharing. Interpretations are the responsibility of study authors

1.6 Mouse models of p53 mutations

Monumental advances have been made in understanding the p53 pathway, greatly owing to advancements in recombinant DNA technology. A number of genetically engineered mouse models (GEMMs) carrying different *p53* mutant alleles have been generated to characterize the role of p53 in development and tumorigenesis, and what these models have taught us is that not all p53 mutations are equal (69, 70). Mice inheriting one copy of a null allele at the *p53* locus ($p53^{+/-}$) are tumor prone and have decreased survival compared to wild-type ($p53^{+/+}$) mice. Interestingly, homozygous *p53* null ($p53^{-/-}$) mice are viable and phenotypically look normal, but exhibit a drastic decrease in tumor latency concomitant with a significant reduction in survival compared to $p53^{+/+}$ or $p53^{+/-}$ mice (36). Exposing $p53^{+/-}$ or $p53^{-/-}$ mice to ionizing radiation or carcinogens further reduces tumor latency and survival (71, 72). However, unlike other tumor suppressor such as *RB* or *PTEN* that most often undergo truncating or deletion-type mutations, the majority *p53* mutations are point mutations that changes a single residue and often results in the expression of a dysfunctional full-length protein (73, 74). Characterization of GEMMs carrying different *p53* mutations revealed a differential impact of between different point mutations, suggesting that there are differences in the activity and function between different p53 mutant proteins (69, 70). A great example is discussed below.

Back in 2004 our lab generated two different p53 knockin mice to better understand the impact of p53 missense mutations *in vivo* (14, 18). Both models carried substitutions at nucleotide 515 but carried different amino acid substitution that resulted from the nucleotide change. One model carried a G to A substitution resulting in an arginine to histidine substitution at amino acid 172 ($p53^{R172H}$) and corresponds to the *TP53*^{R175H} hotspot mutation in human tumors. The histidine substitution abolishes the ability of p53 to bind DNA, thus preventing its ability to transcriptionally activate target genes critical for tumor suppression.

Mice inheriting one copy of the mutant allele ($p53^{R17H/+}$) exhibited increased metastatic potential that was largely absent in $p53^{+/-}$ or $p53^{-/-}$ mice (18, 19). The other mouse model had a G to C substitution at nucleotide 515, this time resulting in an arginine to proline substitution at the same codon 172 ($p53^{R172P}$). At variance with the $p53^{R172H}$ mutant protein, this mutant protein has only a partial loss-of-function since it retains some capacity to bind DNA to induce cell cycle arrest and senescence, but the ability to activate apoptosis is abolished (14). The human tumor data and mouse genetic studies clearly demonstrate the importance of the p53 pathway in maintaining genomic stability and suppressing spontaneous tumorigenesis.

1.7 p53 and therapeutic approaches

The observations that a large portion of p53-mutant tumors are resistant or refractory to standard frontline treatments (i.e. chemo- and radiotherapy) demonstrates a dire need for alternative treatments, particularly ones that do not induce massive DNA damage that increases the likelihood of developing secondary cancers. Since a high proportion of tumors inactivate the p53 pathway, a rational strategy is to reverse this process. Evidence to support that restoring p53 function induces tumor suppressive effects has demonstrated in different cancer models. In 2007 three groups independently showed genetically restoring WT p53 in $p53$ -null tumors induced rapid tumor regression and in some cases, a complete response in mice (75-77). The limitation of these studies is that the efficacy of p53 restoration was evaluated in $p53$ -null tumors and the majority (~75%) of tumors inactivate p53 via point mutations that most often occur of the DBD of p53. These mutations abolish the transcriptional activity of p53 and mutant p53 also exerts dominant repressive effects on its wild-type (WT) counterpart (61). Moreover, *TP53* missense mutations are frequently accompanied by loss of the remaining WT allele, referred as loss-of-heterozygosity (LOH). It is important to note this distinction since mouse models carrying different $p53$ alleles reveal a clear difference between $p53$ deletions and missense mutations. Specifically, mutant p53 has acquired gain-of-function

(GOF) and dominant-negative (DN) activities that endow the mutant-p53 with oncogenic properties by exacerbating malignant transformation, metastatic potential and drug resistance (18, 19, 78). These findings raise the question of whether the presence of mutant p53 may affect response to WT p53 restoration therapy, especially considering that certain p53-mutants proteins (i.e. R175H, R248W & R273H) are capable of inducing drug resistance by transactivating non-canonical target genes such as the multidrug resistance (*MDR1*) gene (79). Based on these observations, it is likely that certain *p53* alterations can affect response to various anticancer agents, including p53 restoration-based therapies. Investigating the factors underlying response to p53 restoration is imperative since the development of p53 pathway activating agents is rapidly evolving in cancer therapeutics research. These include MDM2 inhibitors (broadly referred to as nutlins) (80, 81), agents that deplete mutant p53 proteins (82, 83), and mutant p53 reactivators (84-86), to name a few.

MDM2 inhibitors (MDM2i) have been extensively studied and these small molecules antagonize the negative regulation of p53 by binding the hydrophobic pocket of MDM2 with high affinity to prevent or disrupt its physical interaction with p53 (87, 88). However, MDM2i would in principle, be effective for tumors that retain WT p53 such as liposarcomas where the majority of these tumors are driven by *MDM2* amplification, and as discussed earlier, *TP53* mutation and *MDM2/4* amplification are generally mutually exclusive genetic events (88, 89). Our lab has examined the effects of genetically restoring p53 in *Mdm2*-amplified tumors using an *Mdm2* transgenic mouse model (90). Interestingly, mice with sarcomas responded more favorably to p53 restoration compared to mice with lymphomas, further supporting nutlins may have clinical applicability in *MDM2*-amplified sarcomas.

Another class of p53 activating agents that show promise is mutant p53 reactivators, which have been of particular interest due to the observation that many tumors exhibit high levels of stabilized mutant p53 proteins. Among the different types of mutant p53 reactivators, the most widely studied is a compound called APR-246 (2-(hydroxymethyl)-2-

(methoxymethyl)quinuclidin-3-one), which targets and refolds mutant p53 proteins to its wild-type conformation, thus restoring the ability to bind DNA (86). APR-246 has already been tested in a phase I/IIa clinical trial in patients with hormone-refractory prostate cancer or hematological malignancies and reported that restoring p53 activity was well tolerated with minimal adverse side effects, unlike the severe side effects associated with MDM2i (88, 91). However, this clinical trial only addressed the safety and dosage of APR-246 treatment, thus, an unknown is which p53-mutant tumors and cells, in particular, will respond favorably to p53 restoration therapy.

1.8 Rationale and Aims

The role of p53 has been clearly shown, in both human and murine systems, to be crucial in suppressing cellular transformation, tumor progression, and mediating response to radio- and chemotherapy. It is therefore not surprising that the *p53* gene is the most frequently mutated in all human tumors, prompting many researchers to investigate the utility of restoring the p53 pathway as an alternative treatment approach.

Since the development of mutant-p53 reactivators is rapidly evolving and gaining more attention in cancer therapeutic research, it is important to take into account that resistance is anticipated and remains a frequent impediment to conventional or targeted therapies. Moreover, it remains largely unknown if mutant-p53 reactivators will provide any survival benefits or have an impact on promoting tumor regression and merits further investigation. Prospective studies in conjunction with global gene expression profiling will provide a better understanding of who would benefit from p53-based therapies and a framework for identifying the pathways mediating. ***I hypothesize that mutant p53 gain-of-function drives heterogeneous responses to wild-type p53 reactivation that is dictated by the dynamic interplay of acquired somatic alterations.*** I intend to gain a deeper understanding of the cellular processes accounting for the variable therapeutic response through the following aims:

1. Evaluate the therapeutic efficacy of genetically restoring p53 in tumors with a *p53*^{R172H} missense mutation.
2. Characterize the gene expression profile of p53-mutant tumors subjected to p53 activation using high-throughput RNA-sequencing
3. Examine the effects of p53 restoration with novel drug combinations

I aim to characterize the factors accounting for responses to p53 restoration in addition to novel drug combination to potentiate the anti-tumor effects of p53 reactivation, which will be critical when it comes to translating p53-based therapies into clinical practice.

CHAPTER 2

EVALUATING THERAPEUTIC RESPONSE TO WILD-TYPE P53 RESTORATION IN TUMORS WITH A *P53*^{R172H} MISSENSE MUTATION

2.1 INTRODUCTION

Previously our lab developed a knock-in mouse carrying a hypomorphic *p53* allele (*p53^{neo}*) that can be conditionally reactivated to investigate the effects of restoring p53 activity *in vivo* (92). Using this allele, our lab showed that reinstatement of WT p53 in tumors with a *p53^{R172H}* missense mutation induces apoptosis or senescence, which are potent tumor suppressive mechanisms. However, reduction in tumor volume after p53 restoration was less remarkable compared to tumors that were *p53*-null (75-77, 92). What was not addressed in this study is whether restoring p53 in a p53 mutant background has any impact on prolonging survival and the degree of variability that can occur in response to p53 restoration.

Here I comprehensively examine the impact of restoring p53 in tumors with a *p53^{R172H}* missense mutation. Using the same *p53^{neo}* allele to restore p53, my objective is to characterize the pleiotropic anti-tumorigenic effects of reactivated p53 and to evaluate whether p53 restoration confers any survival benefits.

2.2 METHODS

Animal studies

Rosa26-CreER^{T2}, *Rosa26-tdTomato* and *Rosa26-GNZ* (herein referred to as *R26^{CreER}*, *R26^{tdT}* and *R26^{GNZ}*, respectively) knockin mice were purchased from Jackson Laboratory. *p53^{R172H/+}* mice were crossed to *R26^{CreER}* mice then intercrossed to generate double homozygous *p53^{R172H/R172H};R26^{CreER/CreER}* mice. *p53^{neo/neo}* mice were crossed to either *R26^{tdT}* or *R26^{GNZ}* mice then intercrossed to generate *p53^{neo/neo};R26^{TdT/TdT}* or *p53^{neo/neo};R26^{GNZ/GNZ}* double homozygous mutants. *p53^{neo/neo};R26^{tdT/tdT}* or *p53^{neo/neo};R26^{GNZ/GNZ}* were then crossed to *p53^{R172H/R172H};R26^{CreER/CreER}* or *p53^{R172H/R172H}* to generate *p53^{neo/R172H};R26^{CreER/tdT}*, *p53^{neo/R172H};R26^{CreER/GNZ}* or *p53^{neo/R172H};R26^{tdT/+}*, respectively. All mice were maintained in a >95% C57BL/6J genetic background.

Magnetic Resonance Imaging

All MRI studies were performed on a 7 Tesla (7T) BioSpec small animal imaging system (Bruker BioSpin Corp., Billerica, MA; software: ParaVision) equipped with a 60 mm imaging gradient and a 35 mm RF coil for signal excitation. Prior to imaging, mice were sedated with 5% isoflurane/oxygen (v/v) in an induction chamber and anesthesia was maintained with 1-2% (v/v) isoflurane delivered via nosecone throughout image acquisition. Mice were imaged in the supine position and a scout spin-echo images in the coronal orientation verified proper positioning. Images were acquired by T2-weighted rapid acquisition with relaxation enhancement (RARE) scans sequence (echo time/repetition time, 65 ms/5,000 ms; RARE factor 12; 4 averages) with in plane geometry parameters (50 mm x 30 mm field of view; 256 x 192 voxels image matrix; 1 mm thick slice geometry with 0.25 mm skip) in the sagittal orientation. Image analyses was performed using ImageJ (93). Tumor volumes were calculated by manual segmentation of region of interests drawn on T2-weighted sagittal stacks for each tumor-containing slice.

Tamoxifen treatments

Mice that develop tumors were randomly assigned to tamoxifen or corn-oil vehicle treatment group. Tamoxifen (Sigma-Aldrich) was prepared at a concentration of 30 mg/mL in corn oil and mice were treated at a dose of 3mg/40g body weight via intraperitoneal (IP) injections, while the control group received equal volumes of corn oil IP injections.

Statistics

Statistical analyses were performed using GraphPad Prism 6 software (GraphPad, San Diego, CA, USA) using ANOVA analyses with Bonferroni's correction for multiple testing unless otherwise specified. Mouse survival curves by Kaplan-Meier plots were analyzed by the log-rank (Mantel-Cox) tests. Statistical significance was defined as $p < 0.05$.

Study approval

All mouse experiments were approved by the MD Anderson Cancer Center Institutional Animal Care and Use Committee and conformed to the guidelines of the United States Animal Welfare Act and the National Institutes of Health.

Table 1. Primers used for genotyping and recombination PCR

Primer name	Primer sequence	Assay
pI5	ACCTGTAGCTCCAGCACTGG	Genotyping: p53 alleles
pI6	ACAAGCCGAGTAACGATCAGG	Genotyping: p53 alleles
neo-R	ACCCGCTTCCATTGCTCAGCGG	Genotyping: p53 alleles
tdTom WT FW	AAGGGAGCTGCAGTGGAGTA	Genotyping: Rosa26-tdTomato
tdTom WT Rev	CCGAAAATCTGTGGGAAGTC	Genotyping: Rosa26-tdTomato
tdTom Mut Rev	GGCATTAAAGCAGCGTATCC	Genotyping: Rosa26-tdTomato
tdTom Mut FW	CTGTTCCCTGTACGGCATGG	Genotyping: Rosa26-tdTomato
CreERT2-WT Fw	AAAGTCGCTCTGAGTTGTTAT	Genotyping: Rosa26-CreER ^{T2}
CreERT2-WT Rev	GGAGCGGGAGAAAATGGATATG	Genotyping: Rosa26-CreER ^{T2}
CreERT2-Mut Rev	CCTGATCCTGGCAATTTCCG	Genotyping: Rosa26-CreER ^{T2}
VpCI-FW	GGCCATCTCTGTGAGTTCGA	Recombination PCR
VpCI-2	CTCATGGTGGGGCAGCG	Recombination PCR
VpCI-NeoR	CAGACTGCCTTGGGAAAAGC	Recombination PCR
5end-R-Biotin	[Bt _n] GGGCCCTCGATATCAAGCTT	Recombination pyrosequencing
NeoPS-R1-Biotin	[Bt _n] CAGGGTTTCTCTATGTAGCC	Recombination pyrosequencing
NeoPS-F2	GCCTGGTCTAATTCCGATC	Recombination pyrosequencing
Neo-PSS	TATACGAAGTTATTAGGTC	Recombination pyrosequencing

2.3 RESULTS

Generation and characterization of $p53^{neo/R172H}$ mice with different genetic backgrounds

To comprehensively evaluate how tumors with a p53 missense mutation would respond to wild-type p53 restoration, I generated cohorts of mice with genotypes $p53^{neo/R172H};R26^{CreER/GNZ}$, $p53^{neo/R172H};R26^{CreER/tdT}$ and $p53^{neo/R172H};R26^{tdT/+}$ for our studies. The $p53^{neo}$ allele contains a floxed PGK-neomycin cassette in the fourth intron of the endogenous p53 locus. In the absence of Cre recombinase, p53 is expressed at approximately 7% compared to a wild-type p53 allele, making $p53^{neo}$ a hypomorphic allele (92). This 7% expression confers a survival advantage as $p53^{neo/-}$ mice live longer than mice with homozygous p53 deletions or mutations but develop tumors with a shorter latency than $p53^{+/-}$ mice (92). Removal of the *PGK-neomycin* cassette through Cre-mediated recombination reconstitutes the locus, thus restoring p53 expression (Figure 3). The $p53^{R172H}$ missense mutant corresponds to the $p53^{R175H}$ hotspot mutation in human tumors and has GOF and dominant-negative properties (18, 19). The $R26^{CreER}$ allele constitutively expresses a Cre recombinase fused to a modified ligand-binding domain of the estrogen receptor under the *Rosa26* promoter and this Cre fusion protein is activated only in the presence of the active metabolite of tamoxifen (76). The $R26^{GNZ}$ reporter allele is supposed to express a GFP-LacZ fusion protein upon Cre-mediated recombination but in our hands was non-functional. Specifically, we observed no GFP or LacZ expression in tissues or cells after recombination was induced (data not shown), thereby prompting us to generate the $p53^{neo/R172H};R26^{CreER/tdT}$ cohort that faithfully expresses the red fluorescence protein (RFP) tdTomato upon Cre-mediated recombination. No differences in tumor spectrum were observed and there was no significant difference in survival between the three cohorts indicating that homozygous or heterozygous knock-in at the *Rosa26* locus has minimal to no effects on tumor development (Figure 4).

The mean median survival of untreated $p53^{neo/R172H}$ mice, regardless of the *Rosa26* allele used, is 157.5 days, which is nearly identical to the previously published survival curve of $p53^{neo/R172H};CreER^{TM}$ mice (median survival 160 days) that carry a transgenic *CreERTM* allele and have an intact *Rosa26* locus (92). These mice develop a wide spectrum of tumors that can be detected by conventional T2-weighted magnetic resonance imaging (MRI) (Figure 5), but primarily succumb to lymphomas (~65%) and sarcomas (~30%) (Figure 4B).

It is worthwhile to note that the $p53^{neo/R172H};R26^{CreER/GNZ}$ cohort was studied independently and prior to the $p53^{neo/R172H};R26^{CreER/tdT}$ and $p53^{neo/R172H};R26^{tdT/+}$ cohorts. However, $p53^{neo/R172H};R26^{CreER/tdT}$ and $p53^{neo/R172H};R26^{tdT/+}$ mice were studied in conjunction with each other at the same time.

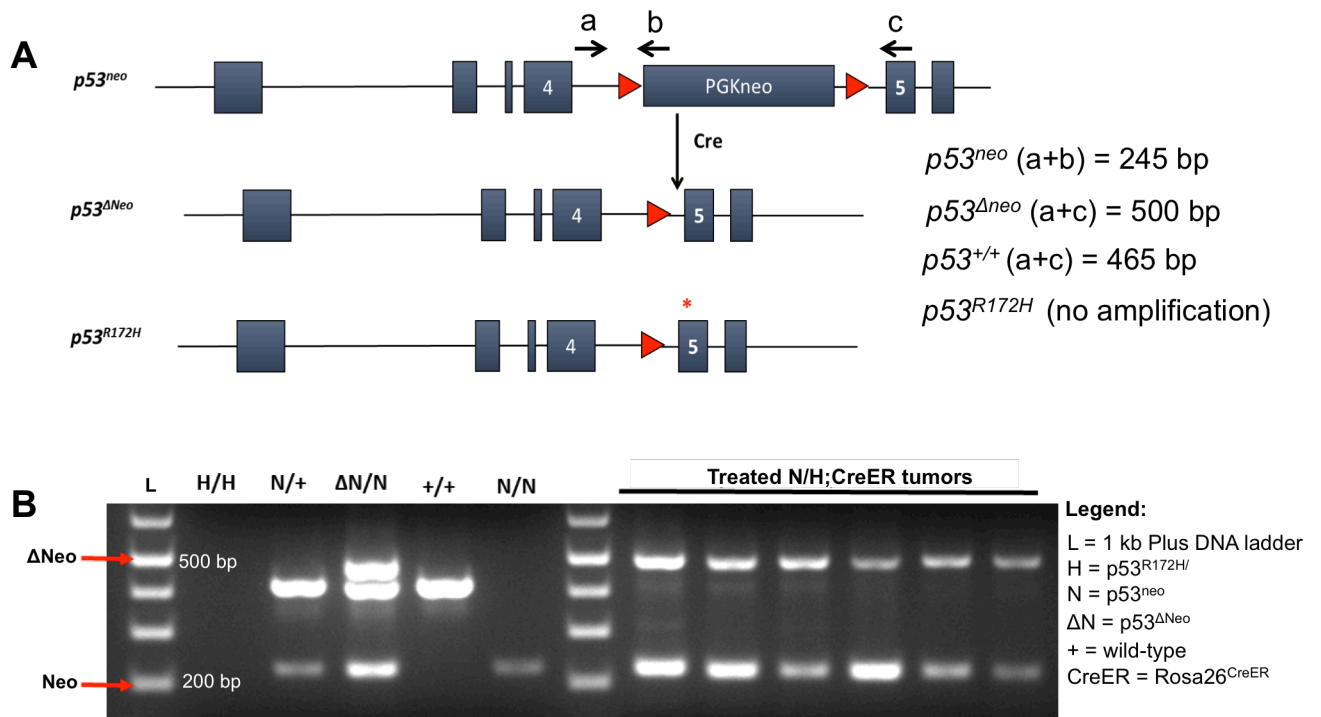


Figure 3. Genetic restoration of wild-type p53 *in vivo*

(A) Schema of the *p53^{neo}* alleles used in this study. The *p53^{neo}* allele contains a floxed *PGKneomycin*-resistance cassette inserted into the fourth intron of the endogenous p53 locus (top). Recombination of the *p53^{neo}* (denoted as *p53^{Δneo}*) allele occurs upon activation of Cre recombinase (middle). The *p53^{R172H}* mutant allele (bottom) corresponds to the *TP53^{R175H}* hotspot mutation in human cancers. To examine recombination, primers (represented as a, b, and c with arrows underneath) were designed to specifically amplify the *p53^{neo}* and *p53^{Δneo}* alleles and not the *p53^{R172H}* allele. **(B)** PCR of tumor DNA showing recombination of the *p53^{neo}* allele after tamoxifen treatment. Primer sequences used in this figure can be found in Table 1 and the names of the primers indicated above are as follows:

- primer a (forward) = VpCI-FW;
- primer b (reverse) = VpCI-NeoR;
- primer c (reverse) = VpCI-2

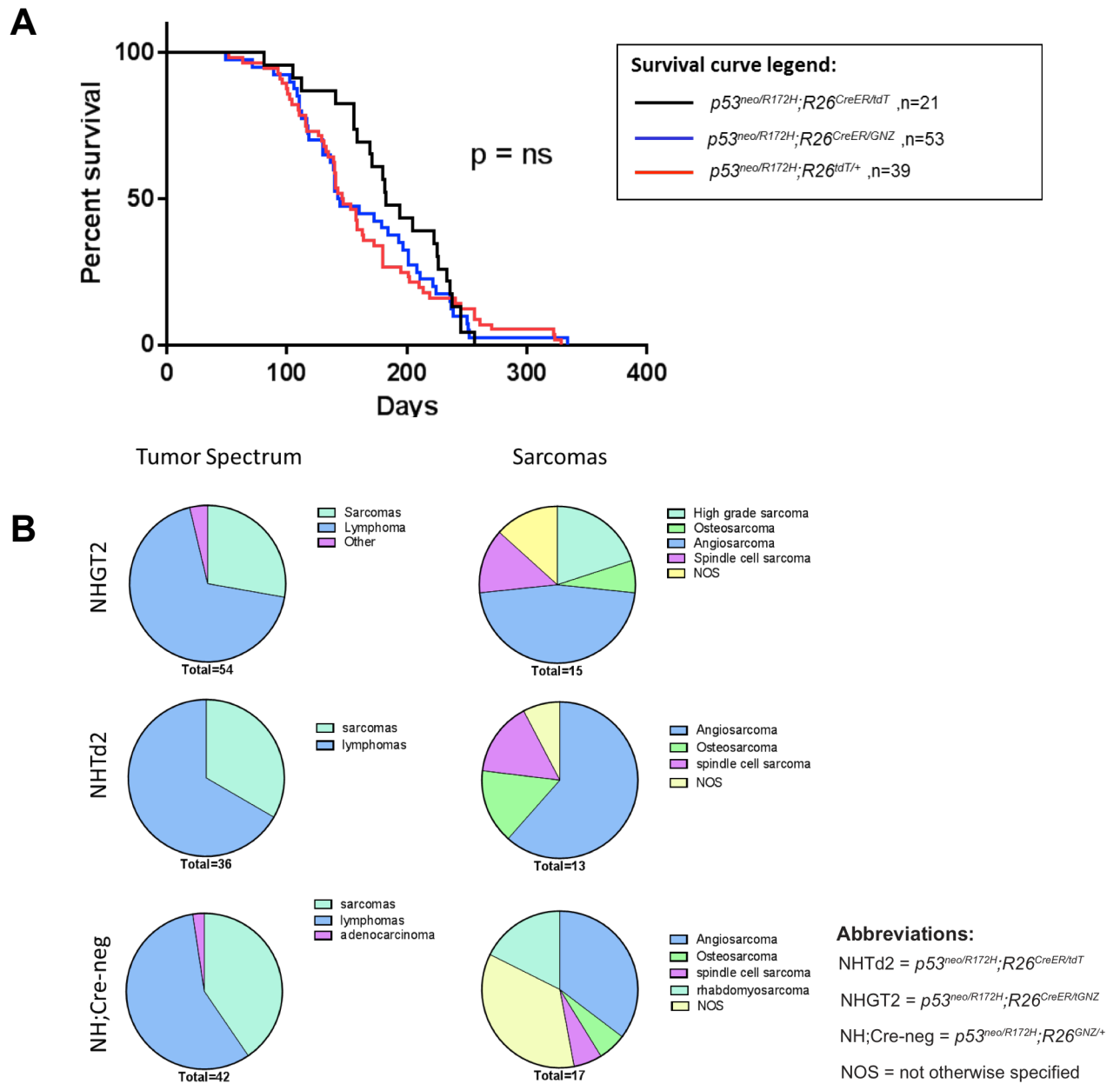


Figure 4. Survival and tumor spectrum of untreated $p53^{neo/R172H}$ mice. No differences in survival (**A**) or tumor spectrum (**B**) observed between $p53^{neo/R172H}$ mice with heterozygous or homozygous knock-in alleles ($Rosa26^{CreERT2}$, $Rosa26^{tdTomato}$ and $Rosa26^{GNZ}$) at the $Rosa26$ locus. Survival was analyzed by Kaplan-Meier test and significance is defined as $p < 0.05$.

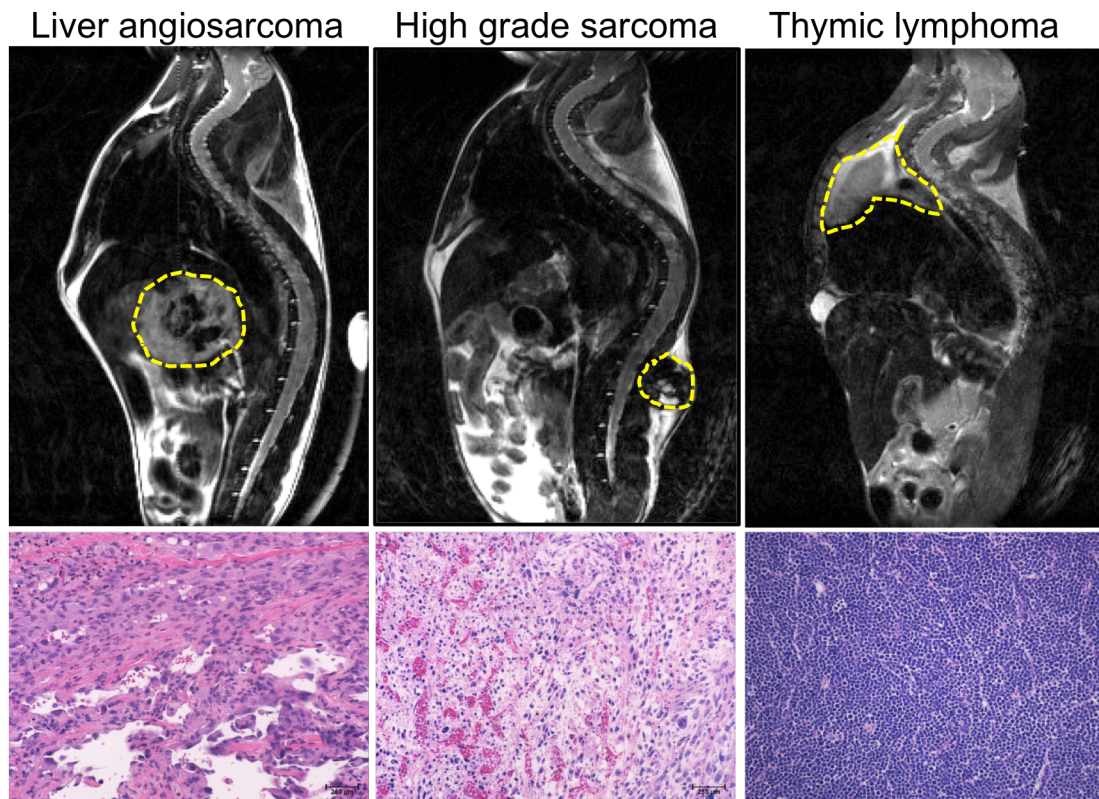


Figure 5. Tumor spectrum diversity in $p53^{neo/R172H};R26^{CreER/tdT}$ mice.

Mice were monitored for tumor formation by T2-weighted magnetic resonance imaging (MRI) (top panels) and tumors were diagnosed by routine histological analyses by hematoxylin & eosin (H&E) staining (bottom panels). MRIs are sagittal sections of a liver angiosarcoma (left panel), while the middle panels represent a mouse with a high-grade sarcoma. The most common tumor type observed were lymphomas of the thymus (right panels).

Restoring wild-type p53 activity in tumor-bearing mice carrying a $p53^{R172H}$ missense mutation significantly prolongs survival

To determine if p53 restoration could prolong overall survival, cohorts of $p53^{neo/R172H};R26^{CreER/tdT}$ or $p53^{neo/R172H};R26^{tdT/+}$ mice were monitored by MRI for tumor formation (Figure 5). To induce recombination of the $p53^{neo}$ allele, mice were administered tamoxifen, resulting in the genomic reconstitution of the $p53$ locus (Figure 3). Tumor-bearing mice were randomized to either tamoxifen or corn-oil vehicle treatment group where they received up to four weekly intraperitoneal (I.P.) injections and overall survival was determined by calculating the number of days survived post start of treatment. Tamoxifen treatments significantly prolonged survival ($p = 0.01$) in $p53^{neo/R172H};R26^{CreER/tdT}$ mice (median survival = 22 days) compared to vehicle-treated mice (median survival = 14 days) or tamoxifen-treated $p53^{neo/R172H};R26^{tdT/+}$ mice lacking CreER ($p = 0.03$) that have a median survival of 17 days (Figure 6A). Further, mice from both control cohorts all died within 27 days after treatment start while 40% of mice subjected to p53 restoration were still alive 40 days after starting treatment, with one mouse living beyond 100 days. The differences in survival were not dependent on initial tumor volume (Figure 6B) or tumor-type (Figure 6C) supporting the notion that restoring wild-type p53 in p53-mutant tumors has therapeutic efficacy.

Interestingly, the increase in survival was also not dependent on tumors regressing since we observed survival benefits in some tumor-bearing mice that failed to show a decrease in tumor volume after tamoxifen treatments. This was demonstrated through routine MRI to follow tumor growth changes in mice undergoing tamoxifen treatment to restore p53 (Figure 7). We followed tumor growth changes in a mouse that started tamoxifen treatments for an abdominal tumor measuring 265 mm^3 on day 0 (Figure 7A, top panels). We imaged the mouse again 29 days after starting weekly tamoxifen treatments and observed the abdominal tumor had grown up to 360 mm^3 , a 35% volume increase, and by day 47 the mouse had developed a sizeable thymic lymphoma that increased nearly 600% over the course of 11

days, whereas the abdominal tumor volume increased by only 43% (Figures 7A, top panels & 7B, left). In this case, it appears that the abdominal tumor stabilized upon p53 restoration but the mouse eventually succumbed to a thymic lymphoma that developed after completing its treatment regimen and had to be sacrificed on day 58. We observed the same delayed growth effect in thymic lymphomas as well (Figure 7A, bottom panels). Over the course of 24 days the thymus tumor grew from 73 to 271 mm³ (Figure 7B, right), but the mouse did not become moribund until day 48 (data not shown). These findings suggest that p53 restoration slows tumor growth even in cases where tumors appear to be more resistant to p53 restoration.

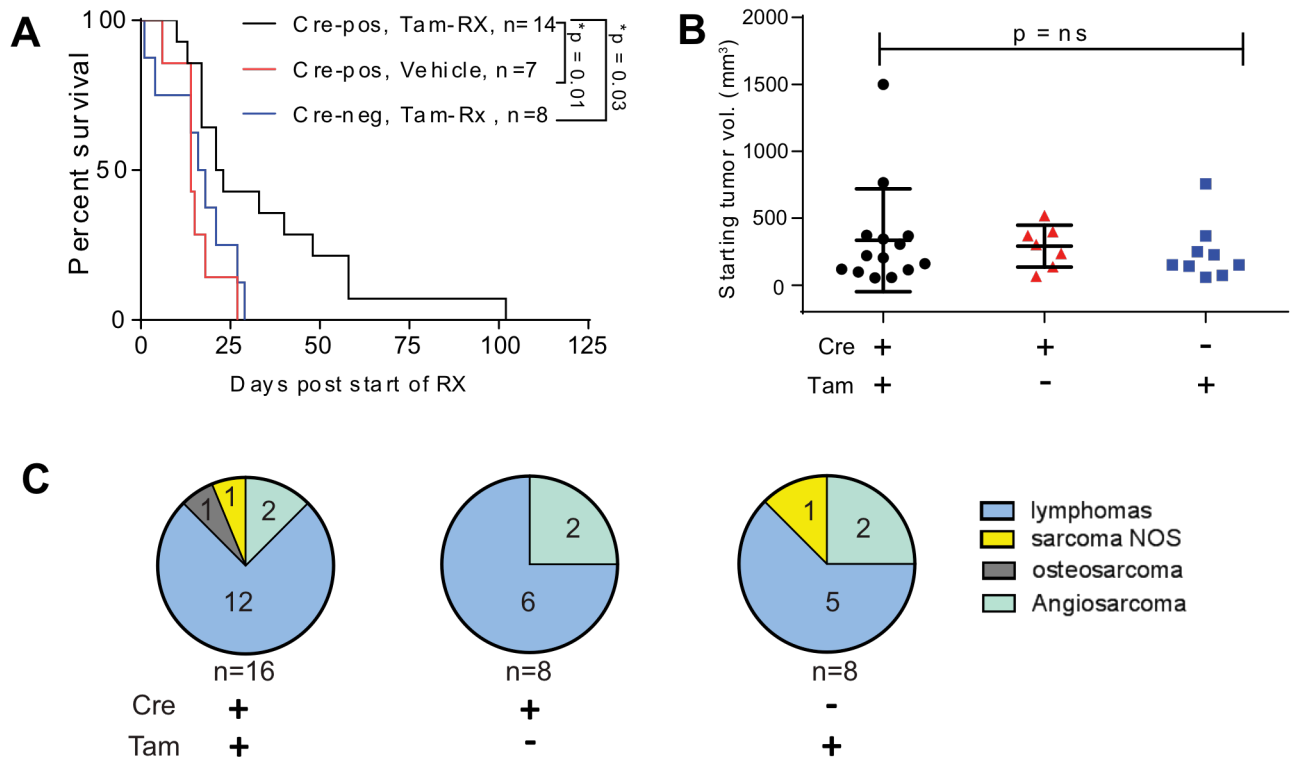


Figure 6. Restoring wild-type p53 in p53-mutant tumors significantly prolongs survival

(A) Kaplan-Meier analysis of $p53^{neo/R172H};R26^{CreER/tdT}$ mice treated with tamoxifen (black curve) or corn-oil vehicle (red curve) and $p53^{neo/R172H};R26^{tdT/+}$ mice (lacking Cre) treated with tamoxifen (blue curve). **B,C**, No significant differences in tumor volume at the start of treatment **(B)** and tumor spectrum **(C)** of mice from the survival cohort.

Abbreviations: Cre-pos = $p53^{neo/R172H};R26^{CreER/tdT}$ mice; Cre-neg = $p53^{neo/R172H};R26^{tdT/+}$ mice; Tam-RX = tamoxifen treated

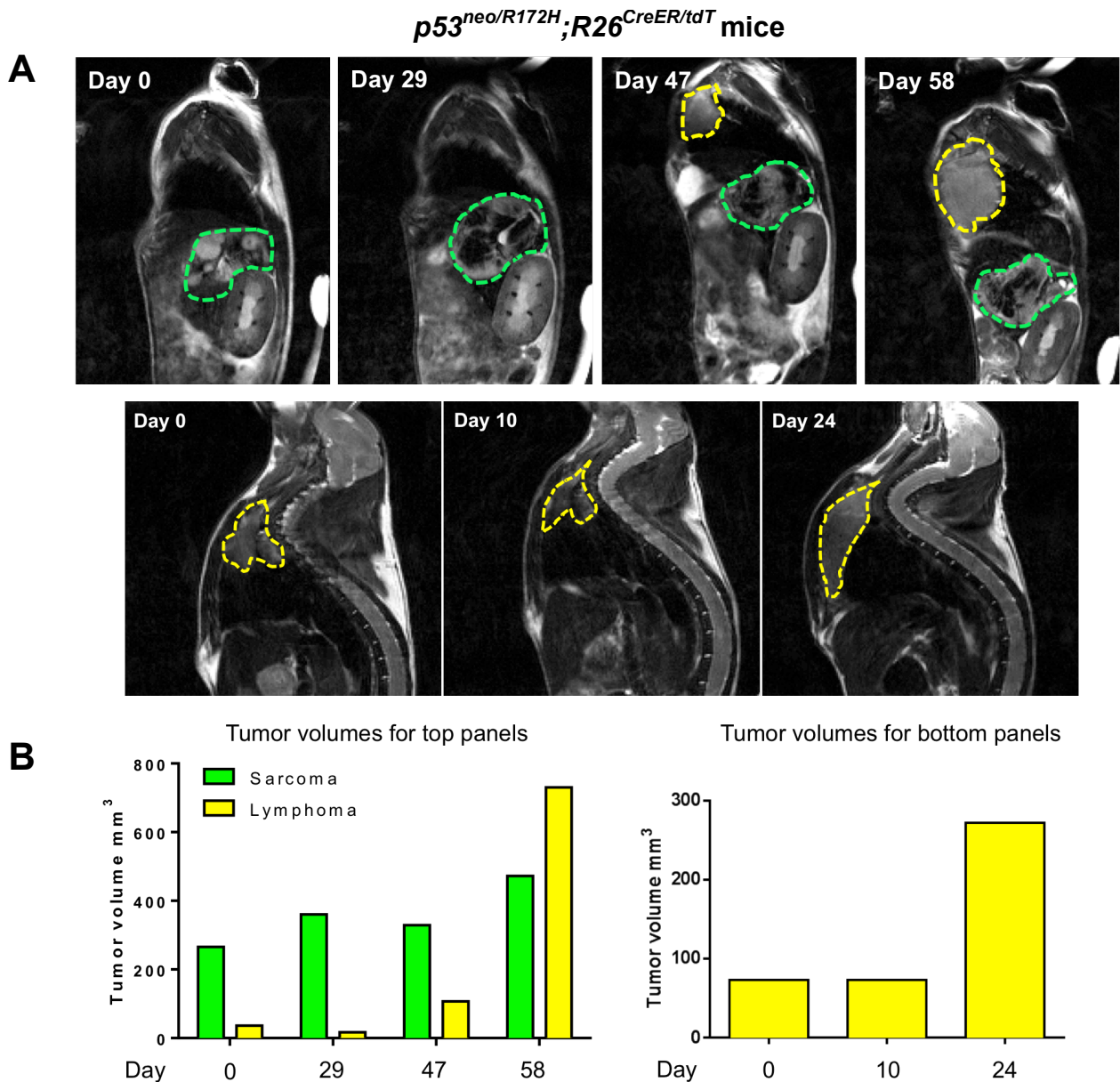


Figure 7. Survival benefits in the absence of tumor regression upon p53 reinstatement
 Representative MRIs (A) and corresponding tumor volume graphs (B) at indicated days in two different tamoxifen-treated *p53^{neo/R172H};R26^{CreER/tdT}* mice. Despite the tumors failing to regress upon tamoxifen-treatment, these mice exhibited an increase in survival that extended beyond 20 days. Although the thymus is not observable in the first two top panels it was present in other MRI sections and measurable, accounting for the lymphoma volumes at day 0 and 29 in the left graph of (B).

Heterogeneous response to p53 restoration in tumors with a p53^{R172H} missense mutation

We then aimed to determine what proportions of spontaneous p53-mutant tumors are sensitive or resistant to wild-type p53 restoration and evaluated the degree of variability that occurs in response to p53 restoration. We monitored a cohort of *p53^{neo/R172H};R26^{CreER/GNZ}* mice for tumor development by MRI. Upon detection of a tumor, mice started weekly tamoxifen injections and were closely monitored for changes in tumor volume (Figure 8). In total, 17 mice with 24 tumors were treated (Table 2) and 50% of treated tumors responded by showing a >20% decrease in total volume while ~37% of tumors were classified as non-responders because they had a >20% increase in total volume and ~12% of tumors stabilized with a change of <5% in volume (Figure 9 & Table 2). Factors that could contribute to the differences in response include loss of heterozygosity (LOH) and recombination efficiency of the *p53^{neo}* allele. To this end, a pyrosequencing assay was developed to quantify recombination efficiency and to assess LOH. Recombination of the *p53-neo* allele was approximately 25% in all treated tumors with the exception of tumor 1, which showed 0% recombination (Figure 9 & Table 2). This tumor also lost the *p53^{R172H}* allele. LOH analysis revealed partial LOH of the *p53^{neo}* allele in two tumors whereas the remaining tumors exhibited no LOH (Table 2).

These data suggest that the heterogeneous therapeutic impact of p53 restoration in p53-mutant tumors are not caused by alterations of the *p53* locus itself, but by other molecular events such as the acquisition of somatic mutations or alterations in gene expression that impact how transformed cells with a *p53^{R172H}* mutation responds to wild-type p53 activation.

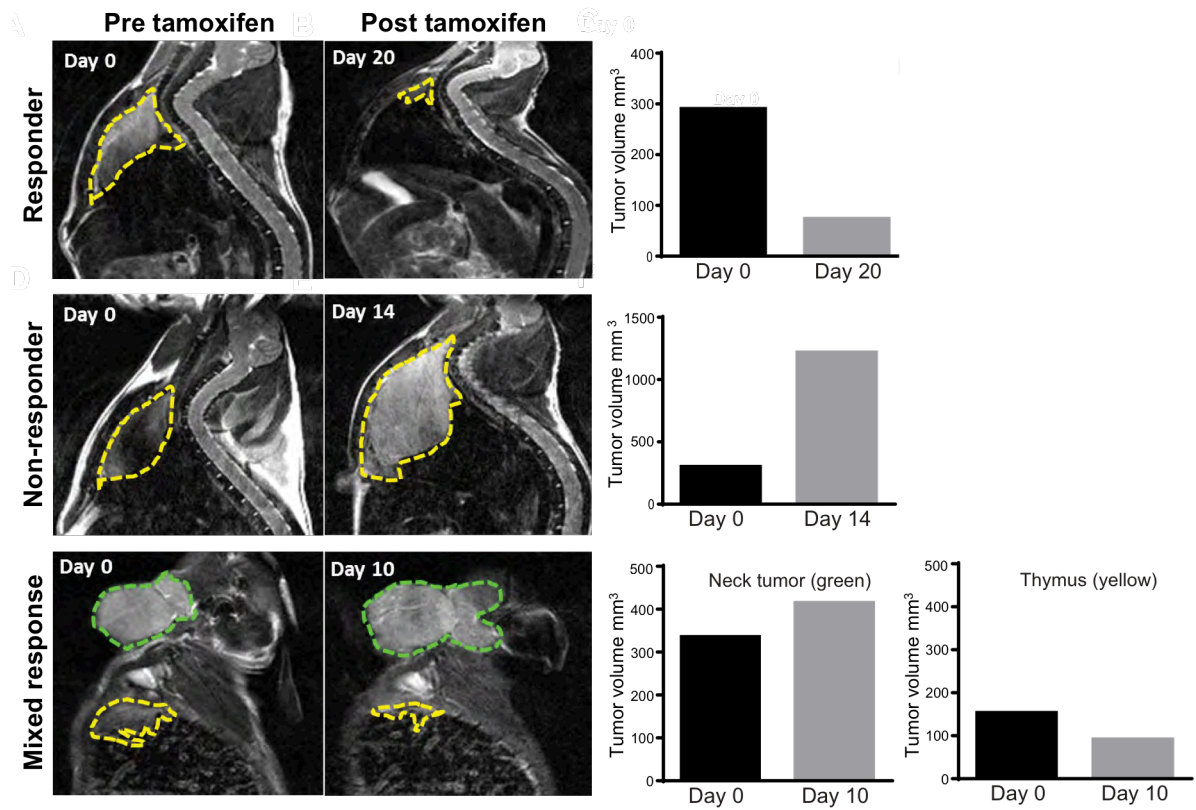


Figure 8. Variations in response to p53 restoration

Sagittal MRIs (left) and corresponding tumor volume graphs (right) of $p53^{neo/R172H};R26^{CreER/GNZ}$ mice before the start of tamoxifen treatment (left MRI panels) and after tamoxifen (right MRI panels) demonstrating variations in treatment response.

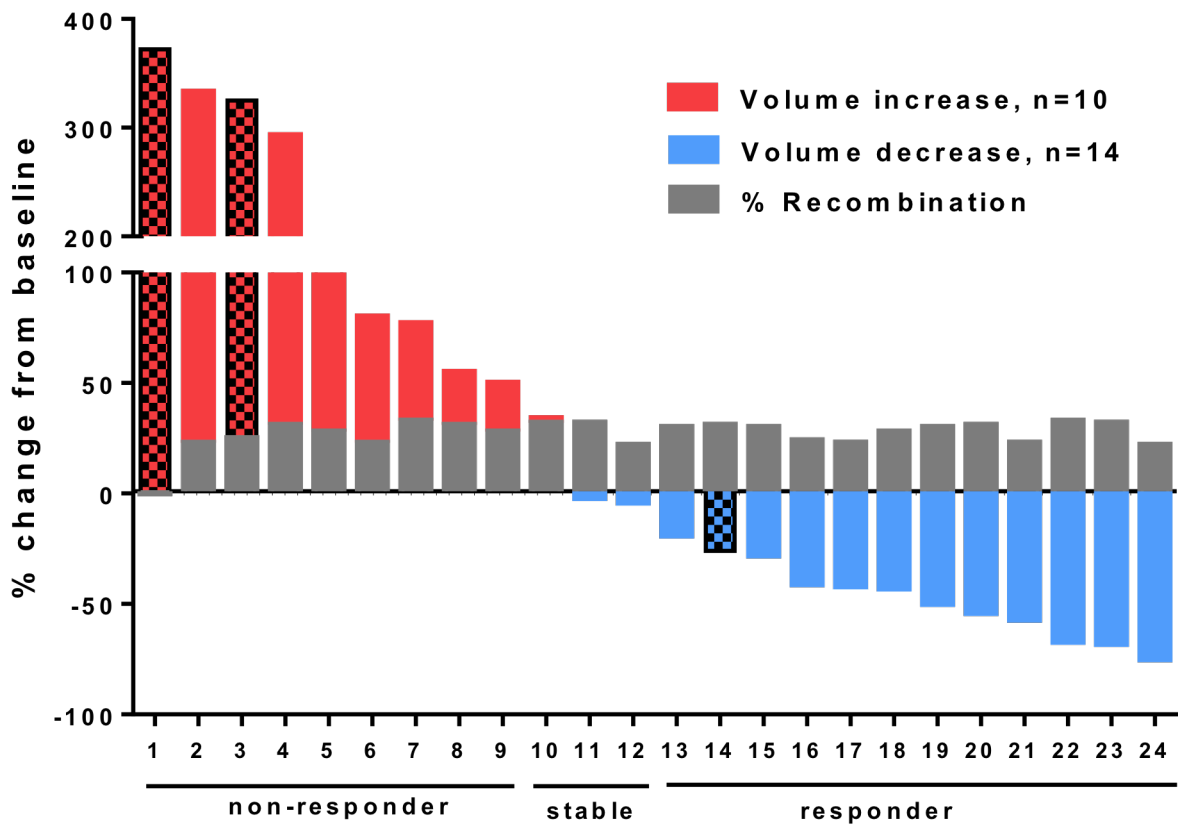


Figure 9. Summary of response to p53 restoration

Waterfall plot of tumor volumetric change from baseline in tamoxifen-treated $p53^{neo/R172H};R26^{CreER/GNZ}$ mice demonstrating the varying degrees of response. Solid bars represent lymphomas while checkered bars are sarcomas. Grey bar represents recombination efficiency of the $p53^{neo}$ allele

Tumor # (Refer to Fig. 9)	Pathological findings	Treatment duration (days)	Tumor Volume (mm ³)		Tumor volume change (%)	Response	p53 ^{neo} allele recombination	LOH status	RNA-seq
			Pre-RX	Post-RX					
1	High grade sarcoma	14	48.2	227.3	372%	NR	0%	Yes	No
2	Thymic lymphoma	14	295.5	1212	310%	NR	23%	No	Yes
3	Spindle cell sarcoma	18	200.7	808.2	300%	NR	25%	No	No
4	Thymic lymphoma	17	343.1	1246	262%	NR	31%	No	Yes
5	Thymic lymphoma	15	15.5	33	112%	NR	28%	No	No
6	Thymic lymphoma	13	1054	1512	57%	NR	23%	No	Yes
7	Intestinal lymphoma	15	61	88.4	45%	NR	33%	No	No
8	Lymphoma of submandibular LN	10	333.7	413.6	24%	NR	31%	No	No
9	Thymic lymphoma	18	95.9	117.7	22%	NR	28%	No	Yes
10	Thymic lymphoma	7	137.5	140	2%	S	32%	Partial	No
11	Thymic lymphoma	15	18	17.6	-2%	S	32%	NA	No
12	Thymic lymphoma	13	382.6	368.7	-4%	S	22%	NA	No
13	Thymic lymphoma	13	196.4	158.5	-19%	R	30%	Partial	Yes
14	Lymphoma	13	16.3	12	-26%	R	31%	No	No
15	Angiosarcoma	13	662.8	476	-28%	R	30%	No	No
16	Thymic lymphoma	10	152.3	89.6	-41%	R	24%	No	Yes
17	Thymic lymphoma	15	1183.4	688.7	-42%	R	23%	No	Yes
18	Thymic lymphoma	12	172.1	98.5	-43%	R	28%	No	Yes
19	Thymic lymphoma	7	112.7	56.6	-50%	R	30%	No	Yes
20	Thymic lymphoma	7	134.3	61.7	-54%	R	31%	No	Yes
21	Thymic lymphoma	13	36.5	15.7	-57%	R	23%	No	Yes
22	Lymphoma in LN	7	76.8	25	-67%	R	33%	No	No
23	Lymphoma of submandibular LN	7	35.7	11.4	-68%	R	32%	No	No
24	Thymic lymphoma	18	289	71.9	-75%	R	22%	No	Yes

Table 2. Detailed log of treated autochthonous tumors from the MRI cohort

Mice in this table represent treated mice from the waterfall plot in Figure 9. Last column indicates the tumor samples used for RNA sequencing experiments.

Abbreviations:

LN = lymph node

NR = non-responder

S = stable

R = responder

RX = tamoxifen treatments

LOH = loss of heterozygosity

2.4 CONCLUSION

In this chapter I characterized the impact of mutant p53 gain-of-function (GOF) on therapeutic response to p53 restoration. I genetically reactivated *p53* in tumor-bearing mice carrying a germline *p53^{R172H}* mutation to examine, *in vivo*, whether restoring p53 restoration promotes any survival advantages. I showed that restoring p53 in *p53*-mutant tumors does have therapeutic potential as it significantly prolonged survival. However, tumor volumetric change upon p53 restoration varied widely, ranging from 75% reduction to a 300% increase in volume. Analyses of the *p53^{neo}* locus revealed the level of restored p53 was equivalent in all tamoxifen-treated tumor samples, with a recombination efficiency of 25%, on average. In addition, I observed minimal to no loss-of-heterozygosity (LOH) of the *p53^{neo}* allele, indicating that variations in response are not likely caused by alterations or differences in the *p53^{neo}* locus and must be attributed to other molecular events. In the following chapter we take a more comprehensive approach to explore the molecular basis driving the widely ranging variability to p53 restoration.

CHAPTER 3

GLOBAL GENE EXPRESSION PROFILING OF P53-MUTANT TUMORS TO IDENTIFY THE PATHWAYS UNDERLYING RESPONSE TO P53 RESTORATION

3.1 INTRODUCTION

High throughput next-generation sequencing (NGS) platforms have provided long beseeched aid to understanding the molecular pathogenesis of many different human diseases. Recent advancements in NGS technologies have led to the identification of novel somatic mutations in a variety of human cancers that have important prognostic value and may serve as potential therapeutic targets. For example, RNA-sequencing is often used to compare tumors sensitive or resistant to a particular treatment to identify the pathways or gene expression signature underlying response and to provide a better understanding of who would benefit from a certain therapy.

In the previous chapter I showed that restoring p53 in p53-mutant tumors led to heterogeneous responses that could not be attributed to LOH or differences in the level of restored p53 and hypothesized that variations in response were attributed to other molecular events. To delineate these events and gain novel insight on the molecular processes accounting for variable responses to p53 restoration, we performed high-throughput RNA sequencing (RNA-seq) across 12 treated $p53^{neo/R172H};R26^{CreER/GNZ}$ mutant tumors that were sensitive (n=8) or resistant (n=4) to p53 restoration. All 12 treated tumors were T-cell lymphomas of the thymus (Table 2). RNA-sequencing data will provide a diagnostic platform to better understand the gene networks and pathways underlying resistance or sensitivity to p53 restoration.

3.2 METHODS

mRNA sequencing and gene expression analyses

Tumors from tamoxifen-treated $p53^{neo/R172H};R26^{CreER/GNZ}$ mice were harvested right after the final MRI during which a response (growth vs. shrinkage) was observed. Total RNA was isolated from tumors using TRIzol reagent (Life Technologies) following standard manufacturer's instruction. Total RNA was submitted to the M.D. Anderson sequencing core facility. Barcoded Illumina compatible libraries were prepared using the Illumina TruSeq mRNA seq Kit, per the manufacturer's protocol. The libraries were multiplexed 4 per lane and sequenced on the HiSeq3000 sequencer using the 75 bp paired end format. The raw RNA-sequencing (RNA-seq) readouts were mapped to the mouse mm10 assembly reference genome using TopHat, an open-source software tool that aligns RNA-seq reads to a reference genome. Differential gene expression analysis was performed with DESeq (an R/Bioconductor package) using a false discovery rate (FDR) of 5%. Gene set analyses were analyzed with the bioinformatics tool "GSEA" (Gene Set Enrichment Analysis) developed by the Broad Institution (94). The enrichment analyses were done with the Gene Ontology biological process gene sets and oncogenic gene sets from the molecular signature databases (MSigDB). The pathway analysis was performed with IPA (Ingenuity Pathway Analysis) developed by Ingenuity Inc. The significantly differentially expressed genes were used as input gene list for the IPA core analysis.

3.3 RESULTS

Distinct molecular profiles between tumors sensitive or resistant to p53 restoration

We performed high-throughput mRNA sequencing (RNA-seq) on 12 treated $p53^{neo/R172H};R26^{CreER/GNZ}$ mutant T-cell lymphomas that were sensitive (n=8) or resistant (n=4) to p53 restoration to determine if a molecular profile of response could be defined. All 12 treated tumors were T-cell lymphomas of the thymus (Table 2). Comparative analyses was performed with DESeq (Bioconductor) using a false discovery rate (FDR) < 5%. Differential expression analysis comparing responders vs. non-responders yielded 2484 significantly differentially expressed genes (DEGs) and hierarchical clustering of the significantly DEGs reveal that 2 out of 8 responders clustered more closely to the 4 non-responders (Figure 10). One plausible explanation is that those two tumors became refractory to tamoxifen treatments and began to relapse even though the tumors were smaller than before starting treatment. This could result in the refractory tumors acquiring a gene expression signature similar to tumors that are resistant to p53 restoration. Despite this, these two samples were analyzed in further pathway analyses and maintained in the responder's category.

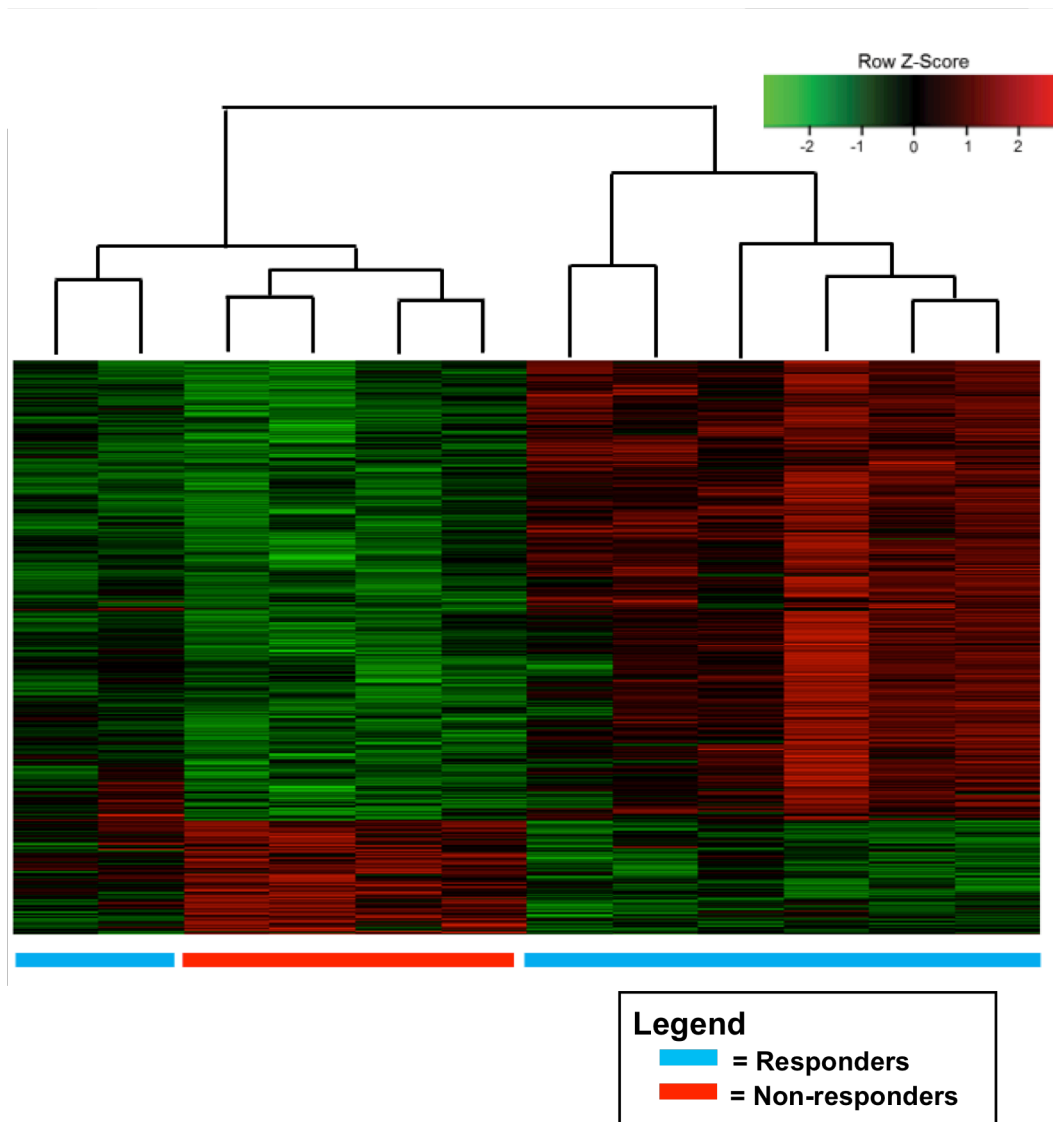


Figure 10. RNA-seq heatmap of significantly differentially expressed genes

Hierarchical clustering and gene expression heatmap of tamoxifen-treated thymic lymphomas yielded 2484 genes that were significantly differentially expressed (false discovery rate [FDR] < 0.05) between responders (n=8) and non-responders (n=4).

The TNF pathway is activated in responders

To identify the top upstream molecules that can explain the observed gene expression changes between responding (n = 8) and non-responding (n = 4) tumors, upstream regulator analysis of the significantly DEGs was performed using the Ingenuity Pathway Analysis (IPA). Among the top 10 most significant upstream regulators 9 molecules were predicted to be activated in responders and 5 of them were cytokines (Figure 11). WNT3A was the only cytokine with an unpredicted activation state. This means that in our dataset the downstream targets of WNT3A showed a random pattern of directional change that could not be correlated with WNT3A being in a state of activation or inhibition. Tumor Necrosis Factor (TNF) was the most significant upstream regulator with a reported activation state (Z-score = 4.76) in responders (Figure 11). TNF promotes an inflammatory response and binding of TNF to its cognate receptors can initiate several pathways such as activation of NF- κ B, MAPK pathways, or induction of death receptor signaling (95).

Notably, NF- κ B was another top upstream regulator with a reported activation state (Z-score = 7.69). Although less significant than TNF, the Z-score was higher due to a higher ratio of genes following a directional change of being in an activated state. Gene set enrichment analysis (GSEA) identified the inflammatory response (Figure 12) as being significantly enriched in responding tumors with a nominal p-value <0.01, providing further support that the TNF pathway may play a substantial role in the therapeutic response to p53 restoration. Additional GSEA results showed that the top 9 most enriched gene sets were biological processes involved in immune response, inflammatory response, and processes that have been linked to TNF pathway activation (Appendix A).

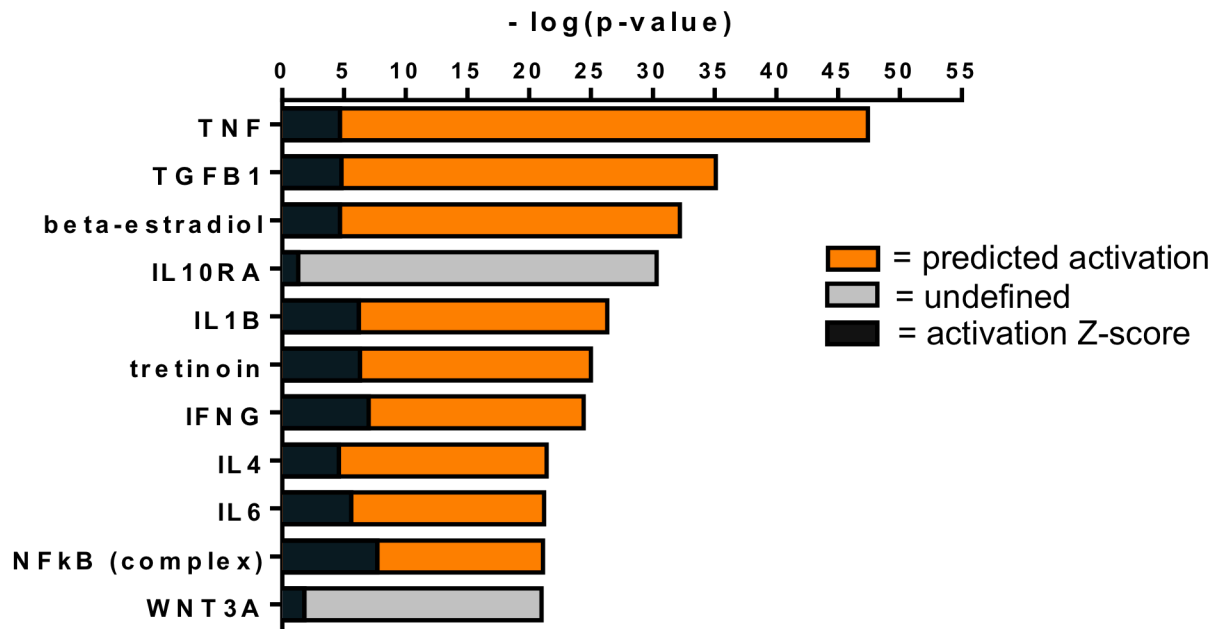


Figure 11. IPA upstream regulator analysis Graphical representation of the top 10 most significant upstream regulators identified from upstream pathway analysis using IPA.

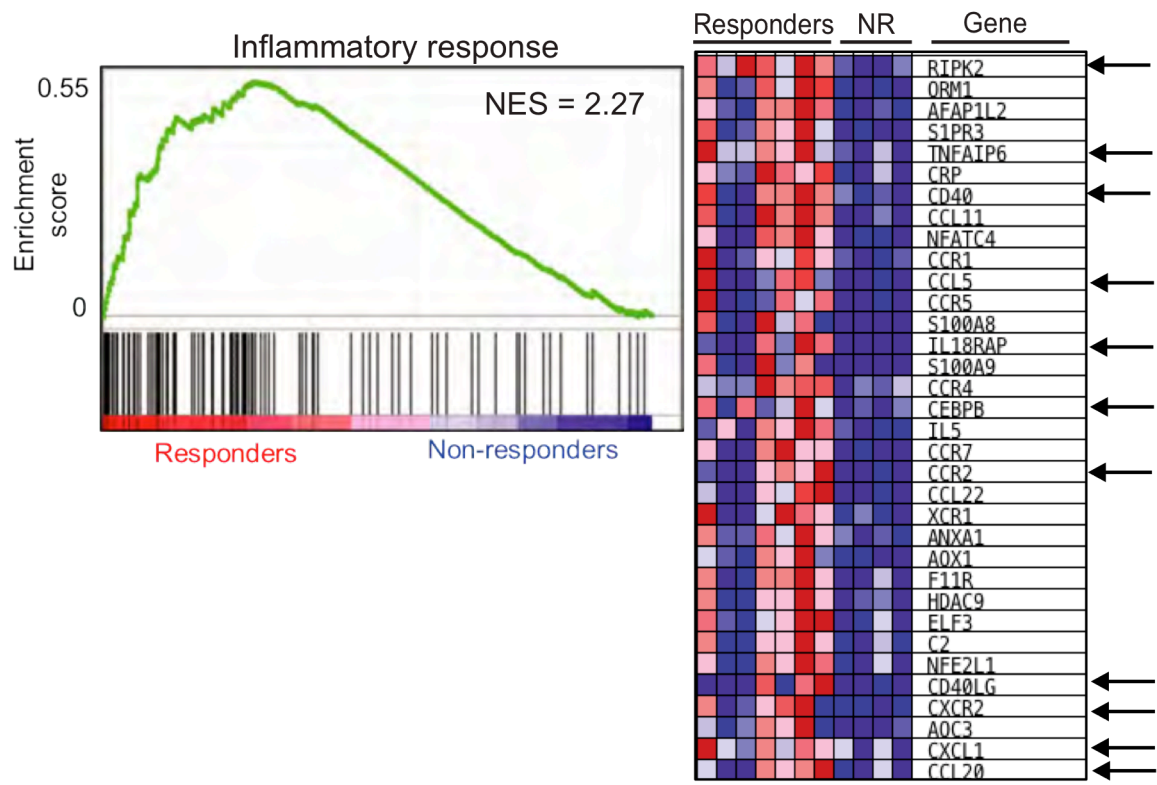


Figure 12. Gene set enrichment analysis of RNA-seq data presented as enrichment score (left), and corresponding heatmap (right) of leading-edge gene expression changes for genes of inflammatory response, which is significantly enriched with a nominal p-value < 0.01. Black arrows on the heatmap (right) point to TNF family members.

Identification of actionable targets in the TNF pathway

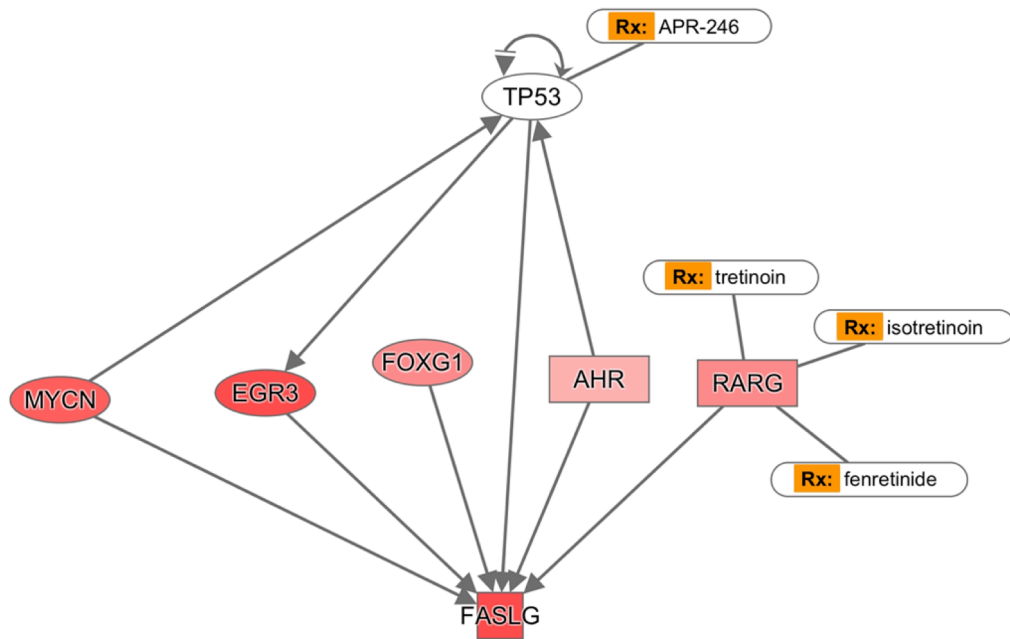
The upstream regulator analysis reported 293 genes from our dataset of significantly DEGs that are downstream effectors of TNF. TNF downstream effector molecules include any genes belonging to the TNF receptor superfamily or genes that are affected as a result of TNF signaling. To narrow down the list of 293 genes, we considered the top 10 most differentially expressed genes with the objective to focus on the molecules that are members of the TNF receptor superfamily while disregarding those that are only affected by TNF activation (Table 3). Of the top 10 most differentially expressed, Fas ligand (*Fasl*) was the only gene belonging to the TNF receptor superfamily. *Fasl* expression was upregulated 3.4 (log₂ fold change) in responders. Binding of *Fasl* to its receptors initiates the extrinsic apoptotic pathway via activation of death receptor signaling (96, 97). Using this knowledge, I used IPA to build a pathway of molecules upstream of *Fasl* then applied the drug overlay function to identify those that are pharmacologically targetable (Figure 13). This led to the identification of RAR γ (denoted as RARG), a retinoic acid receptor (RAR) that was also significantly upregulated in responding tumors (Figure 14). RARs are a type of nuclear receptor that can transactivate target gene expression upon ligand-binding of retinoic acid (RA), such as all-trans retinoic acid (ATRA) (denoted as tretinoin & isotretinoin in Figure 13) that binds to all three retinoic acid receptors, RAR α , RAR β & RAR γ (98). However, RNA-seq expression analysis revealed that RAR γ was significantly upregulated in responding tumors, while no significant differences in RAR α and RAR β expression were observed (*Rarg*, *Rara* & *Rarb*, respectively in Figure 14).

Genes in dataset	Log2 fold change	Adj. p-value from RNA-seq expression analysis
S100A9	4.338	1.46E-05
S100A8	3.849	0.0002
MYH7	3.786	2.18891E-05
CCR8	3.606	0.002
CCND2	3.549	0.0001
IL18R1	3.532	0.00085048
FASL	3.465	0.001
TIMP4	3.438	0.001
CAR2	3.305	0.0009
TREM3	3.282	0.003

Table 3. Top 10 most differentially expressed TNF downstream molecules

Genes in this table include those that belong to the TNF receptor superfamily or any genes known to be directly or indirectly affected by TNF signaling. Among the top 10, *Fasl* was the only gene that is a TNF receptor superfamily member.

fasL



© 2000-2016 QIAGEN. All rights reserved.

Figure 13. Identification of actionable targets in the TNF pathway. IPA was used to build a pathway of significantly differentially expressed genes directly upstream of FasL (denoted as FASLG). Degree of red color indicates genes that are significantly upregulated in responders (darker red = higher fold change).

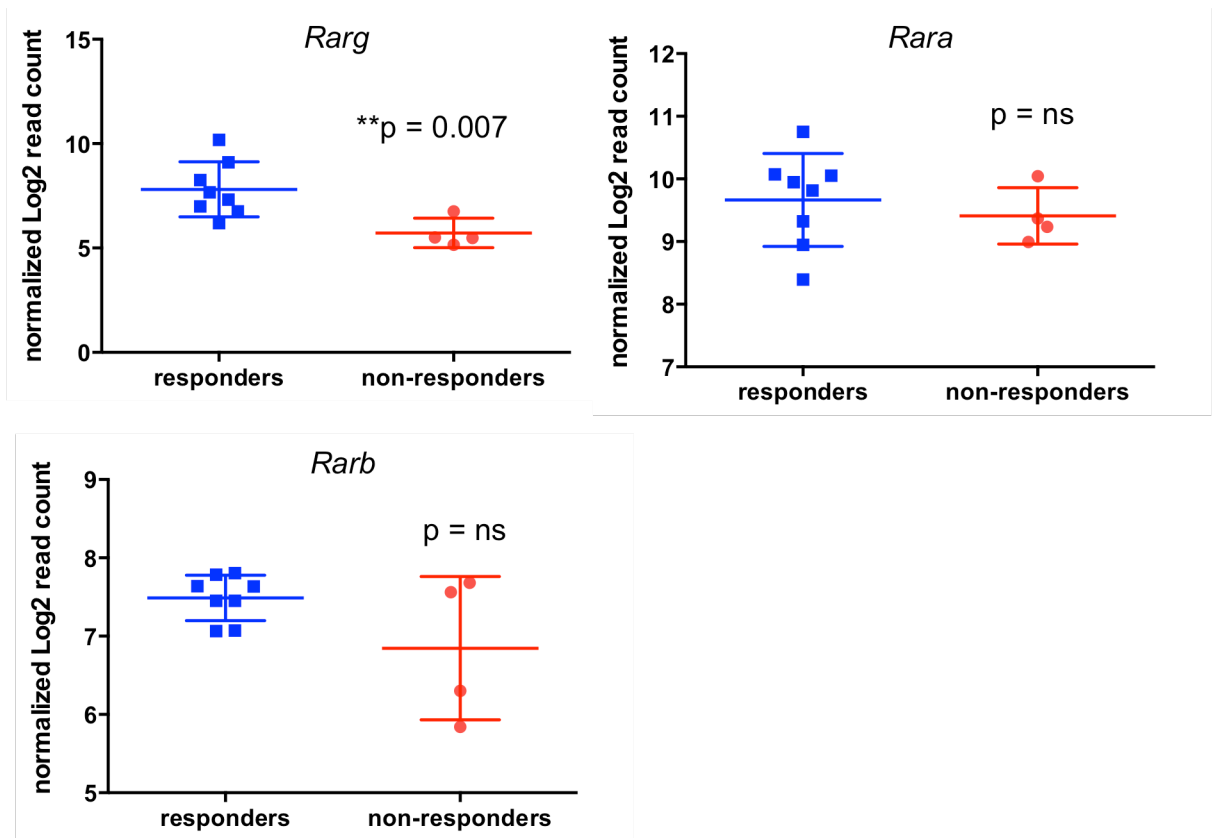


Figure 14. DESeq differential expression analysis of *Rarg*, *Rara*, and *Rarb* presented as normalized Log2 read count with adjusted p-value for Benjamin-Hochberg corrections for multiple testing.

3.4 CONCLUSION

In this chapter I describe using RNA-sequencing as an approach to comprehensively characterize the gene expression profile and molecular networks impacting response to p53 restoration. I genetically reactivated wild-type p53 in *p53^{R172}* mutant tumors then sequenced the transcriptome of 12 treated T-cell lymphomas that were sensitive or resistant to p53 restoration with the goal of identifying the pathways critical for response and actionable targets that may synergize or have an additive effect when combined with p53 restoration therapy. I performed upstream regulator pathway analyses, which revealed that the TNF pathway was activated in p53-sensitive tumors. Further, I identified the retinoic acid receptor, RAR γ , as a druggable target in the TNF pathway and hypothesized that pharmacologically activating RAR γ with a synthetic retinoid will have an additive or synergistic effect with reactivated p53. In the following chapter I evaluate and describe the effects of combining retinoic acid treatment with p53 restoration therapy.

CHAPTER 4

EVALUATING THE THERAPEUTIC EFFICACY OF A COMBINATION THERAPY WITH RETINOIC ACID AND P53 RESTORATION

4.1 INTRODUCTION

In the previous chapter I identified the TNF pathway and RAR γ , an effector in the TNF pathway, as critical mediators in response. Like p53, activation of RARs can promote cell death by initiating apoptosis through the intrinsic or extrinsic pathway. RARs are a type of nuclear receptor that heterodimerizes with RXR, and this complex functions as a transcription factor that can be activated upon ligand binding of retinoic acid (RA). RARs and p53 share some common transcriptional target genes including *Fas*, *Fasl*, *Pidd*, *Trail*, and several pro-apoptotic genes (99-101). In addition, cytosolic p53 and RXR/Nurr77 are both capable of inducing intrinsic cell death by directly interacting with anti-apoptotic Bcl-2 family members on the outer mitochondrial membrane as illustrated in Figure 15 (96, 100).

Based on the overlapping roles of p53 and RARs in activating cell death (Figure 15), I hypothesized that treating tumors with a synthetic retinoid would improve therapeutic response to p53 restoration. Using treatment-naïve thymic lymphomas from $p53^{neo/R172H};R26^{CreER/tdT}$ mice, I developed a syngeneic transplant model to propagate tumors for parallel combinatorial therapy studies that can be achieved in a single tumor type (Figure 16A). I performed an initial baseline study to determine sensitivity to p53 restoration and acquired T-cell thymic lymphoma lines that were sensitive (Figure 16B, top panels) and resistant to p53 restoration (Figure 15B, middle panels). As with the treated autochthonous tumors from the MRI study, the reduction in tumor growth and prolonged survival were not caused by tamoxifen since tamoxifen-treated $p53^{neo/R172H};R26^{tdT/+}$ mice exhibited no reduction in tumor volume or survival advantages (Figure 16B, bottom panels).

In this chapter we investigated the effects of a combination therapy regimen to determine if response to p53 restoration can be augmented when combined with retinoic acid treatment.

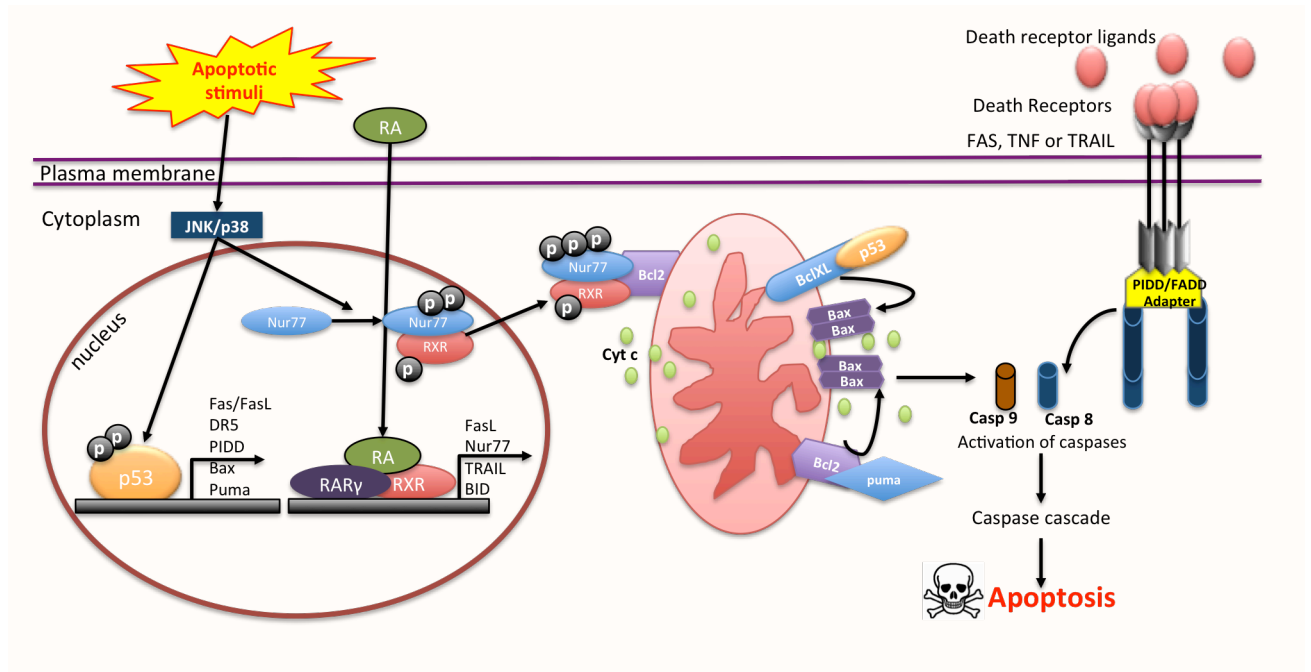
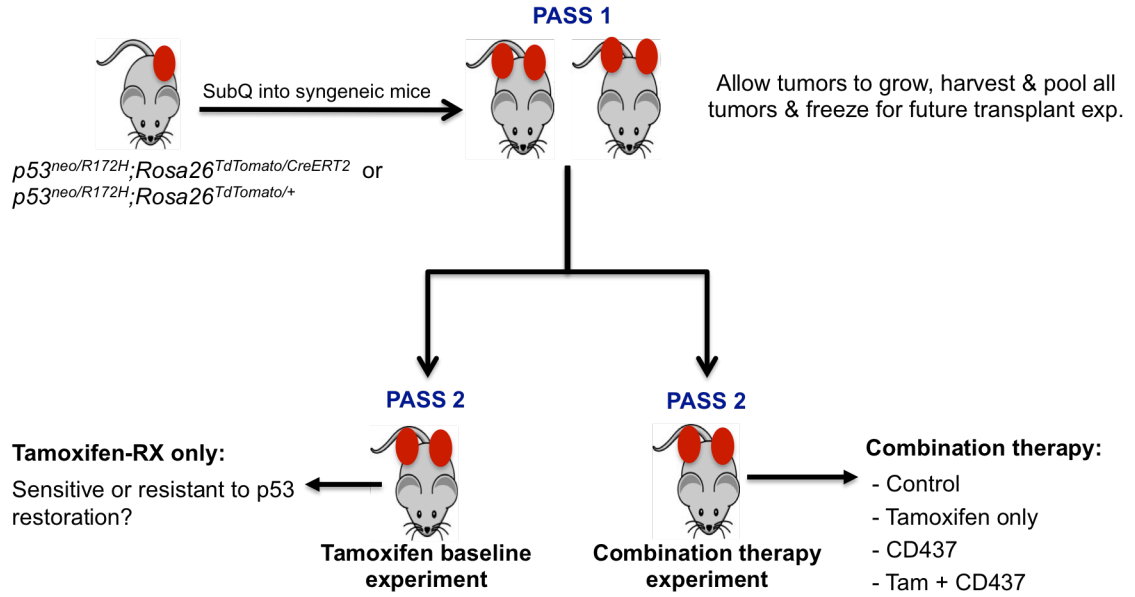


Figure 15. Overlapping roles of p53 and RARs in activating cell death

Both p53 and RAR can initiate cell death via the extrinsic pathway by transcriptionally activating death receptor genes such as *Fas*, *Fasl*, *Pidd*, and *Trail*, to name a few. In addition, p53 and RAR are capable of inducing cell death via the intrinsic pathway by physically associating with anti-apoptotic factors on the mitochondrial outer member.

A



B

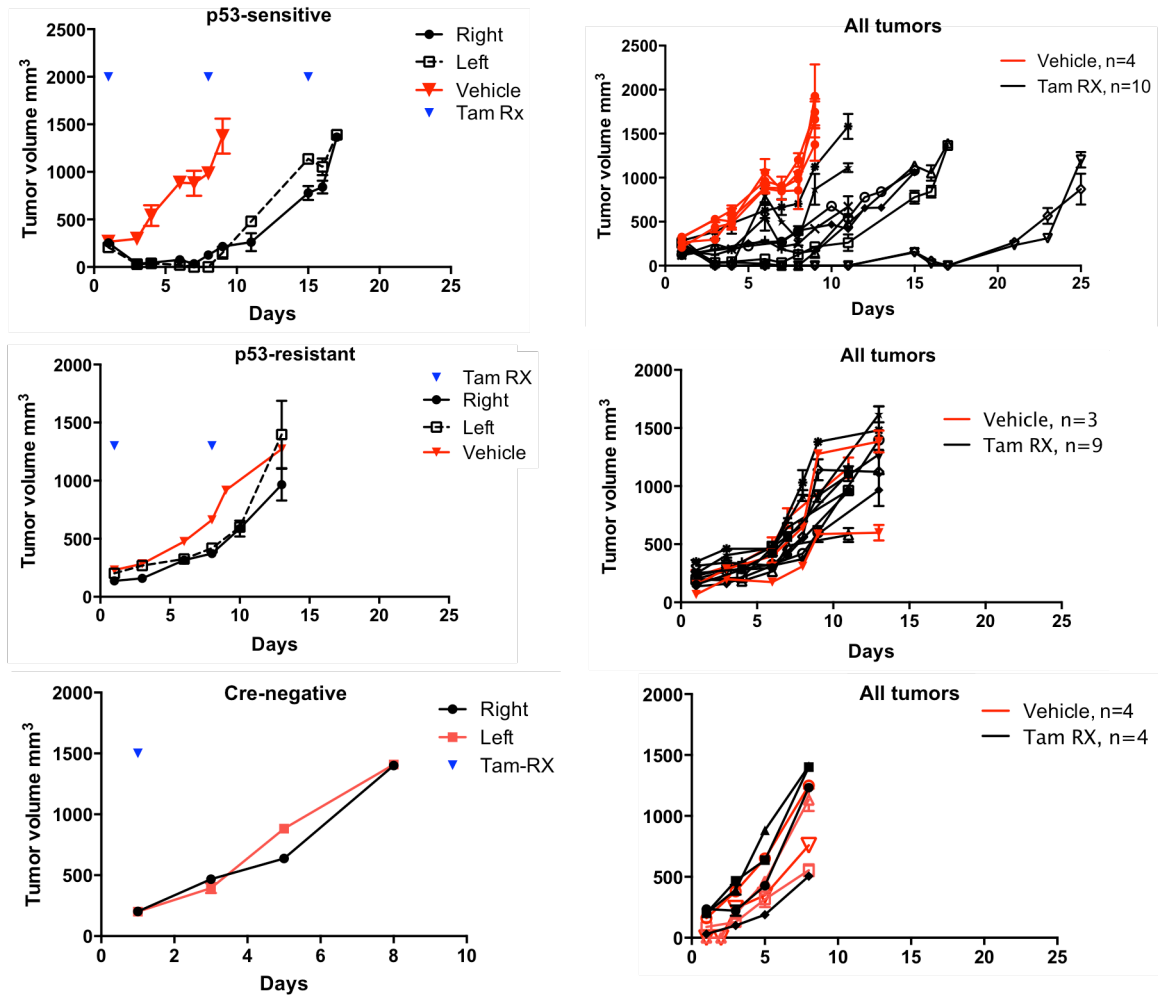


Figure 16. Generation & treatment of syngeneic tumor models

(A) Syngeneic transplant model used to propagate treatment-naïve tumors from $p53^{neo/R172H};R26^{CreER/tdT}$ or $p53^{neo/R172H};R26^{tdT/+}$ mice. (B) Tumor growth curves of syngeneic thymic lymphomas from the tamoxifen baseline study. (Top panels) a $p53^{neo/R172H};R26^{CreER/tdT}$ thymic lymphoma that was classified as p53-sensitive, (middle panels) a $p53^{neo/R172H};R26^{CreER/tdT}$ thymic lymphoma that was classified as p53-resistant, (bottom panels) a $p53^{neo/R172H};R26^{tdT/+}$ thymic lymphoma line used as a negative control to demonstrate that tamoxifen treatment alone does not affect tumor growth.

4.2 METHODS

Syngeneic tumor transplants

All procedures were carried out using aseptic techniques. Treatment-naïve thymic lymphomas were harvested from euthanized $p53^{neo/R172H};R26^{CreER/tdT}$ or $p53^{neo/R172H};R26^{tdT/+}$ mice and dissociated using two 18 gauge needles in a petri dish with DMEM culture media supplemented with 10% fetal bovine serum. Tumor cells were then strained through a 70 micron cell strainer, pelleted by centrifugation, then resuspended in a solution of Matrigel:PBS (1:2 v/v) (BD Bioscience). Tumor cells (5×10^6 cells/injection site) were subcutaneously injected into the left and right fat pads of 8 week old syngeneic C57BL/6J mice ($n \geq 32$ for each combination therapy experiment) purchased from The Jackson Laboratory.

Treatment of syngeneic mice

Stock solutions of CD437 (Tocris) were prepared by dissolving in DMSO to a concentration of 25 mg/mL then further diluted to 2.5 mg/mL in 10% (w/v) 2-hydroxypropyl- β -cyclodextrin (Sigma, Cat # H107) right before treatment. For each combination therapy cohort, mice were randomly divided to one of four different treatment groups before exhibiting tumor growth: vehicle (2-hydroxypropyl- β -cyclodextrin) ($n \geq 7$), tamoxifen ($n \geq 6$), (3 mg per injection); CD437 ($n \geq 6$) (0.3 mg per injection) and tamoxifen + CD437 ($n \geq 8$) (3 mg & 0.3 mg, respectively) and treatments did not start until a tumor reached 150-250 mm³ in volume. Tumors were measured with digital calipers every 1-2 days and tumor volumes were calculated using the equation $[(\text{length} \times \text{width}^2)/2]$ as previously described (67). Mice were sacrificed once a tumor reached 1500 mm³ in volume or 1.5 cm in any direction. All syngeneic mice that developed tumors were included in the analyses.

Flow cytometry

Tumors were harvested from euthanized mice and disassociated into a single cell suspension in phosphate buffered saline (PBS) supplemented with bovine serum albumin (BSA). Red blood cells (RBC) were depleted by incubating in RBC lysis buffer. For immunophenotypic analyses, 1×10^6 tumor cells were incubated in an antibody cocktail of α -mouse CD4-APC (Biolegend, 100411), α -mouseCD8a-APC-Cy7 (Biolegend, 100713), and α -mouse CD3-FITC (Biolegend, 100203) at a concentration per the manufacturer's recommendation. After DAPI exclusion, cells were gated on singlets. Annexin-V flow cytometry was performed following the same protocol with Annexin V-FITC (Biolegend, 640905). All antibody incubations were performed on ice, protected from light. Flow analyses were performed on the Gallios 561 flow cytometer and data were analyzed using Kaluza software (Beckman Coulter, Indianapolis, IN, USA).

Quantitative real-time PCR (qPCR)

Total RNA was isolated from harvested tissues of euthanized mice using TRIzol reagent (Life Technologies) following standard manufacturer's instruction. For each tumor sample, 1 μ g of total RNA using was reverse transcribed using iScript 5X supermix (BioRad) according to manufacturer's protocol. qPCR analyses were performed in triplicates on a 7900HT Fast Real-time PCR system (Applied Biosystems, software: SDS). All primers used were for mouse mRNA sequences and are as follows: *Cd38* (forward, 5'-GAAGACTACGCCCCACTTGT; reverse primer, 5'- ATGGGCCAGGTGTTTGGATT), *FasI* (forward, 5'- ACCGCTCTGATCTCTGGAGT; reverse, 5'- GGCTGGTTGTTGCAAGACTG); *Bid* (forward, 5'- CCAGTCACGCACCATCTTTG; reverse, 5'- GTCCATCTCGTTTCTAACCAAGT), *Rplp0* (forward, 5' CCCTGAAGTGCTCGACATCA; reverse, 5'- TGCGGACACCCTCCAGAA), p21 (forward, 5'- CCTGACAGATTTCTATCACTCCA, reverse, 5'- AGGCAGCGTATATCAGGAG); and *Puma* (forward, 5'-GTACGAGCGGCGGAGACAAG; reverse, 5'- GCACCTAGTTGGGCTCCATTTCTG).

Statistics

Statistical analyses were performed using GraphPad Prism 6 software (GraphPad, San Diego, CA, USA) using ANOVA analyses with Bonferroni's correction for multiple testing unless otherwise specified. Mouse survival curves by Kaplan-Meier plots were analyzed by the log-rank (Mantel-Cox) tests. Statistical significance was defined as $p < 0.05$.

Study approval

All mouse experiments were approved by the MD Anderson Cancer Center Institutional Animal Care and Use Committee and conformed to the guidelines of the United States Animal Welfare Act and the National Institutes of Health.

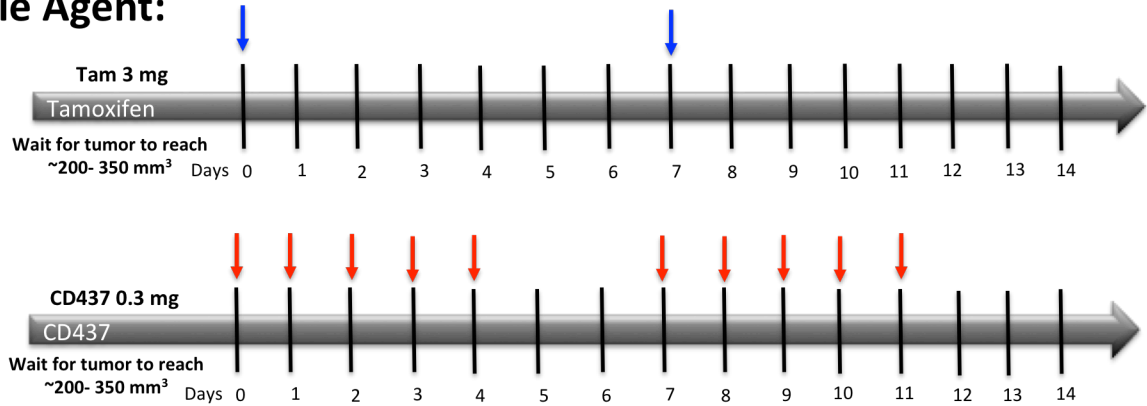
4.3 RESULTS

Designing a combination therapy regimen with the RAR γ -specific retinoid, CD437, for combination therapy experiments

To assay if combining retinoic acid treatments with p53 restoration via tamoxifen could improve response, I designed a combination therapy drug study to evaluate the synthetic retinoid, CD437 (6-[3-(1-Adamantyl)-4-hydroxyphenyl]-2-naphthalene carboxylic acid). I chose CD437 since it is a RAR γ -selective agonist and RNA-seq expression analysis revealed that *Rarg* was significantly upregulated in responding tumors, whereas as *Rara* & *Rarb* showed no differences in expression (Figure 14).

I used a syngeneic transplant model where tumor cells are subcutaneously injected into both the right and left fat pads of recipient mice to allow so that more tumors could be evaluated without increasing the number of mice. In addition, since tumor cells were subcutaneously injected, tumor growth could easily be tracked and measured on a daily basis with digital calipers. A treatment regimen was designed to evaluate and compare the efficacy of p53 restoration and CD437 treatment as a monotherapy or combination therapy approach. Mice in the tamoxifen treatment group were administered 3 mg/dose once a week (2 treatments total) via IP injection, which is the same regimen used on mice from the MRI cohort. Mice treated with CD437 were administered 0.3 mg/dose via IP injections for 5 consecutive days for two weeks, with a two-day break between each round. I designed this regimen based on literature search and found that this is one of the standard regimens commonly used for administering retinoic acid in mice. Mice in the combination therapy cohort were administered the same dosage of both drugs, starting with tamoxifen first (Figure 17).

Single Agent:



Combination therapy:

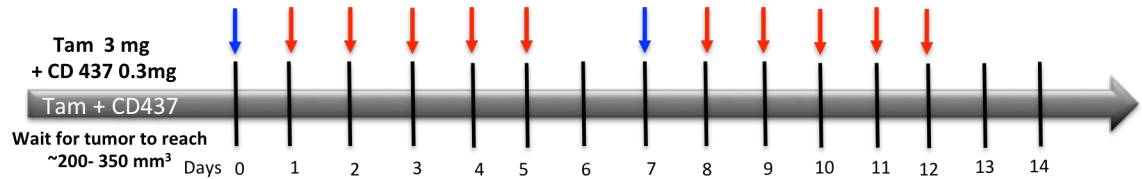


Figure 17. Treatment regimen for combination therapy experiments

For the tamoxifen cohort (top), mice were administered 3 mg per dose via IP injections once a week for up to two weeks then followed for survival. For the CD437 cohort (middle), mice were treated with 0.3 mg/dose via IP injections for 5 consecutive days for two weeks, with a two-day break between each round. The combination therapy cohort received the same dose of tamoxifen and CD437 as single-agent treated mice (bottom).

The RAR γ -selective retinoid, CD437, sensitizes resistant tumors to p53 restoration

We first evaluated the effects of combining CD437 treatment with p53 restoration via tamoxifen treatment in the p53-resistant T-cell lymphoma. Equivalent numbers (5×10^6) of treatment-naïve *p53^{neo/R172H};R26^{CreER/tdT}* lymphoma cells were subcutaneously injected into the right and left fat pads of wild-type C57BL6/J syngeneic mice ($n = 42$). Of the 42 mice injected, 80% ($n=34$) developed at least one tumor. Mice were randomized to different treatment groups and treatments did not start until a tumor reached at least 150 mm^3 in size (Figure 17). Survival was measured as days survived post treatment start, in which mice were sacrificed once a tumor reached 1500 mm^3 in volume or measured 1.5 cm in any direction.

In the p53-resistant T-cell lymphoma line, monotherapy with tamoxifen or CD437 was insufficient to promote tumor regression (Figure 18) or prolong survival (Figure 19) since the tumor volumes measured at each day and survival overlapped with vehicle-treated mice. However, mice treated with tamoxifen (to restore p53) in conjunction with CD437 exhibited a reduction in tumor growth that corresponded with a significant increase in survival (Figure 20 & Figure 21A). When we looked at tumor volumes 12 days after the start of treatment, the mean tumor volume of combo-treated mice was 385.1 mm^3 , which was significantly lower ($p < 0.01$) compared to vehicle-treated mice (mean tumor volume = 931.7 mm^3) or mice treated with tamoxifen (mean tumor volume = 807 mm^3) or CD437 (mean tumor volume = 927.1 mm^3) alone (Figure 21B). In conclusion, the combination of CD437 and p53 restoration sensitized p53-resistant tumors, as it effectively promoted tumor regression whereas single agent treatment had minimal to no effect in reducing tumor burden or prolonging survival compared to vehicle-treated mice.

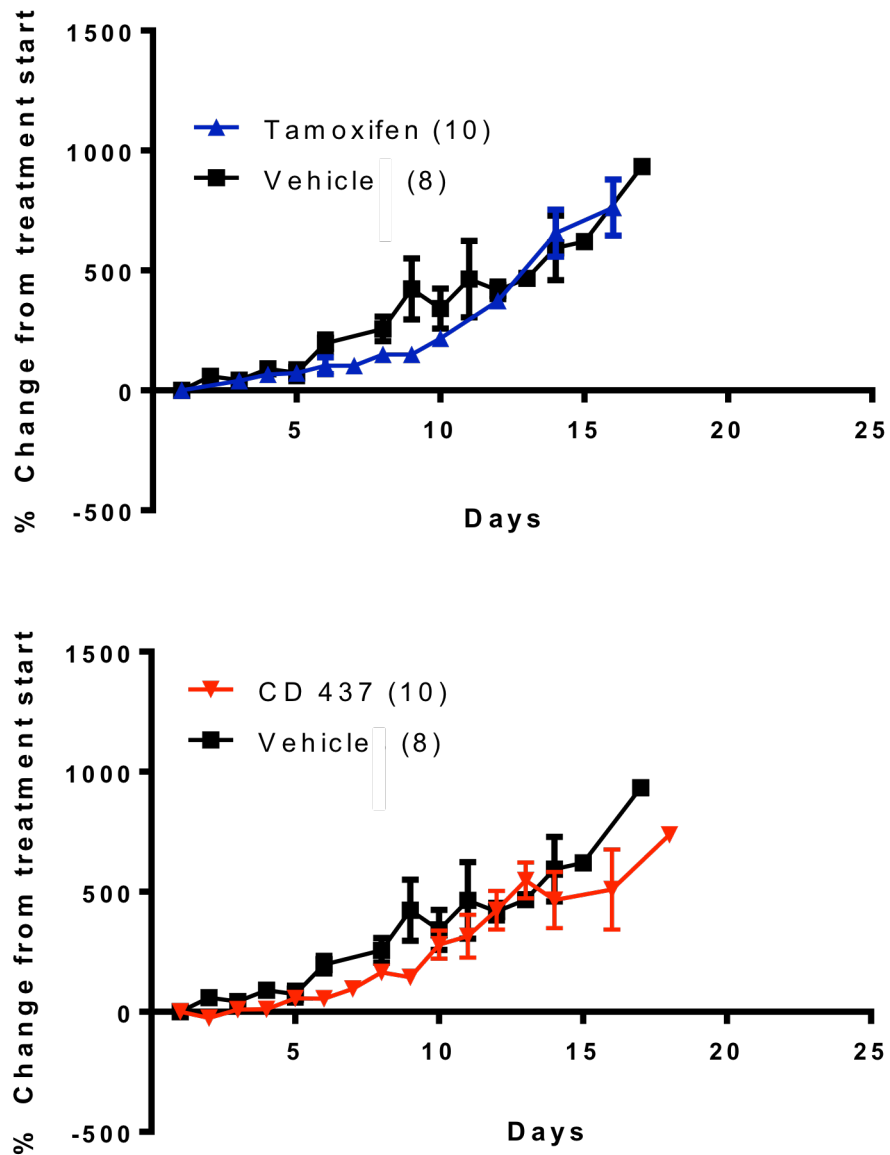


Figure 18. Tumor growth curves of single-agent treated p53-resistant tumors

Mean \pm s.e.m. of tumor growth curve (mm^3) plotted as percent change from baseline for mice treated with tamoxifen (top) or CD437 (lower).

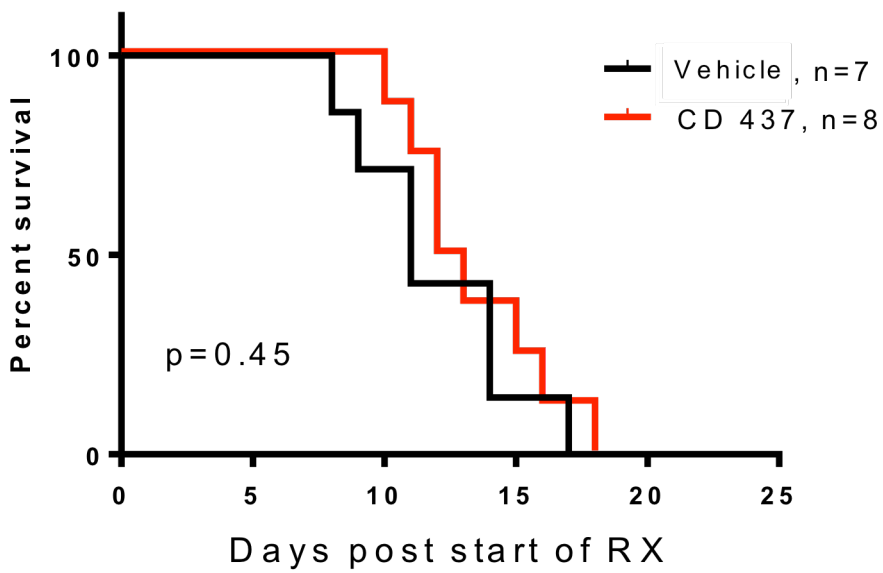
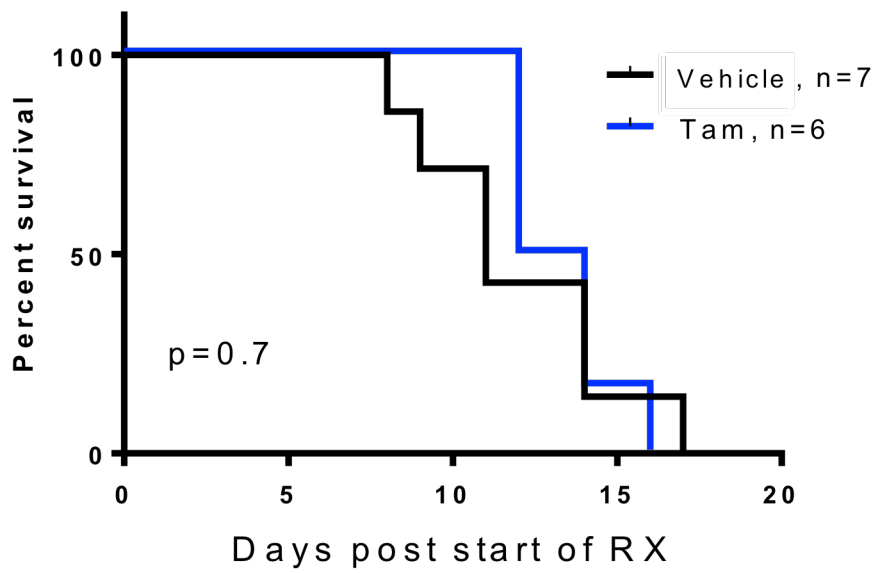


Figure 19. Survival of single-agent treated mice with p53-resistant tumors

Kaplan-Meier analyses of mice from Figure 18 with tumor size reaching 1500 mm³ as the end-point.

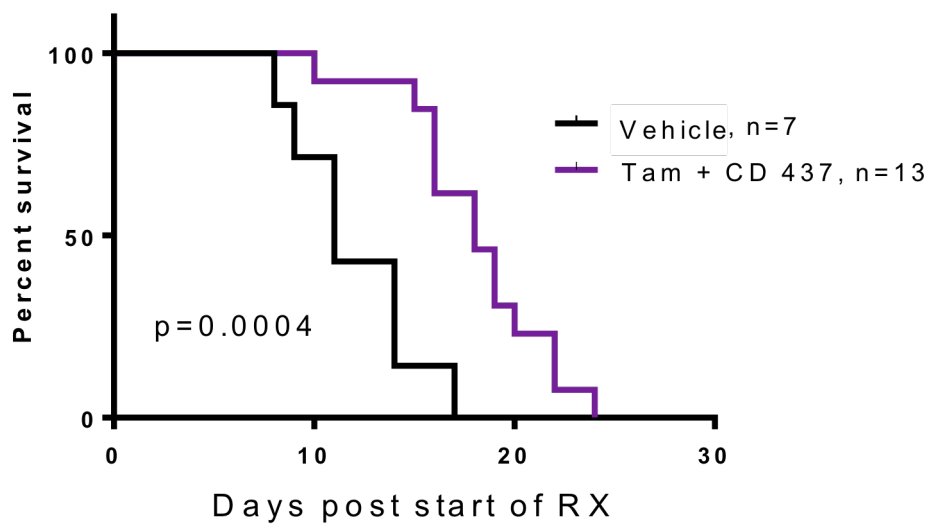
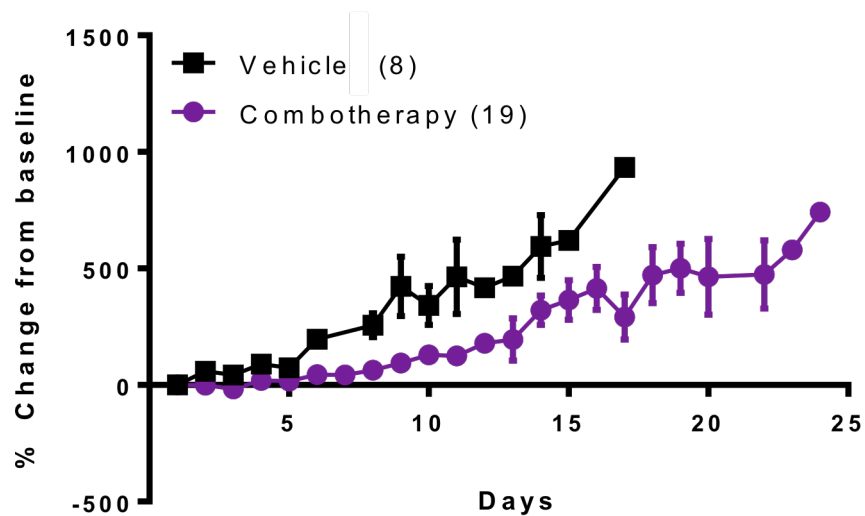


Figure 20. Tumor growth & survival of combo-treated p53-resistant tumors

Mean \pm s.e.m. of tumor growth curve (mm^3) plotted as percent change from baseline (top) of mice treated with tamoxifen plus CD437 and Kaplan-Meier analyses of mice with tumor size reaching 1500 mm^3 as the end-point of data shown in growth curve above.

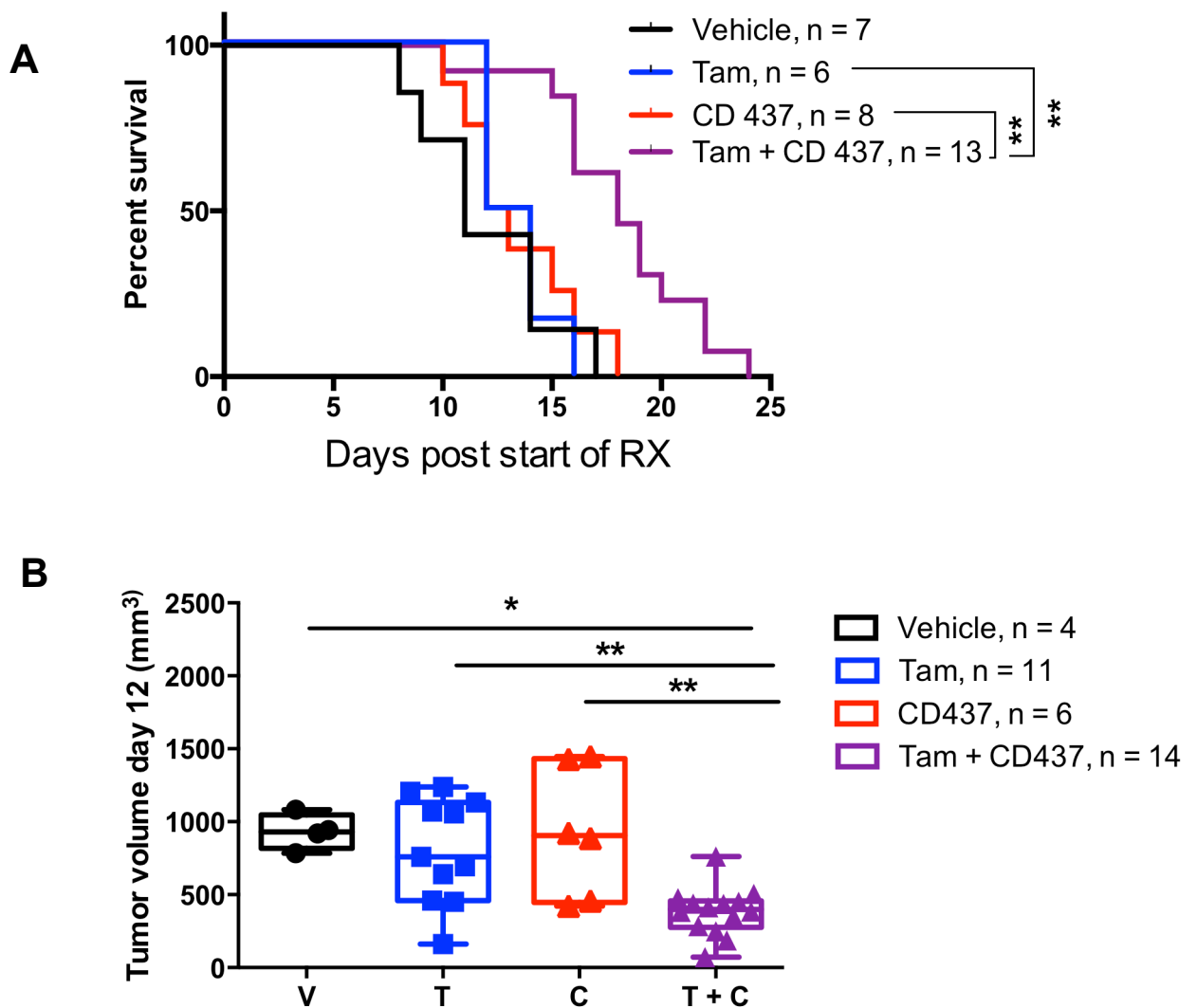


Figure 21. Summary of treatment for p53-resistant tumors

(A) Kaplan-Meier analyses for all treatment groups of mice with tumor size reaching 1500 mm³ as the end-point of data shown in the p53 resistant line. **(B)** Mean \pm s.e.m. of tumor size distribution (mm³) at day 12 of data shown in Figures 18 & 20. Data were analyzed by ANOVA with Bonferroni corrections for multiple comparisons (B).

Levels of significance: *p < 0.05, **p < 0.01,

CD437 additively improves response and survival in p53-sensitive tumors

Next we evaluated therapeutic response to CD437 in the p53-sensitive thymic lymphoma line. For this cohort, 33 mice were injected with equivalent numbers (5×10^6) of tumor cells and 88% of mice ($n = 29$) developed tumors. In line with the results of the baseline study (Figure 16), we observed that p53 restoration alone promoted rapid tumor regression as tamoxifen-treated mice exhibited smaller tumor volumes across all measured days (Figure 22A) as well as a significant ($p = 0.005$) increase in survival (Figure 22B). Mice treated with CD437 as a monotherapy also showed tumor regression (Figure 23A) that corresponded with a significant ($p = 0.002$) increase in survival (Figure 23B) compared to vehicle-treated mice. This is contrary to what we observed in the p53-resistant cohort where CD437-treated mice showed no changes in tumor volume or survival benefits compared to vehicle-treated mice (Figure 21).

Interestingly, combination therapy showed a superior response by additively increasing survival tumor regression in mice. The combination of tamoxifen and CD427 promoted rapid tumor regression that extended for a longer duration of time compared to vehicle or single-agent-treated mice (Figure 24A) and corresponded with an even more significant increase ($p = 0.0001$) in survival compared to controls (Figure 24B). Moreover, combo-treated mice also showed a significant increase in survival compared to tamoxifen-treated mice (Figure 25A). When we looked at tumor volumes 12 days after the start of treatment; the mean tumor volume of combo-treated mice was significantly smaller ($p < 0.0001$) compared to mice treated with vehicle (187.6 mm^3 vs. 1315 mm^3 , respectively), tamoxifen (187.6 mm^3 vs. 787 mm^3 , respectively), or CD437 (187.6 mm^3 vs. 747.6 mm^3 , respectively) alone (Figure 25B).

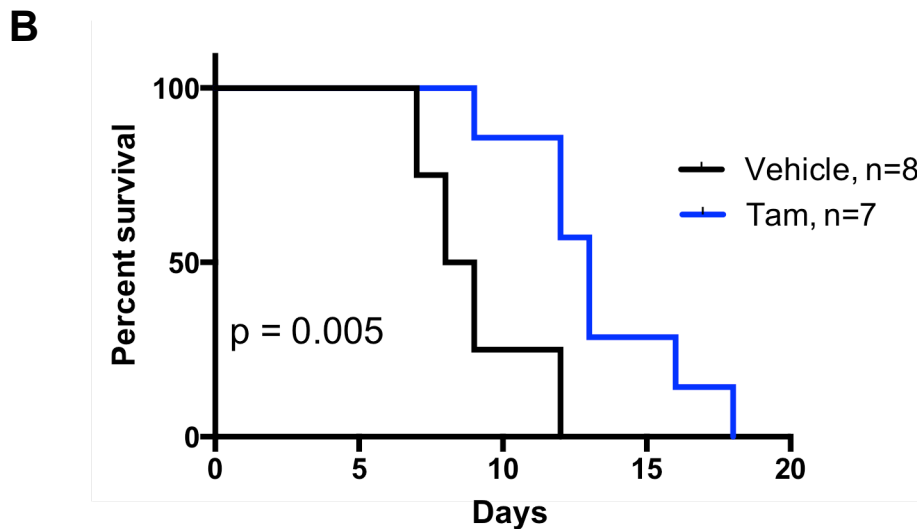
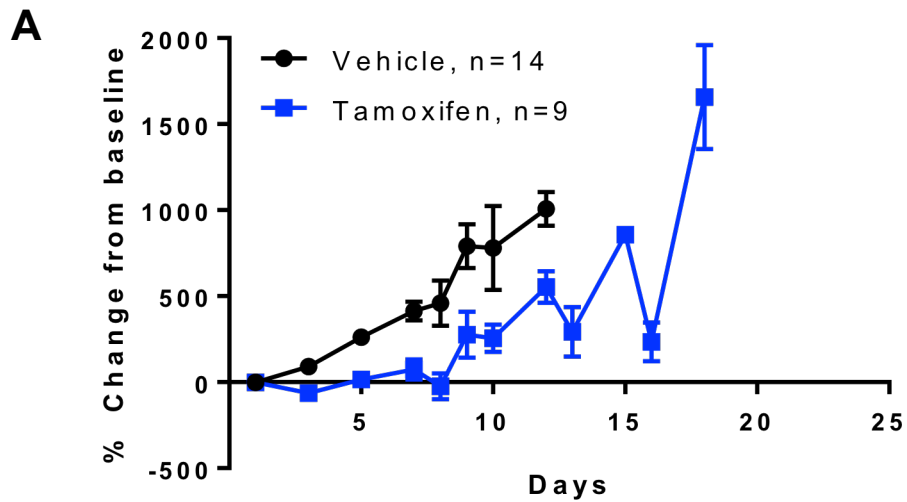


Figure 22. Tumor growth curve & survival of tamoxifen-treated p53-sensitive tumors

(A) Tumor growth curves plotted as mean \pm s.e.m. of percent change from baseline for tamoxifen-treated syngeneic mice harboring tumors from $p53^{neo/R172H};R26^{CreER/tdT}$ mice sensitive to p53 restoration. (B) Kaplan Meier analysis of tumor size reaching 1500 mm³ as an endpoint for data shown in (A).

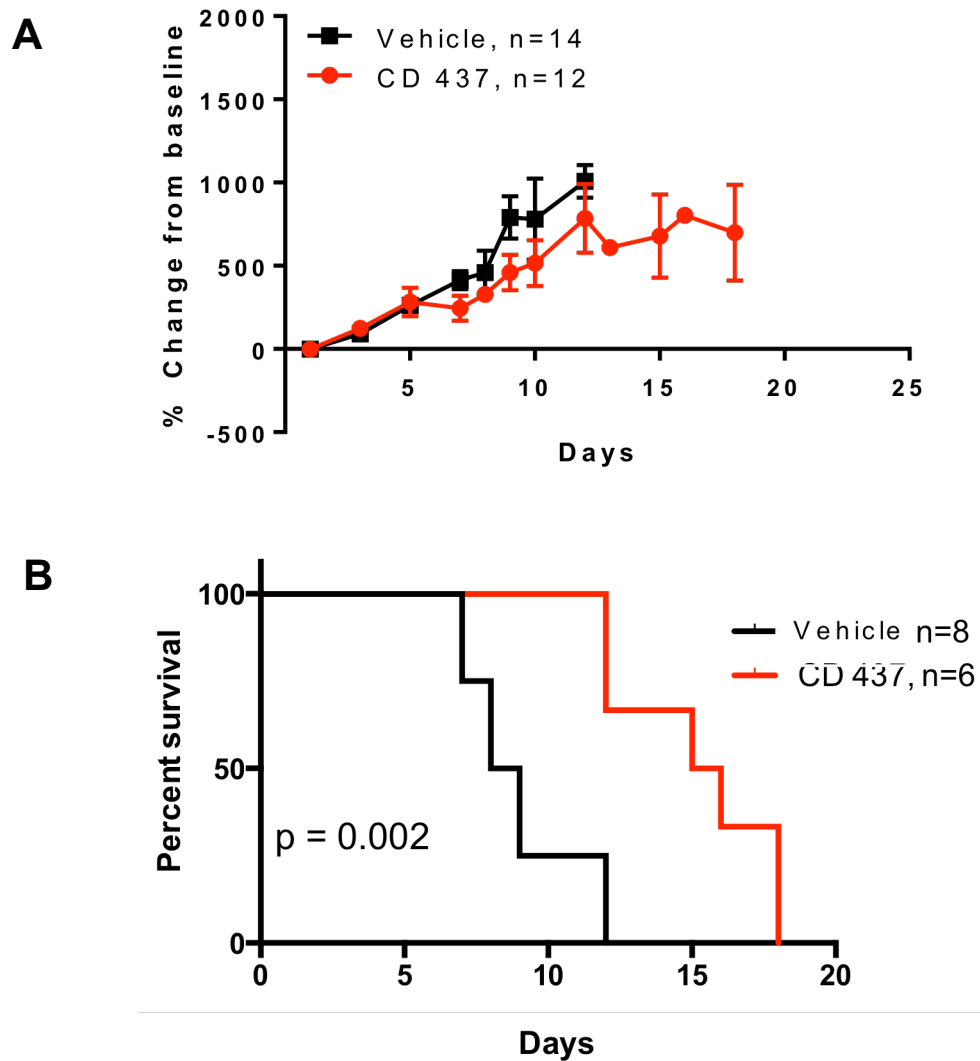


Figure 23. Tumor growth curve & survival of CD437-treated p53-sensitive tumors

(A) Mean \pm s.e.m of tumor growth curves plotted as percent change from baseline for CD437-treated syngeneic mice harboring tumors from $p53^{neo/R172H};R26^{CreER/tdT}$ mice sensitive to p53 restoration. (B) Kaplan Meier analysis of tumor size reaching 1500 mm³ as an endpoint for data shown in (A).

f

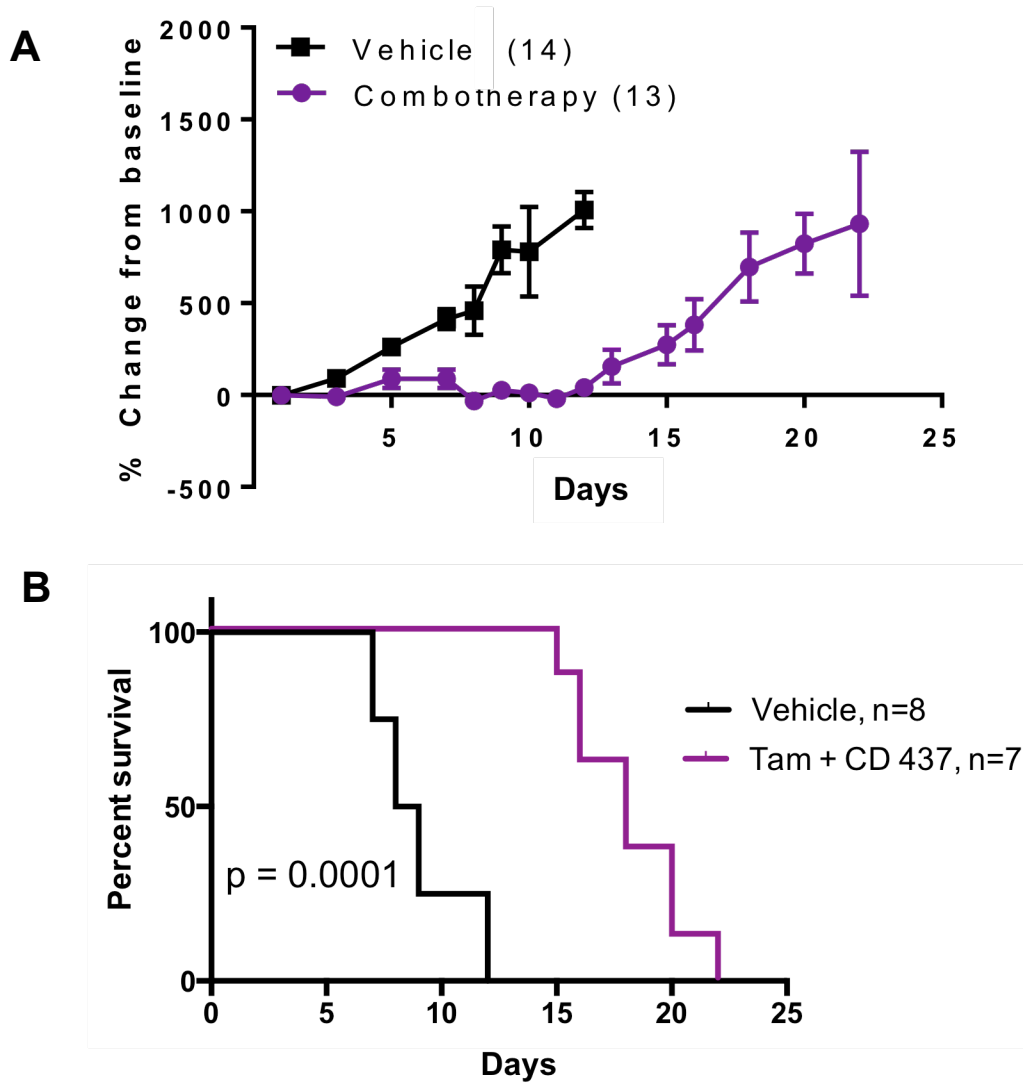


Figure 24. Tumor growth curve & survival o combo-treated p53-sensitive tumors

(A) Tumor growth curves plotted as mean \pm s.e.m. of percent change from baseline for tamoxifen-treated syngeneic mice harboring tumors from $p53^{neo/R172H};R26^{CreER/tdT}$ mice sensitive to p53 restoration. **(B)** Kaplan Meier analysis of tumor size reaching 1500 mm³ as an endpoint for data shown in (A).

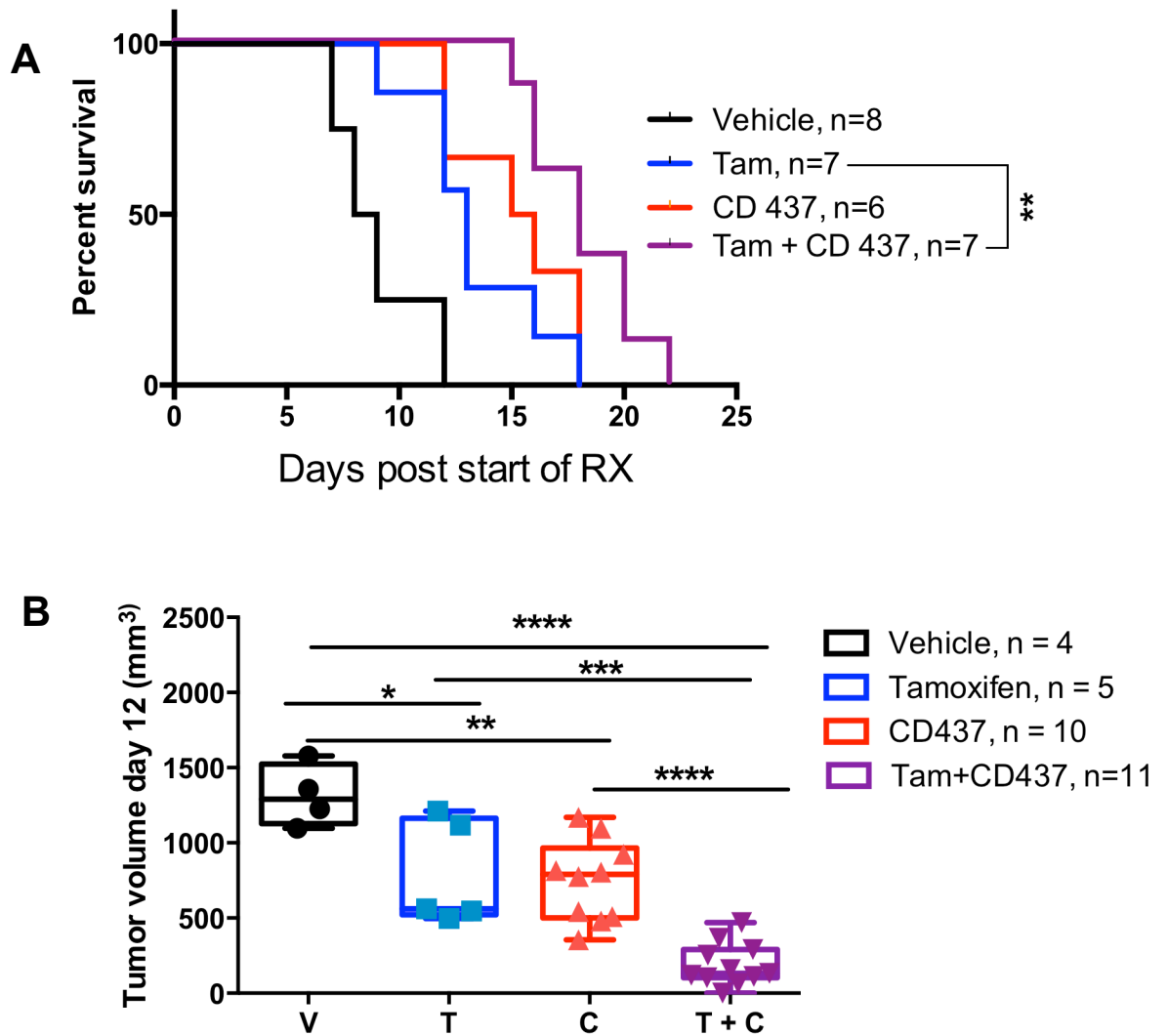


Figure 25: Treatment summary for p53-sensitive tumors

(A) Kaplan-Meier analyses for all treatment groups of mice with tumor size reaching 1500 mm³ at end-point. **(B)** Mean \pm s.e.m. of tumor size distribution (mm³) at day 12 of data shown in Figures 22-24. Data were analyzed by ANOVA with Bonferroni corrections for multiple comparisons. Levels of significance: *p < 0.05, **p < 0.01, ***p < 0.001, **** p < 0.0001.

Histological differences between p53- sensitive and resistant T-cell lymphomas

To better understand why two genetically identical thymic lymphomas carrying the same *p53* missense mutation could exhibit such striking differences in treatment responses, we compared the pathology of treatment-naïve syngeneic *p53^{neo/R172H};R26^{CreER/tdT}* lymphomas resistant or sensitive to p53 restoration by Hematoxylin & Eosin (H&E) staining. Histological analysis was done with the help of an expert human pathology, Dr. Adel El-Naggar. Together, we observed that p53-resistant lymphomas exhibited higher number of mitotic cells, indicative of proliferation, compared to the sensitive tumors (Figure 26, red arrows). Additionally, there was a marked difference in basal apoptosis as the number of apoptotic bodies per field of view was much higher in sensitive tumors compared to resistant tumors where the presence of apoptotic bodies was sparse (Figure 26, yellow arrows).

The observation that the proportion of mitotic vs apoptotic cells was much higher in p53-resistant tumors provides some insight as to why these tumors were inherently more difficult to treat. It is plausible that restoring p53 or CD437 treatment as a monotherapy was insufficient to shift the balance from proliferation to apoptosis. To further explore how combination therapy with CD437 sensitizes resistant tumors to p53 restoration, we evaluated the treatment-induced molecular and cellular changes in p53-resistant tumors.

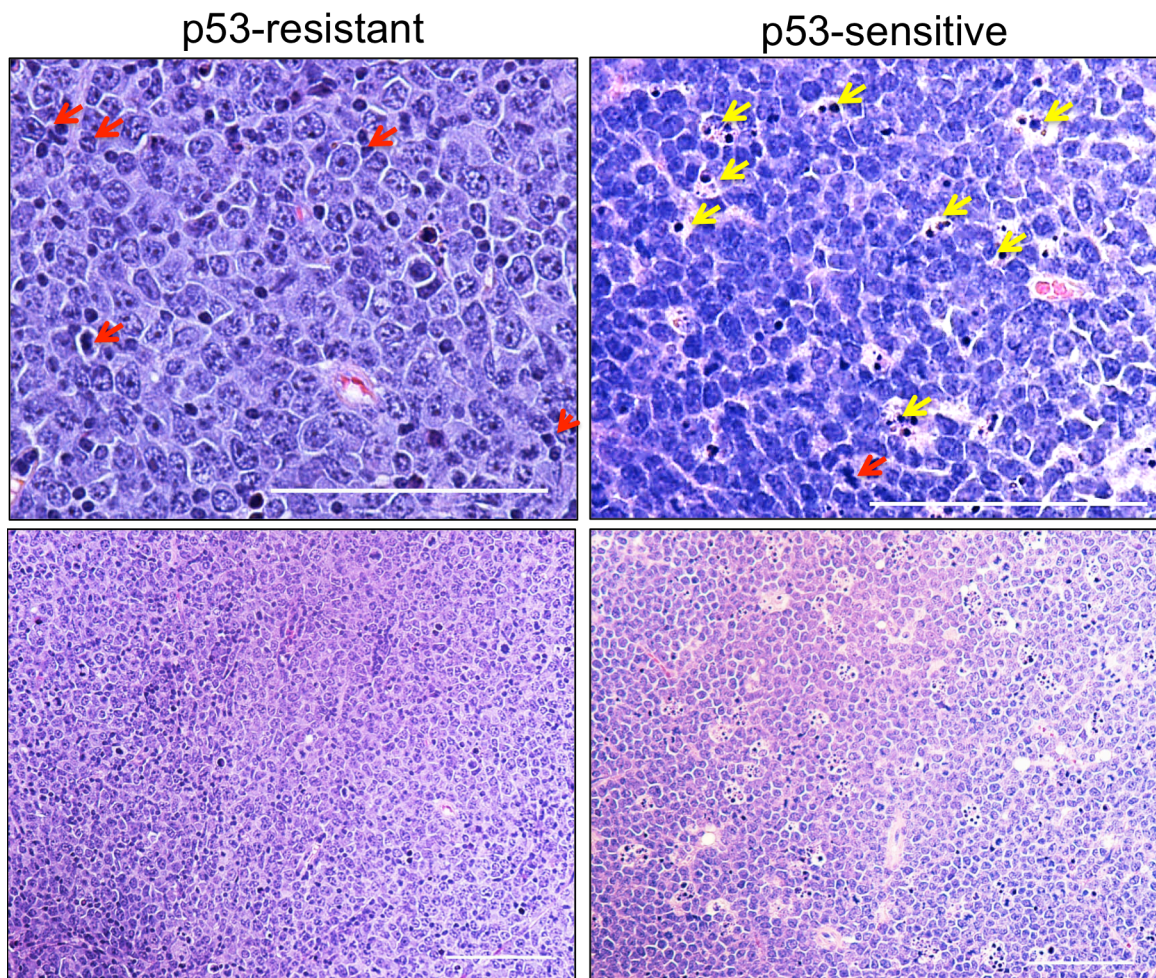


Figure 26. Histological differences between resistant and sensitive T-cell lymphomas

H&E staining of treatment-naïve $p53^{neo/R172H};R26^{CreER/tdT}$ syngeneic T-cell lymphomas reveal resistant tumors (left panels) exhibit more frequent mitotic cells (red arrows) with fewer apoptotic bodies (yellow arrows) per field of view compared to sensitive tumors (right panels). Lower panels are lower magnification of top panels. Scale bar: 100 μ M

CD437 in conjunction with tamoxifen potentiates the transcriptional activity of RAR γ and p53 in p53-resistant syngeneic tumors

Following the observation that CD437 treatment in conjunction with p53 restoration therapeutically improved response in p53-mutant tumors, we next evaluated the acute molecular and cellular changes in p53-resistant tumors to elucidate the mode of tumor regression. Syngeneic mice were administered a single dose of vehicle, tamoxifen, CD437, or tamoxifen + CD437 once tumors reached a minimum of 250 mm³ and tumors were harvested 24 – 48 hours post treatment (Figure 27A). We chose to harvest any tam-treated tumors at the 48 hour time point to allow for maximal recombination of the *p53^{neo}* allele and to ensure consistency, in the context of time, for evaluating tumors treated with tamoxifen as a single-agent approach or in combination with CD437. We performed qPCR analyses on p53-resistant syngeneic tumors to examine the transcriptional activity of p53 and RAR γ induced by tamoxifen and CD437, respectively. Single agent treatment with tamoxifen or CD437 had minimal effect at inducing the p53 targets, *Puma*, *p21*, *Bid*, and *CCng1* or the RAR target, *Cd38*, compared to controls. However, in combo-treated tumors, the level of *p21* is significantly higher ($p < 0.01$) compared to controls or single-agent treated tumors (Figure 27B). Indeed, the *p21* promoter contains an RA response element (RARE) and exposing cells to retinoic acid induces *p21* expression in various cancer cell lines without functional p53 (102, 103). Additionally, combo-treated tumors also exhibited significantly higher levels the p53 targets, *Ccng1* ($p < 0.001$), *Puma* ($p < 0.05$) and *Bid* ($p < 0.05$). Although not validated as RAR transcriptional targets, CD437 has been shown to induce pro-apoptotic-related proteins including BID and PUMA (104-107). The RAR target *Cd38*, a marker of differentiation and T-cell activation (108, 109), was the most significantly upregulated in combo-treated tumors ($p < 0.0001$).

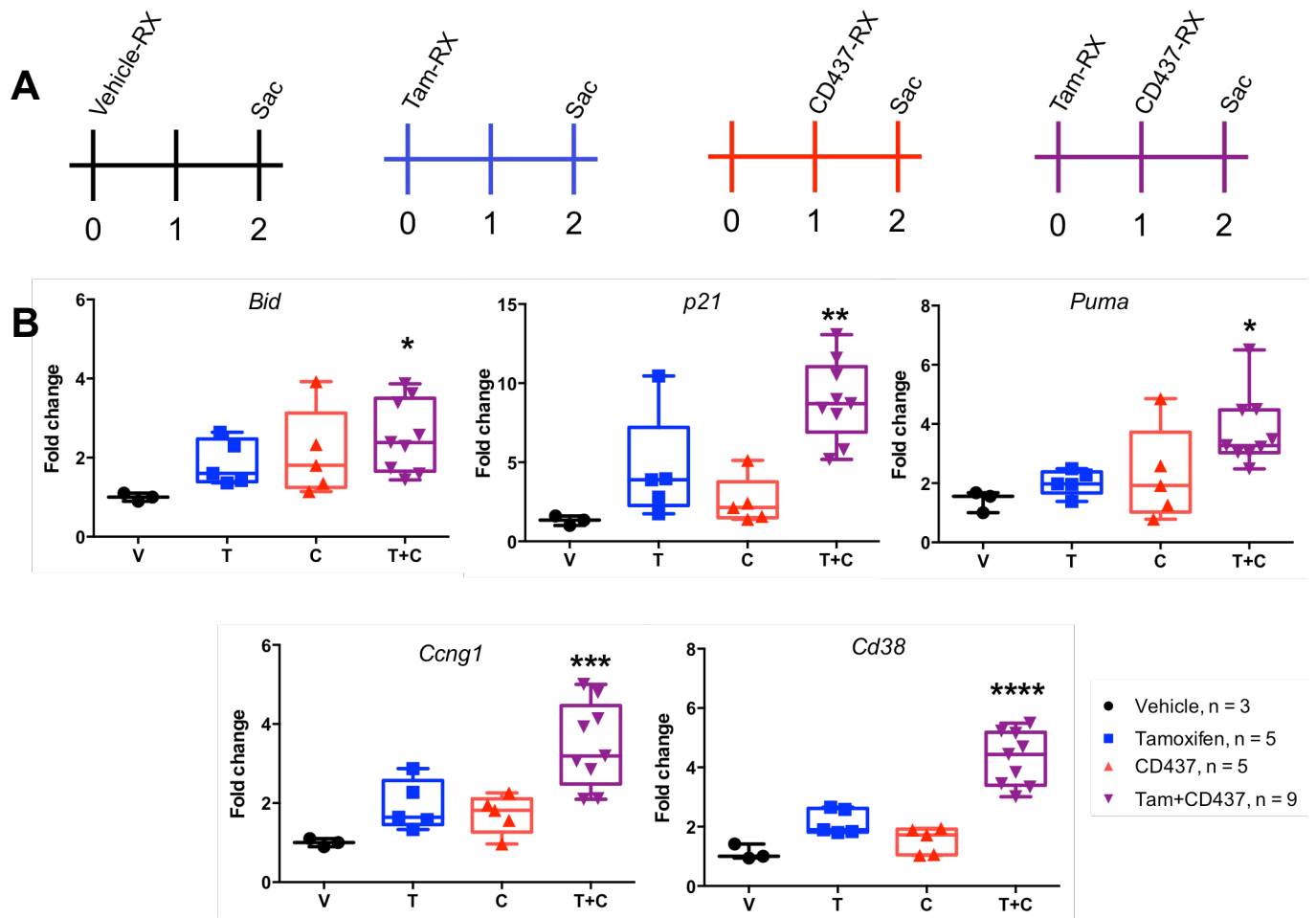


Figure 27. Activation of p53 and RAR target genes in treated syngeneic tumors

(A) Experimental timeline for evaluating the acute molecular changes in tumors induced by tamoxifen and CD437. Wild-type C57BL6/J syngeneic mice were injected with equivalent number (5×10^6) of tumor cells subcutaneously. Once tumors reached a minimum of 250 mm³ mice were administered a single dose of drug then sacrificed 24-48 hours post treatment. **(B)** qPCR analysis of target genes of p53 (*Bid*, *Puma*, *Ccng1* and *p21*) and RAR γ (*CD38*). Results are representative of biologically independent tumor samples treated with vehicle (V, n=3), tamoxifen (T, n=5), CD437 (C, n=5) or tam + CD437 (T+C, n=9) and plotted as fold change relative to vehicle, ANOVA test with Bonferroni's correction for multiple comparisons against vehicle. Levels of significance: *p < 0.05, **p < 0.01, ***p < 0.001, **** p < 0.0001

Combination therapy induces cell death in p53-resistant syngeneic tumors

To examine if up-regulation of pro-apoptotic genes on the mRNA level corresponded with increased cell death, we performed cleaved caspase-3 (CC3) immunohistochemical (IHC) staining, TUNEL assay, and Annexin-V flow cytometric analysis on treated p53-resistant syngeneic tumors. Again, equivalent number of tumors cells (5×10^6 per site) were injected into the right and left fat pads of syngeneic mice (two mice per treatment group) and administered a single dose of vehicle, tamoxifen, CD437, or tamoxifen + CD437 once tumors reached a minimum of 250 mm^3 and tumors were harvested 24 – 48 hours post treatment. Apoptosis was observably higher in combo-treated tumors, as indicated by CC3 and TUNEL positivity, compared to controls or single-agent treated tumors (Figure 28A). This was further substantiated by flow cytometric analysis where the number of Annexin V positive cells was significantly higher in combo-treated tumors compared to vehicle or single-agent treated tumors (Figure 28B). One CD437-treated tumor had to be excluded from the flow analyses due to insufficient number of tumor cells that could be analyzed ($< 2,000$ cells).

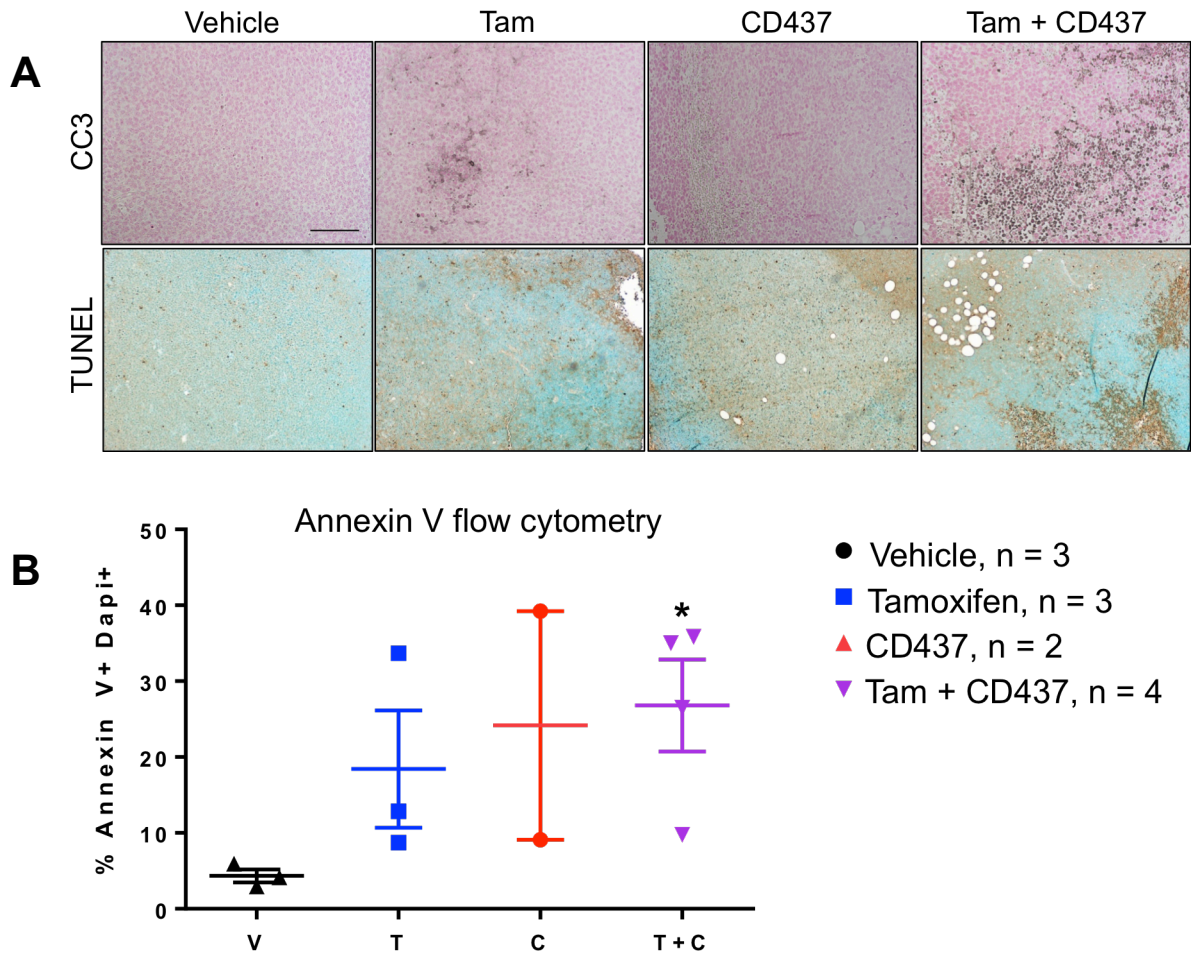


Figure 28. Evaluation of apoptosis in p53-resistant syngeneic tumors

Syngeneic mice were injected with equivalent numbers of p53-resistant tumor cells, then treated with one dose either vehicle, tamoxifen, CD437, or tamoxifen followed by CD437 and tumors were harvested 24-48 hours post treatment. **(A)** Histological analyses of IHC staining against cleaved caspase-3 (CC3) (top panels) and TUNEL (bottom panels). Scale bar: 100 μ M. **(B)** Flow cytometric analysis of single-cell gated Annexin V+/DAPI+ cells processed from biologically independent tumor samples treated with vehicle (V, n=3), tamoxifen (T, n=3), CD437 (C, n=2) or tam + CD437 (T+C, n=4), ANOVA test with Bonferroni's correction for multiple comparisons against vehicle. Level of significance: *p < 0.05

Treatment-induced histological and morphological changes in syngeneic tumors

Our observation that *Cd38* was significantly upregulated in combo-treated tumors prompted us to investigate whether this impacted the morphology or immunophenotype of tumor cells since CD38 is a marker of differentiation as well as T-cell activation (108). Tumors harvested from p53-resistant syngeneic mice 24-48 hours after a single dose of treatment revealed distinct histological changes in combo-treated tumors that were largely absent in vehicle or monotherapy-treated tumors (Figure 29). In accordance with the apoptosis assay performed, combo-treated tumors exhibited higher numbers of apoptotic bodies per field of view compared to vehicle or single-agent treated tumors (indicated by yellow arrows in Figure 29). Additionally, combo-treated tumors exhibited a higher density of smaller, round-shaped lymphocytes (diameter < 8 μ M), which are phenotypic characteristics of normal lymphocytes while lymphoma cells are larger (< 15 μ M diameter) and atypical in shape (Figure 29).

Examination of p53-sensitive lymphomas revealed single-agent treated tumors had an observable increase in the number of apoptotic bodies present per field of view (Figure 30). However, combo-treated tumors exhibited drastic histological changes characteristic of massive cell death compared to vehicle or single-agent treated tumors, further supporting data presented earlier indicating that combining CD437 with p53 restoration additively improves response in tumors inherently sensitive to p53 restoration.

p53-resistant syngeneic tumors

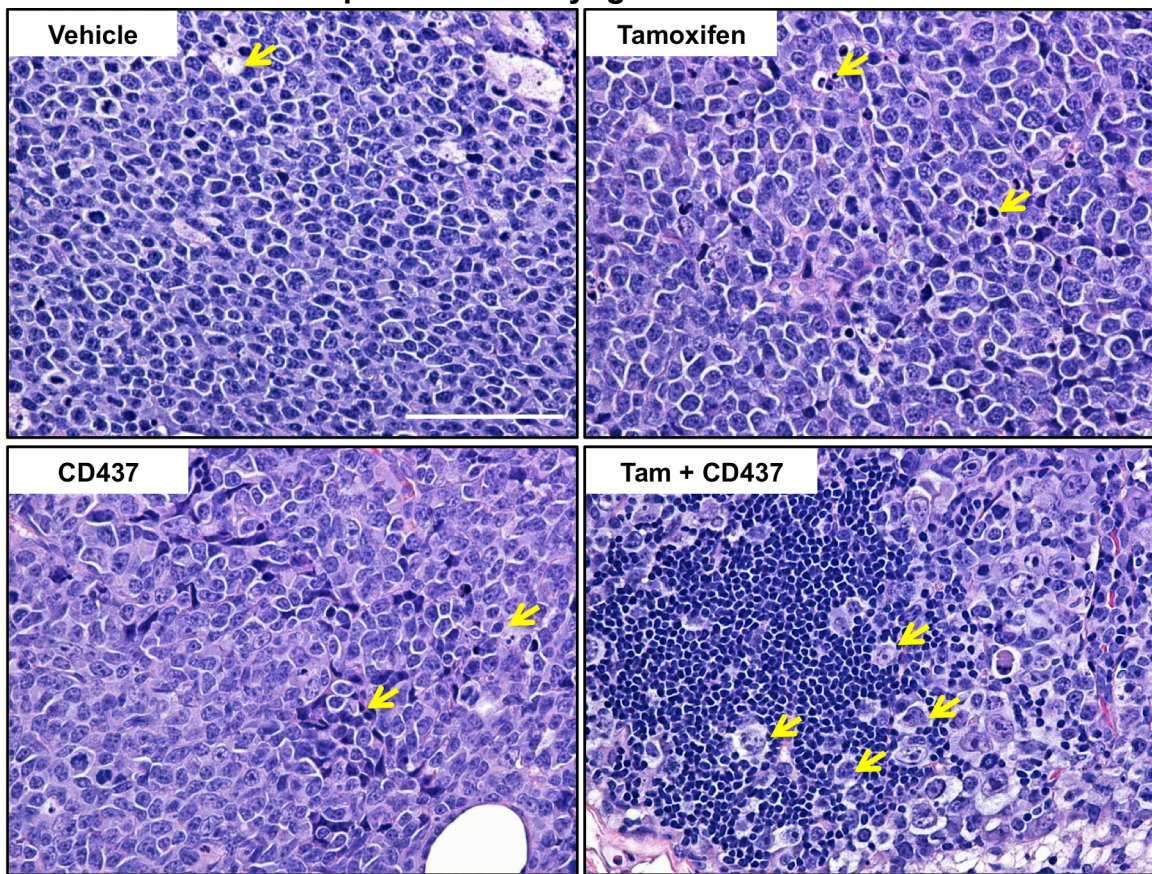


Figure 29. Histology of treated syngeneic resistant T-cell lymphomas

H&E staining of treated p53-resistant lymphomas demonstrating combo-treated tumors exhibit markedly different histological features such as increased apoptosis (yellow arrows) and a higher density of phenotypically normal lymphocytes, compared to vehicle control or single-agent treated tumors.

Scale bar: 100 μ M

p53-sensitive syngeneic tumors

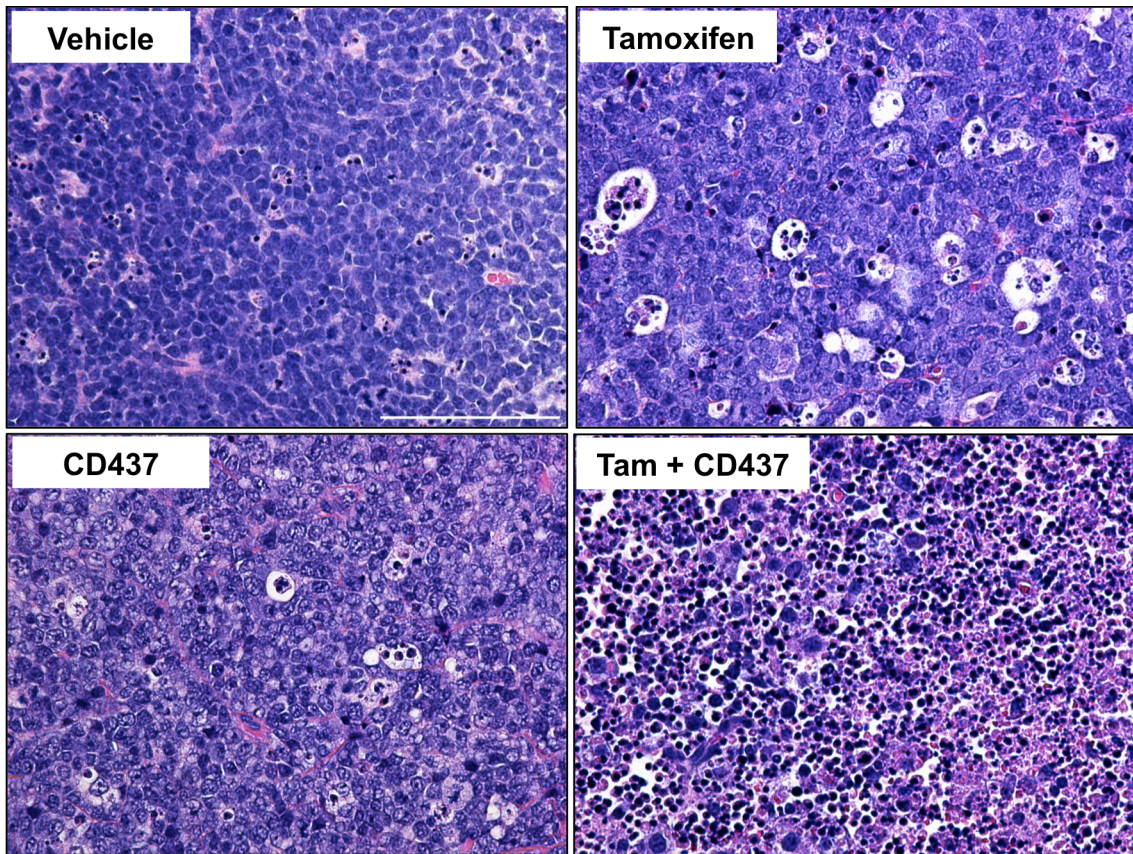


Figure 30. Histology of treated syngeneic sensitive T-cell lymphomas

H&E staining of treated p53-sensitive lymphomas. Combo-treated tumors exhibit histological features of massive cell death or necrosis. Monotherapy treated tumors showed increases in apoptotic bodies and with moderate morphological changes compared to vehicle tumors.

Scale bar: 100 μ M

Combination therapy induces immunophenotypic changes in syngeneic p53-sensitive lymphomas

Since the majority of thymic lymphomas from p53-mutant mice are characterized as being CD4+/CD8+ DP (110), we wanted to examine if treatments impacted the population of T-cells. We performed multicolor flow cytometric analyses with antibodies against CD4+ and CD8+ on syngeneic tumors harvested 24-48 hours after a single dose of treatment. To our surprise, the p53 resistant lymphoma line was not CD4+/CD8+ DP as anticipated (Figure 31A). However, immunofluorescence staining with an antibody against the T-cell marker, CD3, demonstrates that this tumor is a T-cell lymphoma (Figure 31B).

On the other hand, examination of the p53-sensitive line was more telling, as the majority of vehicle-treated tumor cells were double positive for both CD4+ and CD8+. Intriguingly, combo-treated tumors exhibited a significant reduction in the population of immature CD4+/CD8+ double positive (DP) T-cells that corresponded with increased levels of mature CD4+ or CD8+ single positive T-cells, whereas single-agent treatment had minimal impact on the T-cell population (Figure 32), suggesting a differentiation program may be contributing to tumor regression.

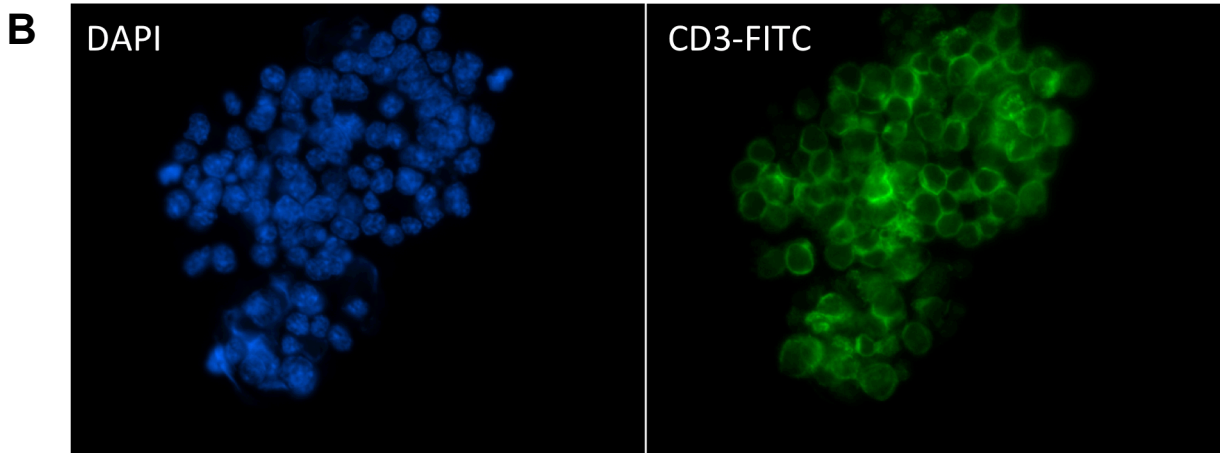
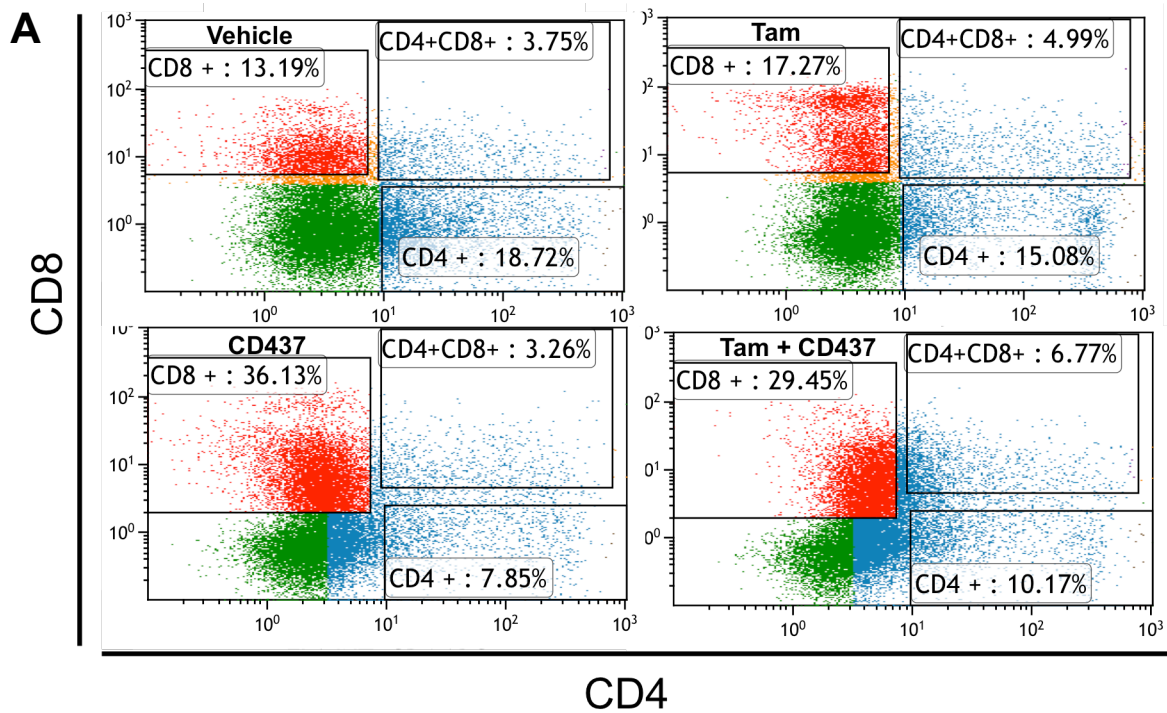


Figure 31. Immunophenotypic analyses of p53-resistant lymphomas

(A) Flow cytometry scatter plot for CD4+,CD8+, and CD4+/CD8+ cells on single-gated cells reveal p53-resistant lymphomas, both vehicle and treated, are not are not CD4+/CD8+ double positive. (B) Immunofluorescence staining of p53-resistant lymphoma cells with the CD3-FITC antibody.

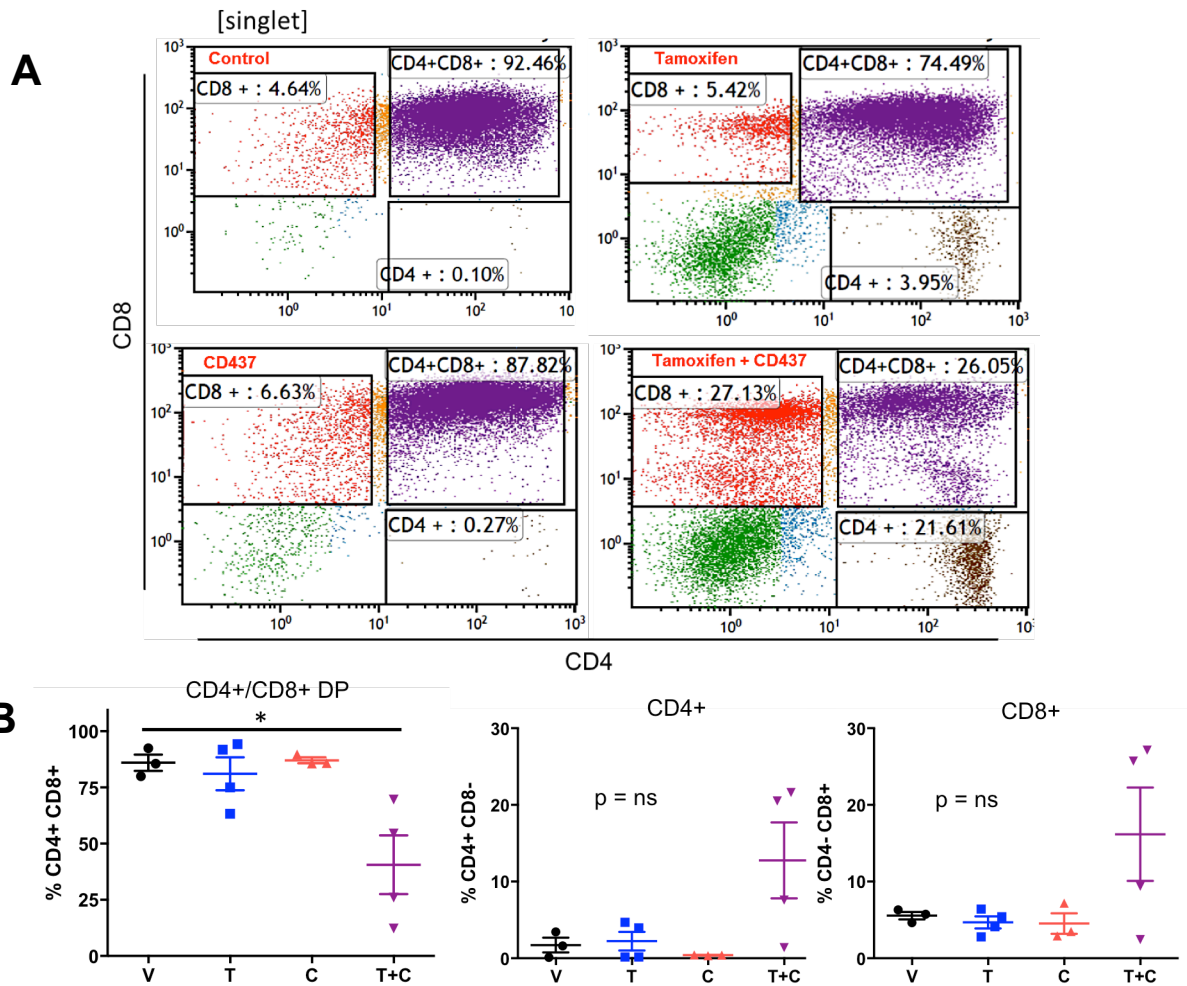


Figure 32. Combination therapy reduces the population of immature CD4+/CD8+ double positive T-cells in p53-sensitive syngeneic tumors

(A) Scatter plot for CD4+, CD8+, and CD4+/CD8+ double positive T-cells on single-gated cells. **(B)** Graphical representation of data from (A) of the population of CD4+/CD8+ double positive T-cells (top left), CD4+ (top right graph), and CD8+ (bottom graph) single-positive T-cells. Data are representative of biologically independent tumor samples treated with vehicle (V, n = 3), tamoxifen (T, n = 4), CD437 (C, n = 3) or tamoxifen plus CD437 (T+C, n = 4), ANOVA test with Bonferroni's correction for multiple comparisons against vehicle: *p < 0.05.

4.4 CONCLUSION

Using a syngeneic tumor transplant mode, I show that restoring p53 in combination the RAR γ -selective agonist, CD437, promoted a better response in T-cell lymphomas with a *p53*^{R172} missense mutation. Combination therapy sensitized treatment-resistant tumors by significantly inducing cell death. Interestingly, combination therapy also additively improved response in T-cell lymphomas inherently sensitive to p53 restoration.

Histological analyses of treatment-naïve tumors revealed that the resistant lymphomas were highly aggressive and proliferative compared to sensitive lymphomas. Additionally, basal apoptosis was comparatively higher in sensitive tumors whereas apoptotic bodies were infrequent and sparse in resistant tumors. This may explain why this tumor line was more resistant to single-agent treatments. It is plausible that restoring p53 or CD437 treatment as a monotherapy was insufficient to induce the level of cellular death programs needed to promote tumor regression, but the combination of the two therapies shifted the balance from a proliferative state towards a dying state in tumor cells.

CHAPTER 5

DISCUSSION

Summary

Using a genetic approach, I show that restoring wild-type p53 in a p53-mutant background has therapeutic potential as it significantly prolonged survival, but due to the heterogeneous nature in response, will unlikely be effective as a monotherapy. To better understand these differences, we performed RNA-sequencing on treated tumors to comprehensively characterize the gene expression profile and molecular networks impacting response to p53 restoration in tumors with a *p53^{R172H}* missense mutation. Gene expression profiling of treated autochthonous T-cell lymphomas suggested a critical role for the TNF pathway in promoting response, as it was upregulated in tumors sensitive to p53 restoration. Further, I identified retinoic acid receptor gamma (RAR γ), an effector in the TNF pathway, as an actionable target. Both TNF and RAR γ play critical roles in the regulation of immune cells and T-cell homeostasis (98, 108, 111). Further, TNF signaling aberrations are implicated in variety of human cancers while loss of RAR γ leads to the development of myeloproliferative syndromes in mice (112).

To investigate if pharmacologically activating RAR γ in conjunction with p53 restoration would improve response in T-cell lymphomas, I performed combination therapy drug studies using a RAR γ -selective retinoid (CD437) in a syngeneic tumor transplant model. In tumors that were resistant to p53 restoration as a monotherapy, I show that combination therapy with CD437 sensitized T-cell lymphomas that were resistant to p53 restoration as a monotherapy. Overall, a combination of p53 restoration (via tamoxifen injections) and CD437 resulted in significant tumor regression with a significant increase in survival compared to mice in the vehicle or monotherapy treatment groups. I provide compelling evidence that RAR γ cooperates with p53 in circumventing resistance in p53-resistant lymphomas significantly by activating pro-apoptotic genes that corresponded a significant induction in apoptosis. In contrast, p53 restoration or CD437 as a monotherapy was insufficient to induce the expression

of p53 or RAR γ target genes and exerted minimal cytotoxic effects. One explanation for this is that CD437 has been shown to increase p53 protein levels that corresponded with increased expression of pro-apoptotic and cell cycle arrest genes in non-small cell lung carcinoma (NSCLC) cell lines with wild-type, but not mutant p53 (105, 107). Moreover, additional studies demonstrate that CD437 promotes both p53-dependent and independent cell death via activation of extrinsic and intrinsic apoptotic pathways (107, 113). Since we observed that this resistant T-cell lymphoma exhibited histological features characteristic of an aggressive tumor (i.e. abundant mitosis with low basal apoptosis), it is plausible that restoring p53 or CD437 as a monotherapy was insufficient at inducing the level of cellular death programs to shift the cell from a proliferative state into a dying state.

We show that sensitive T-cell lymphomas had basally higher levels of apoptosis while resistant T-cell lymphomas were inherently more proliferative and aggressive. Indeed, when we examined the effects of different treatments, sensitive tumors showed a favorable response to both p53 restoration and CD437 as a monotherapy and combining the two therapies additively improved response and survival in mice. We also show that combination therapy in sensitive T-cell lymphomas impacted the population of T-cells by significantly reducing the number of immature T-cells. Interestingly, single-agent treatment had exerted minimal changes on the T-cell population compared to vehicle mice, suggesting a differentiation program may be contributing to the enhanced response.

Clinical implications

Since the p53 pathway is impaired or attenuated in the majority of human tumors, restoring the pathway has become an attractive treatment approach. Several strategies to reactivate the p53 pathway have been evaluated in various cancer models, such as inhibiting the negative regulation of MDM2 and/or MDM4, depleting mutant p53 protein, and restoring wild-type p53 function, to name a few. Moreover, the development of p53 pathway activating agents has become a rapidly evolving field in cancer therapeutics research (114).

For example, the nutlin derivative RG7112 has already progressed from pre-clinical testing and into clinical trials (87, 88). Results from early phase clinical trials in patients with liposarcoma or hematological malignancies revealed RG7112 treatment leads to p53 activation, with some patients achieving a complete response. However, all patients experienced at least one adverse event, while a large proportion exhibited severe adverse events, primarily renal, hematological and gastrointestinal toxicities. This is not surprising considering that excessive p53 activity can have dire cellular consequences. For example, homozygous deletion of either *Mdm2* or *Mdm4* from the germline leads to embryonic lethality in mice, which can be rescued by concomitantly deleting both p53 alleles (42, 43). Moreover, unrestricted p53 activity has deleterious effects in fully developed radio-sensitive and insensitive tissues. Using a conditional *Mdm2* allele, our lab has showed that global loss of *Mdm2* in adult mice leads to a multitude of pathological defects, resulting in lethality (37). Aside from the deleterious effects of excessive p53 activity, Mdm2 inhibitors would, in principle, be effective only for tumors that retain wild-type p53 and about 50% of tumors harbor inactivating p53 mutations. Therefore, an attractive surrogate for reactivating the p53 pathway is to restore wild-type p53 function.

Initially, it was long-held though that p53 would be undruggable since it is a transcription factor (TF). Since the majority of TFs, with the exception of nuclear hormone

receptors, do not have substrates or small molecule regulators, they are inherently more difficult proteins to target in comparison to kinases or cell surface receptors. In addition, since TFs are nuclear proteins this precludes them from antibody-based therapies whereas cytosolic or membrane bound proteins are more accessible to an array of compounds and antibodies (115). However, the use of high-throughput chemical compound and drug screens to identify the agents that could suppress growth in p53-mutant cell lines led to the identification of several compounds that could restore p53 function (114).

Mutant-p53 reactivators have been of particular interest due to the fact that many tumors exhibit high levels of stabilized mutant p53 proteins. Among the different types of mutant p53 reactivators, the most widely studied is a compound called APR-246 (2-(hydroxymethyl)-2-(methoxymethyl)quinuclidin-3-one), which targets and refolds mutant p53 proteins to its wild-type conformation, thus restoring DNA binding capabilities (86) . Notably, APR-246 has already been tested in a phase I/IIa clinical trial in patients with hormone-refractory prostate cancer or hematological malignancies (91). In contrast to the phase I/IIa clinical trial with the Mdm2 inhibitor RG7112, results this clinical trial reported that APR-246 treatment was well tolerated with minimal adverse side effects. Since this clinical trial only addressed the safety and dosage of APR-246 treatment, an important unknown is which p53-mutant tumors and cells, in particular, will respond favorably to p53 restoration therapy. However, as with most anticancer therapies it is anticipated that a proportion of tumors will be resistant. Therefore, identifying the mediators of response or resistance mechanisms will provide a better understanding of who would benefit from p53-based therapies and provide a framework for identifying rational drug combinations to potentiate the tumor suppressive effects of p53 restoration.

Advantages of our model

In our model, mice spontaneously develop tumors over time as they would in patients with Li Fraumeni Syndrome have germline *p53* missense mutations and heterogeneous response provided an ideal system to model what might be observed in a clinical setting. Additionally, since the majority of human tumors (~75%) acquire *p53* missense mutations as opposed to truncating or deletion-type mutations, we believe the genetic model used here is more relevant compared to previous mouse models where p53 was genetically restored in a p53-null background, (75-77). It is important to note this distinction because mutant p53 has acquired GOF that often promotes drug resistance and mutant p53 protein also exerts transdominant repressive effects on its WT counterpart to prevent DNA binding as an additional measure to inhibit its transcriptional activity (18, 19).

Considering the mice used in the present were genetically identical and the level of p53 that was restored was equivalent in all tumor samples (approximately 25%), it was surprising that response to p53 restoration was strikingly divergent, even between mice with the same type of tumor type. However, this provided us with the ideal system to effectively evaluate the molecular changes defining response to p53 restoration therapy. Assuming that mutant p53 reactivating agents are unlikely to be 100% efficient *in vivo* (i.e. binding and restoring 100% of mutant p53 proteins to WT conformation), the level of p53 restoration that was induced in our genetic model from one *p53* allele may be more physiologically representative to what may be observed in a clinical setting. Further, since we genetically restored p53 we were able to avoid any off-target effects associated with pharmacological p53 restoration using mutant p53 reactivators. For example, APR-246 has been shown to have off-target effects such as binding and activating the p53 family members, p63 and p73. In addition, other groups previously described p53-independent cytotoxic activities exerted by APR-246 in various cancer cell lines with wild-type p53 or have p53 deletions (116, 117). Additionally, by using a syngeneic model for the combination therapy experiments we were able to evaluate the effects of different

treatments within a single tumor type in a more controlled environment to mitigate experimental artifacts that could lead to inconclusive or inaccurate interpretations of results. Another advantage of using a syngeneic tumor model is that we were able to maintain a normal wild-type stroma and immune compartment.

Significance

To our knowledge, this is the first time the global gene expression profile of p53-mutant tumors was used as a method to understand the molecular basis driving sensitivity to p53 restoration. Based on our findings and the supporting results of the validation experiments designed to test our hypothesis, we feel the approach used here can be applied to multiple p53-mutant cancer types as a method to identify the critical pathways impacting response p53-restoration therapy while providing the capability of identifying novel drug combination to circumvent resistance or enhance therapeutic response,

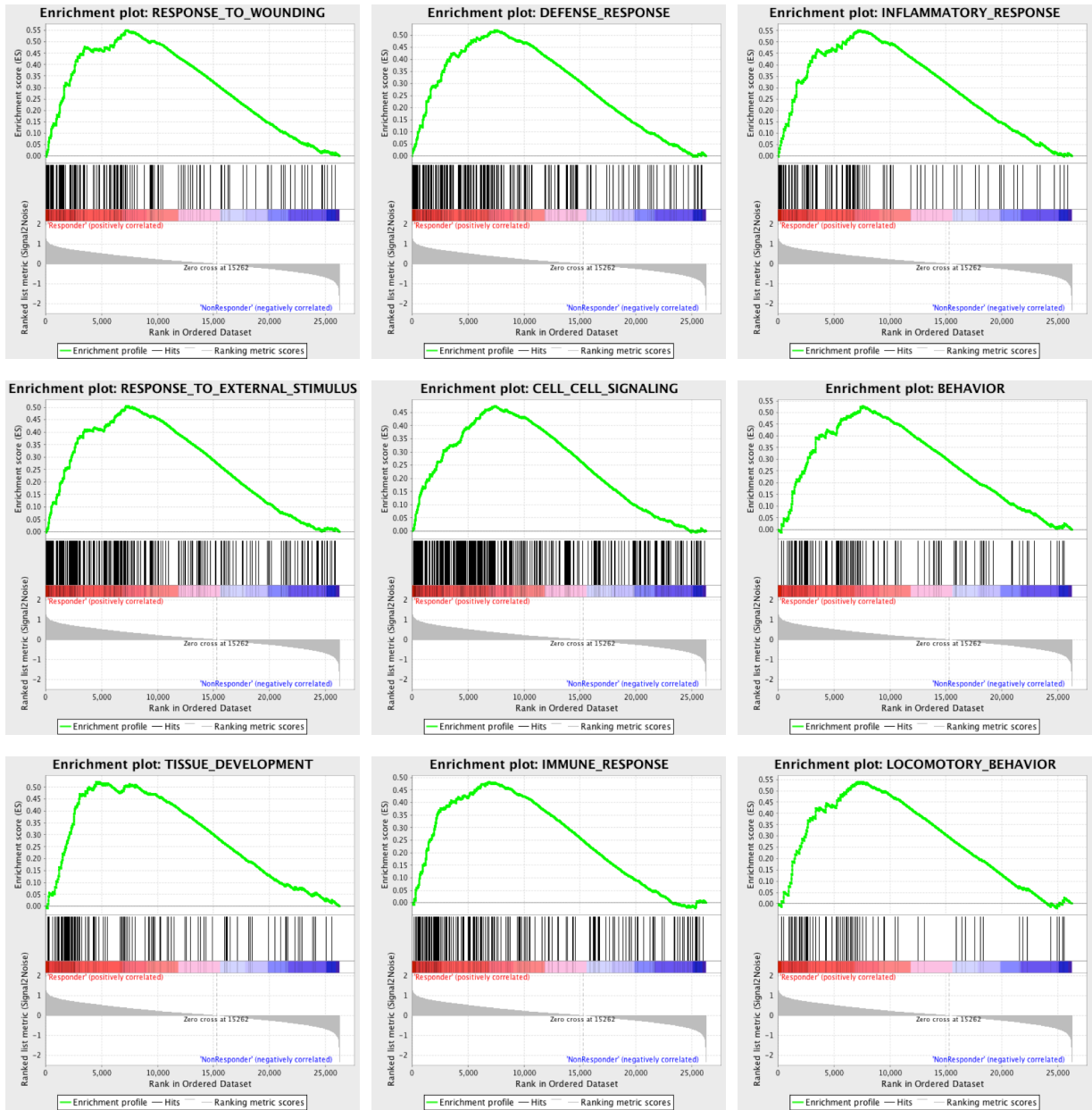
Additionally, the recent advancement in the era of genomics has allowed the utilization of high-throughput next generation sequencing (NGS) approaches to become very affordable, thus feasible for researchers worldwide. Resultantly, NGS approaches, such as whole genome or exome sequencing, is frequently and widely used as a tool to better understand the etiology of a spectrum of human diseases, including cancer. In addition to identifying mutations that are causally implicated in tumorigenesis, called driver mutations, NGS is frequently utilized as a tool for defining molecular signatures contributing to a phenotype. For example, RNA-sequencing is often used to characterize the molecular profile or gene expression signatures mediating response to a certain treatment or for determining who may benefit from a certain therapy. Among the multiple utilities for NGS approaches, one of the most propitious is to identify novel or alternative therapeutic targets in tumors that are resistant to standard frontline treatments, such as radio- and chemotherapy.

Future direction

Further work is needed to delineate the mechanism by which p53 and RAR γ cooperate in mediating tumor suppression. Additionally, a limitation to my study is that bulk tumors were sequenced, so it remains unknown which cell-types were responsive or resistant to p53 and merits further investigation. However, the groundbreaking development of single-cell sequencing has illuminated the complexity and heterogeneity that exists within a tumor, often referred to as intratumor heterogeneity. Moreover, the use of single cell sequencing on different tumor cell populations and metastatic sites has furnished important clues into the evolution of malignant clones and their roles in drug resistance, invasion & metastasis (118-120). Since I observed that CD437 treatment sensitized T-cell lymphomas to p53 restoration, whereas monotherapy exerted minimal cytotoxic effects, identifying the specific cell-type or clones that responded to combination therapy may provide insight into the mechanisms of resistance or how co-activating p53 and RAR γ promotes a synergistic-type effect at inducing cell death. Therefore, performing single-cell sequencing on these tumors may be warranted in the future.

Noteworthy, this drug combination may exert the same anticancer activities in other non-lymphoid cancers, particularly ovarian carcinomas, since they almost universally carry p53 mutations (63). Ancillary to this is that CD437 has been shown to have growth inhibitory effects in p53-mutant, chemo-resistant ovarian carcinoma cell lines, providing a strong rationale for evaluating this drug combination in this tumor type (104, 106, 121)

APPENDIX



Appendix A. Snapshot of RNA- sequencing gene set enrichment analyses of the top 9 most significant gene sets with a nominal p- value < 1% and nominal enrichment score > 2.10.

BIBLIOGRAPHY

1. Lane DP, Crawford LV. T antigen is bound to a host protein in SV40-transformed cells. *Nature*. 1979;278(5701):261-3. PubMed PMID: 218111.
2. Linzer DI, Levine AJ. Characterization of a 54K dalton cellular SV40 tumor antigen present in SV40-transformed cells and uninfected embryonal carcinoma cells. *Cell*. 1979;17(1):43-52. PubMed PMID: 222475.
3. Sarnow P, Ho YS, Williams J, Levine AJ. Adenovirus E1b-58kd tumor antigen and SV40 large tumor antigen are physically associated with the same 54 kd cellular protein in transformed cells. *Cell*. 1982;28(2):387-94. PubMed PMID: 6277513.
4. Oren M, Maltzman W, Levine AJ. Post-translational regulation of the 54K cellular tumor antigen in normal and transformed cells. *Mol Cell Biol*. 1981;1(2):101-10. PubMed PMID: 6100960; PMCID: PMC369648.
5. Ben David Y, Prideaux VR, Chow V, Benchimol S, Bernstein A. Inactivation of the p53 oncogene by internal deletion or retroviral integration in erythroleukemic cell lines induced by Friend leukemia virus. *Oncogene*. 1988;3(2):179-85. PubMed PMID: 2842714.
6. Chow V, Ben-David Y, Bernstein A, Benchimol S, Mowat M. Multistage Friend erythroleukemia: independent origin of tumor clones with normal or rearranged p53 cellular oncogenes. *J Virol*. 1987;61(9):2777-81. PubMed PMID: 3302314; PMCID: PMC255786.
7. Mowat M, Cheng A, Kimura N, Bernstein A, Benchimol S. Rearrangements of the cellular p53 gene in erythroleukaemic cells transformed by Friend virus. *Nature*. 1985;314(6012):633-6. PubMed PMID: 3990796.

8. Eliyahu D, Michalovitz D, Eliyahu S, Pinhasi-Kimhi O, Oren M. Wild-type p53 can inhibit oncogene-mediated focus formation. *Proc Natl Acad Sci U S A*. 1989;86(22):8763-7. PubMed PMID: 2530586; PMCID: PMC298370.
9. Finlay CA, Hinds PW, Levine AJ. The p53 proto-oncogene can act as a suppressor of transformation. *Cell*. 1989;57(7):1083-93. PubMed PMID: 2525423.
10. Kenzelmann Broz D, Spano Mello S, Biegging KT, Jiang D, Dusek RL, Brady CA, Sidow A, Attardi LD. Global genomic profiling reveals an extensive p53-regulated autophagy program contributing to key p53 responses. *Genes Dev*. 2013;27(9):1016-31. doi: 10.1101/gad.212282.112. PubMed PMID: 23651856; PMCID: PMC3656320.
11. Riley T, Sontag E, Chen P, Levine A. Transcriptional control of human p53-regulated genes. *Nat Rev Mol Cell Biol*. 2008;9(5):402-12. doi: 10.1038/nrm2395. PubMed PMID: 18431400.
12. Baker SJ, Markowitz S, Fearon ER, Willson JK, Vogelstein B. Suppression of human colorectal carcinoma cell growth by wild-type p53. *Science*. 1990;249(4971):912-5. PubMed PMID: 2144057.
13. Chen PL, Chen YM, Bookstein R, Lee WH. Genetic mechanisms of tumor suppression by the human p53 gene. *Science*. 1990;250(4987):1576-80. PubMed PMID: 2274789.
14. Liu G, Parant JM, Lang G, Chau P, Chavez-Reyes A, El-Naggar AK, Multani A, Chang S, Lozano G. Chromosome stability, in the absence of apoptosis, is critical for suppression of tumorigenesis in Trp53 mutant mice. *Nat Genet*. 2004;36(1):63-8. doi: 10.1038/ng1282. PubMed PMID: 14702042.

15. Kastan MB, Onyekwere O, Sidransky D, Vogelstein B, Craig RW. Participation of p53 protein in the cellular response to DNA damage. *Cancer Res.* 1991;51(23 Pt 1):6304-11. PubMed PMID: 1933891.
16. Lu X, Lane DP. Differential induction of transcriptionally active p53 following UV or ionizing radiation: defects in chromosome instability syndromes? *Cell.* 1993;75(4):765-78. PubMed PMID: 8242748.
17. Horn HF, Vousden KH. Coping with stress: multiple ways to activate p53. *Oncogene.* 2007;26(9):1306-16. doi: 10.1038/sj.onc.1210263. PubMed PMID: 17322916.
18. Lang GA, Iwakuma T, Suh YA, Liu G, Rao VA, Parant JM, Valentin-Vega YA, Terzian T, Caldwell LC, Strong LC, El-Naggar AK, Lozano G. Gain of function of a p53 hot spot mutation in a mouse model of Li-Fraumeni syndrome. *Cell.* 2004;119(6):861-72. doi: 10.1016/j.cell.2004.11.006. PubMed PMID: 15607981.
19. Olive KP, Tuveson DA, Ruhe ZC, Yin B, Willis NA, Bronson RT, Crowley D, Jacks T. Mutant p53 gain of function in two mouse models of Li-Fraumeni syndrome. *Cell.* 2004;119(6):847-60. doi: 10.1016/j.cell.2004.11.004. PubMed PMID: 15607980.
20. Zerdoumi Y, Aury-Landas J, Bonaiti-Pellie C, Derambure C, Sesboue R, Renaux-Petel M, Frebourg T, Bougeard G, Flaman JM. Drastic effect of germline TP53 missense mutations in Li-Fraumeni patients. *Hum Mutat.* 2013;34(3):453-61. doi: 10.1002/humu.22254. PubMed PMID: 23172776.
21. Nakano K, Vousden KH. PUMA, a novel proapoptotic gene, is induced by p53. *Mol Cell.* 2001;7(3):683-94. PubMed PMID: 11463392.
22. Miyashita T, Reed JC. Tumor suppressor p53 is a direct transcriptional activator of the human bax gene. *Cell.* 1995;80(2):293-9. PubMed PMID: 7834749.

23. Oda E, Ohki R, Murasawa H, Nemoto J, Shibue T, Yamashita T, Tokino T, Taniguchi T, Tanaka N. Noxa, a BH3-only member of the Bcl-2 family and candidate mediator of p53-induced apoptosis. *Science*. 2000;288(5468):1053-8. PubMed PMID: 10807576.
24. Attardi LD, Reczek EE, Cosmas C, Demicco EG, McCurrach ME, Lowe SW, Jacks T. PERP, an apoptosis-associated target of p53, is a novel member of the PMP-22/gas3 family. *Genes Dev*. 2000;14(6):704-18. PubMed PMID: 10733530; PMCID: PMC316461.
25. Oda K, Arakawa H, Tanaka T, Matsuda K, Tanikawa C, Mori T, Nishimori H, Tamai K, Tokino T, Nakamura Y, Taya Y. p53AIP1, a potential mediator of p53-dependent apoptosis, and its regulation by Ser-46-phosphorylated p53. *Cell*. 2000;102(6):849-62. PubMed PMID: 11030628.
26. el-Deiry WS, Tokino T, Velculescu VE, Levy DB, Parsons R, Trent JM, Lin D, Mercer WE, Kinzler KW, Vogelstein B. WAF1, a potential mediator of p53 tumor suppression. *Cell*. 1993;75(4):817-25. PubMed PMID: 8242752.
27. Zhao L, Samuels T, Winckler S, Korgaonkar C, Tompkins V, Horne MC, Quelle DE. Cyclin G1 has growth inhibitory activity linked to the ARF-Mdm2-p53 and pRb tumor suppressor pathways. *Mol Cancer Res*. 2003;1(3):195-206. PubMed PMID: 12556559.
28. Kastan MB, Zhan Q, el-Deiry WS, Carrier F, Jacks T, Walsh WV, Plunkett BS, Vogelstein B, Fornace AJ, Jr. A mammalian cell cycle checkpoint pathway utilizing p53 and GADD45 is defective in ataxia-telangiectasia. *Cell*. 1992;71(4):587-97. PubMed PMID: 1423616.
29. Floter J, Kaymak I, Schulze A. Regulation of Metabolic Activity by p53. *Metabolites*. 2017;7(2). doi: 10.3390/metabo7020021. PubMed PMID: 28531108; PMCID: PMC5487992.

30. Galluzzi L, Bravo-San Pedro JM, Kroemer G. Ferroptosis in p53-dependent oncosuppression and organismal homeostasis. *Cell Death Differ.* 2015;22(8):1237-8. doi: 10.1038/cdd.2015.54. PubMed PMID: 26143748; PMCID: PMC4495364.
31. Jiang L, Kon N, Li T, Wang SJ, Su T, Hibshoosh H, Baer R, Gu W. Ferroptosis as a p53-mediated activity during tumour suppression. *Nature.* 2015;520(7545):57-62. doi: 10.1038/nature14344. PubMed PMID: 25799988; PMCID: PMC4455927.
32. Laptenko O, Prives C. Transcriptional regulation by p53: one protein, many possibilities. *Cell Death Differ.* 2006;13(6):951-61. doi: 10.1038/sj.cdd.4401916. PubMed PMID: 16575405.
33. Petitjean A, Achatz MI, Borresen-Dale AL, Hainaut P, Olivier M. TP53 mutations in human cancers: functional selection and impact on cancer prognosis and outcomes. *Oncogene.* 2007;26(15):2157-65. doi: 10.1038/sj.onc.1210302. PubMed PMID: 17401424.
34. Petitjean A, Mathe E, Kato S, Ishioka C, Tavtigian SV, Hainaut P, Olivier M. Impact of mutant p53 functional properties on TP53 mutation patterns and tumor phenotype: lessons from recent developments in the IARC TP53 database. *Hum Mutat.* 2007;28(6):622-9. doi: 10.1002/humu.20495. PubMed PMID: 17311302.
35. Freed-Pastor WA, Prives C. Mutant p53: one name, many proteins. *Genes Dev.* 2012;26(12):1268-86. doi: 10.1101/gad.190678.112. PubMed PMID: 22713868; PMCID: PMC3387655.
36. Donehower LA, Harvey M, Slagle BL, McArthur MJ, Montgomery CA, Jr., Butel JS, Bradley A. Mice deficient for p53 are developmentally normal but susceptible to spontaneous tumours. *Nature.* 1992;356(6366):215-21. doi: 10.1038/356215a0. PubMed PMID: 1552940.

37. Zhang Y, Xiong S, Li Q, Hu S, Tashakori M, Van Pelt C, You MJ, Pajeon L, Lozano G. Tissue-specific and age-dependent effects of global Mdm2 loss. *J Pathol.* 2014;233(4):380-91. doi: 10.1002/path.4368. PubMed PMID: 24789767; PMCID: PMC4151977.
38. Itahana K, Mao H, Jin A, Itahana Y, Clegg HV, Lindstrom MS, Bhat KP, Godfrey VL, Evan GI, Zhang Y. Targeted inactivation of Mdm2 RING finger E3 ubiquitin ligase activity in the mouse reveals mechanistic insights into p53 regulation. *Cancer Cell.* 2007;12(4):355-66. doi: 10.1016/j.ccr.2007.09.007. PubMed PMID: 17936560.
39. Meek DW, Anderson CW. Posttranslational modification of p53: cooperative integrators of function. *Cold Spring Harb Perspect Biol.* 2009;1(6):a000950. doi: 10.1101/cshperspect.a000950. PubMed PMID: 20457558; PMCID: PMC2882125.
40. Pant V, Lozano G. Limiting the power of p53 through the ubiquitin proteasome pathway. *Genes Dev.* 2014;28(16):1739-51. doi: 10.1101/gad.247452.114. PubMed PMID: 25128494; PMCID: PMC4197966.
41. Honda R, Tanaka H, Yasuda H. Oncoprotein MDM2 is a ubiquitin ligase E3 for tumor suppressor p53. *FEBS Lett.* 1997;420(1):25-7. PubMed PMID: 9450543.
42. Jones SN, Roe AE, Donehower LA, Bradley A. Rescue of embryonic lethality in Mdm2-deficient mice by absence of p53. *Nature.* 1995;378(6553):206-8. doi: 10.1038/378206a0. PubMed PMID: 7477327.
43. Parant J, Chavez-Reyes A, Little NA, Yan W, Reinke V, Jochemsen AG, Lozano G. Rescue of embryonic lethality in Mdm4-null mice by loss of Trp53 suggests a nonoverlapping pathway with MDM2 to regulate p53. *Nat Genet.* 2001;29(1):92-5. doi: 10.1038/ng714. PubMed PMID: 11528400.

44. Shvarts A, Steegenga WT, Riteco N, van Laar T, Dekker P, Bazuine M, van Ham RC, van der Houven van Oordt W, Hateboer G, van der Eb AJ, Jochemsen AG. MDMX: a novel p53-binding protein with some functional properties of MDM2. *EMBO J.* 1996;15(19):5349-57. PubMed PMID: 8895579; PMCID: PMC452278.
45. Tanimura S, Ohtsuka S, Mitsui K, Shirouzu K, Yoshimura A, Ohtsubo M. MDM2 interacts with MDMX through their RING finger domains. *FEBS Lett.* 1999;447(1):5-9. PubMed PMID: 10218570.
46. Wu X, Bayle JH, Olson D, Levine AJ. The p53-mdm-2 autoregulatory feedback loop. *Genes Dev.* 1993;7(7A):1126-32. PubMed PMID: 8319905.
47. Rodriguez MS, Desterro JM, Lain S, Lane DP, Hay RT. Multiple C-terminal lysine residues target p53 for ubiquitin-proteasome-mediated degradation. *Mol Cell Biol.* 2000;20(22):8458-67. PubMed PMID: 11046142; PMCID: PMC102152.
48. Huang L, Yan Z, Liao X, Li Y, Yang J, Wang ZG, Zuo Y, Kawai H, Shadfan M, Ganapathy S, Yuan ZM. The p53 inhibitors MDM2/MDMX complex is required for control of p53 activity in vivo. *Proc Natl Acad Sci U S A.* 2011;108(29):12001-6. doi: 10.1073/pnas.1102309108. PubMed PMID: 21730163; PMCID: PMC3141917.
49. Pant V, Xiong S, Iwakuma T, Quintas-Cardama A, Lozano G. Heterodimerization of Mdm2 and Mdm4 is critical for regulating p53 activity during embryogenesis but dispensable for p53 and Mdm2 stability. *Proc Natl Acad Sci U S A.* 2011;108(29):11995-2000. doi: 10.1073/pnas.1102241108. PubMed PMID: 21730132; PMCID: PMC3141986.
50. Haupt Y, Maya R, Kazaz A, Oren M. Mdm2 promotes the rapid degradation of p53. *Nature.* 1997;387(6630):296-9. doi: 10.1038/387296a0. PubMed PMID: 9153395.

51. Montes de Oca Luna R, Wagner DS, Lozano G. Rescue of early embryonic lethality in mdm2-deficient mice by deletion of p53. *Nature*. 1995;378(6553):203-6. doi: 10.1038/378203a0. PubMed PMID: 7477326.
52. Allton K, Jain AK, Herz HM, Tsai WW, Jung SY, Qin J, Bergmann A, Johnson RL, Barton MC. Trim24 targets endogenous p53 for degradation. *Proc Natl Acad Sci U S A*. 2009;106(28):11612-6. doi: 10.1073/pnas.0813177106. PubMed PMID: 19556538; PMCID: PMC2710642.
53. Jain AK, Barton MC. Regulation of p53: TRIM24 enters the RING. *Cell Cycle*. 2009;8(22):3668-74. doi: 10.4161/cc.8.22.9979. PubMed PMID: 19844164.
54. Dornan D, Wertz I, Shimizu H, Arnott D, Frantz GD, Dowd P, O'Rourke K, Koeppen H, Dixit VM. The ubiquitin ligase COP1 is a critical negative regulator of p53. *Nature*. 2004;429(6987):86-92. doi: 10.1038/nature02514. PubMed PMID: 15103385.
55. Leng RP, Lin Y, Ma W, Wu H, Lemmers B, Chung S, Parant JM, Lozano G, Hakem R, Benchimol S. Pirh2, a p53-induced ubiquitin-protein ligase, promotes p53 degradation. *Cell*. 2003;112(6):779-91. PubMed PMID: 12654245.
56. Hakem A, Bohgaki M, Lemmers B, Tai E, Salmena L, Matysiak-Zablocki E, Jung YS, Karaskova J, Kaustov L, Duan S, Madore J, Boutros P, Sheng Y, Chesi M, Bergsagel PL, Perez-Ordenez B, Mes-Masson AM, Penn L, Squire J, Chen X, Jurisica I, Arrowsmith C, Sanchez O, Benchimol S, Hakem R. Role of Pirh2 in mediating the regulation of p53 and c-Myc. *PLoS Genet*. 2011;7(11):e1002360. doi: 10.1371/journal.pgen.1002360. PubMed PMID: 22125490; PMCID: PMC3219591.
57. Khetchoumian K, Teletin M, Tisserand J, Mark M, Herquel B, Ignat M, Zucman-Rossi J, Cammas F, Lerouge T, Thibault C, Metzger D, Chambon P, Losson R. Loss of Trim24

(Tif1alpha) gene function confers oncogenic activity to retinoic acid receptor alpha. *Nat Genet.* 2007;39(12):1500-6. doi: 10.1038/ng.2007.15. PubMed PMID: 18026104.

58. Migliorini D, Bogaerts S, Defever D, Vyas R, Denecker G, Radaelli E, Zwolinska A, Depaepe V, Hochepped T, Skarnes WC, Marine JC. Cop1 constitutively regulates c-Jun protein stability and functions as a tumor suppressor in mice. *J Clin Invest.* 2011;121(4):1329-43. doi: 10.1172/JCI45784. PubMed PMID: 21403399; PMCID: PMC3070608.

59. Vitari AC, Leong KG, Newton K, Yee C, O'Rourke K, Liu J, Phu L, Vij R, Ferrando R, Couto SS, Mohan S, Pandita A, Hongo JA, Arnott D, Wertz IE, Gao WQ, French DM, Dixit VM. COP1 is a tumour suppressor that causes degradation of ETS transcription factors. *Nature.* 2011;474(7351):403-6. doi: 10.1038/nature10005. PubMed PMID: 21572435.

60. Pant V, Xiong S, Jackson JG, Post SM, Abbas HA, Quintas-Cardama A, Hamir AN, Lozano G. The p53-Mdm2 feedback loop protects against DNA damage by inhibiting p53 activity but is dispensable for p53 stability, development, and longevity. *Genes Dev.* 2013;27(17):1857-67. doi: 10.1101/gad.227249.113. PubMed PMID: 23973961; PMCID: PMC3778240.

61. Consortium APG. AACR Project GENIE: Powering Precision Medicine through an International Consortium. *Cancer Discovery.* 2017;7(8):818-31. Epub 2017 Jun 1. doi: <https://doi.org/10.1158/2159-8290.CD-17-0151>.

62. Onel K, Cordon-Cardo C. MDM2 and prognosis. *Mol Cancer Res.* 2004;2(1):1-8. PubMed PMID: 14757840.

63. Cancer Genome Atlas Research N. Integrated genomic analyses of ovarian carcinoma. *Nature.* 2011;474(7353):609-15. doi: 10.1038/nature10166. PubMed PMID: 21720365; PMCID: PMC3163504.

64. Sharpless NE, DePinho RA. The INK4A/ARF locus and its two gene products. *Curr Opin Genet Dev.* 1999;9(1):22-30. PubMed PMID: 10072356.
65. Wasylishen AR, Lozano G. Attenuating the p53 Pathway in Human Cancers: Many Means to the Same End. *Cold Spring Harb Perspect Med.* 2016;6(8). doi: 10.1101/cshperspect.a026211. PubMed PMID: 27329033.
66. Malkin D, Li FP, Strong LC, Fraumeni JF, Jr., Nelson CE, Kim DH, Kassel J, Gryka MA, Bischoff FZ, Tainsky MA, et al. Germ line p53 mutations in a familial syndrome of breast cancer, sarcomas, and other neoplasms. *Science.* 1990;250(4985):1233-8. PubMed PMID: 1978757.
67. Jackson JG, Pant V, Li Q, Chang LL, Quintas-Cardama A, Garza D, Tavana O, Yang P, Manshouri T, Li Y, El-Naggar AK, Lozano G. p53-mediated senescence impairs the apoptotic response to chemotherapy and clinical outcome in breast cancer. *Cancer Cell.* 2012;21(6):793-806. doi: 10.1016/j.ccr.2012.04.027. PubMed PMID: 22698404; PMCID: PMC3376352.
68. Choi W, Porten S, Kim S, Willis D, Plimack ER, Hoffman-Censits J, Roth B, Cheng T, Tran M, Lee IL, Melquist J, Bondaruk J, Majewski T, Zhang S, Pretzsch S, Baggerly K, Siefker-Radtke A, Czerniak B, Dinney CP, McConkey DJ. Identification of distinct basal and luminal subtypes of muscle-invasive bladder cancer with different sensitivities to frontline chemotherapy. *Cancer Cell.* 2014;25(2):152-65. doi: 10.1016/j.ccr.2014.01.009. PubMed PMID: 24525232; PMCID: PMC4011497.
69. Donehower LA, Lozano G. 20 years studying p53 functions in genetically engineered mice. *Nat Rev Cancer.* 2009;9(11):831-41. doi: 10.1038/nrc2731. PubMed PMID: 19776746.

70. Lozano G. Mouse models of p53 functions. *Cold Spring Harb Perspect Biol.* 2010;2(4):a001115. doi: 10.1101/cshperspect.a001115. PubMed PMID: 20452944; PMCID: PMC2845198.
71. Harvey M, McArthur MJ, Montgomery CA, Jr., Butel JS, Bradley A, Donehower LA. Spontaneous and carcinogen-induced tumorigenesis in p53-deficient mice. *Nat Genet.* 1993;5(3):225-9. doi: 10.1038/ng1193-225. PubMed PMID: 8275085.
72. Kemp CJ, Wheldon T, Balmain A. p53-deficient mice are extremely susceptible to radiation-induced tumorigenesis. *Nat Genet.* 1994;8(1):66-9. doi: 10.1038/ng0994-66. PubMed PMID: 7987394.
73. Bartek J, Bartkova J, Vojtesek B, Staskova Z, Lukas J, Rejthar A, Kovarik J, Midgley CA, Gannon JV, Lane DP. Aberrant expression of the p53 oncoprotein is a common feature of a wide spectrum of human malignancies. *Oncogene.* 1991;6(9):1699-703. PubMed PMID: 1923535.
74. Levine AJ. 11th Ernst Klenk Lecture. The p53 tumor suppressor gene and product. *Biol Chem Hoppe Seyler.* 1993;374(4):227-35. PubMed PMID: 8329141.
75. Martins CP, Brown-Swigart L, Evan GI. Modeling the therapeutic efficacy of p53 restoration in tumors. *Cell.* 2006;127(7):1323-34. doi: 10.1016/j.cell.2006.12.007. PubMed PMID: 17182091.
76. Ventura A, Kirsch DG, McLaughlin ME, Tuveson DA, Grimm J, Lintault L, Newman J, Reczek EE, Weissleder R, Jacks T. Restoration of p53 function leads to tumour regression in vivo. *Nature.* 2007;445(7128):661-5. doi: 10.1038/nature05541. PubMed PMID: 17251932.
77. Xue W, Zender L, Miething C, Dickins RA, Hernando E, Krizhanovsky V, Cordon-Cardo C, Lowe SW. Senescence and tumour clearance is triggered by p53 restoration in murine liver

carcinomas. *Nature*. 2007;445(7128):656-60. doi: 10.1038/nature05529. PubMed PMID: 17251933.

78. Doyle B, Morton JP, Delaney DW, Ridgway RA, Wilkins JA, Sansom OJ. p53 mutation and loss have different effects on tumorigenesis in a novel mouse model of pleomorphic rhabdomyosarcoma. *J Pathol*. 2010;222(2):129-37. doi: 10.1002/path.2748. PubMed PMID: 20662002.

79. Nguyen KT, Liu B, Ueda K, Gottesman MM, Pastan I, Chin KV. Transactivation of the human multidrug resistance (MDR1) gene promoter by p53 mutants. *Oncol Res*. 1994;6(2):71-7. PubMed PMID: 7949467.

80. Biswas S, Killick E, Jochemsen AG, Lunec J. The clinical development of p53-reactivating drugs in sarcomas - charting future therapeutic approaches and understanding the clinical molecular toxicology of Nutlins. *Expert Opin Investig Drugs*. 2014;23(5):629-45. doi: 10.1517/13543784.2014.892924. PubMed PMID: 24579771.

81. Secchiero P, di Iasio MG, Gonelli A, Zauli G. The MDM2 inhibitor Nutlins as an innovative therapeutic tool for the treatment of haematological malignancies. *Curr Pharm Des*. 2008;14(21):2100-10. PubMed PMID: 18691119.

82. Li D, Marchenko ND, Moll UM. SAHA shows preferential cytotoxicity in mutant p53 cancer cells by destabilizing mutant p53 through inhibition of the HDAC6-Hsp90 chaperone axis. *Cell Death Differ*. 2011;18(12):1904-13. doi: 10.1038/cdd.2011.71. PubMed PMID: 21637290; PMCID: PMC3170683.

83. Alexandrova EM, Yallowitz AR, Li D, Xu S, Schulz R, Proia DA, Lozano G, Dobbstein M, Moll UM. Improving survival by exploiting tumour dependence on stabilized mutant p53 for

treatment. *Nature*. 2015;523(7560):352-6. doi: 10.1038/nature14430. PubMed PMID: 26009011; PMCID: PMC4506213.

84. Blanden AR, Yu X, Loh SN, Levine AJ, Carpizo DR. Reactivating mutant p53 using small molecules as zinc metallochaperones: awakening a sleeping giant in cancer. *Drug Discov Today*. 2015. doi: 10.1016/j.drudis.2015.07.006. PubMed PMID: 26205328.

85. Bykov VJ, Issaeva N, Shilov A, Hultcrantz M, Pugacheva E, Chumakov P, Bergman J, Wiman KG, Selivanova G. Restoration of the tumor suppressor function to mutant p53 by a low-molecular-weight compound. *Nat Med*. 2002;8(3):282-8. doi: 10.1038/nm0302-282. PubMed PMID: 11875500.

86. Lambert JM, Gorzov P, Veprintsev DB, Soderqvist M, Segerback D, Bergman J, Fersht AR, Hainaut P, Wiman KG, Bykov VJ. PRIMA-1 reactivates mutant p53 by covalent binding to the core domain. *Cancer Cell*. 2009;15(5):376-88. doi: 10.1016/j.ccr.2009.03.003. PubMed PMID: 19411067.

87. Andreeff M, Kelly KR, Yee K, Assouline S, Strair R, Popplewell L, Bowen D, Martinelli G, Drummond MW, Vyas P, Kirschbaum M, Iyer SP, Ruvolo V, Gonzalez GM, Huang X, Chen G, Graves B, Blotner S, Bridge P, Jukofsky L, Middleton S, Reckner M, Rueger R, Zhi J, Nichols G, Kojima K. Results of the Phase I Trial of RG7112, a Small-Molecule MDM2 Antagonist in Leukemia. *Clin Cancer Res*. 2016;22(4):868-76. doi: 10.1158/1078-0432.CCR-15-0481. PubMed PMID: 26459177; PMCID: PMC4809642.

88. Ray-Coquard I, Blay JY, Italiano A, Le Cesne A, Penel N, Zhi J, Heil F, Rueger R, Graves B, Ding M, Geho D, Middleton SA, Vassilev LT, Nichols GL, Bui BN. Effect of the MDM2 antagonist RG7112 on the P53 pathway in patients with MDM2-amplified, well-differentiated or dedifferentiated liposarcoma: an exploratory proof-of-mechanism study.

Lancet Oncol. 2012;13(11):1133-40. doi: 10.1016/S1470-2045(12)70474-6. PubMed PMID: 23084521.

89. Ware PL, Snow AN, Gvalani M, Pettenati MJ, Qasem SA. MDM2 copy numbers in well-differentiated and dedifferentiated liposarcoma: characterizing progression to high-grade tumors. *Am J Clin Pathol*. 2014;141(3):334-41. doi: 10.1309/AJCPLYU89XHSNHQO. PubMed PMID: 24515760.

90. Li Q, Zhang Y, El-Naggar AK, Xiong S, Yang P, Jackson JG, Chau G, Lozano G. Therapeutic efficacy of p53 restoration in Mdm2-overexpressing tumors. *Mol Cancer Res*. 2014;12(6):901-11. doi: 10.1158/1541-7786.MCR-14-0089. PubMed PMID: 24598047; PMCID: PMC4058386.

91. Lehmann S, Bykov VJ, Ali D, Andren O, Cherif H, Tidefelt U, Uggla B, Yachnin J, Juliusson G, Moshfegh A, Paul C, Wiman KG, Andersson PO. Targeting p53 in vivo: a first-in-human study with p53-targeting compound APR-246 in refractory hematologic malignancies and prostate cancer. *J Clin Oncol*. 2012;30(29):3633-9. doi: 10.1200/JCO.2011.40.7783. PubMed PMID: 22965953.

92. Wang Y, Suh YA, Fuller MY, Jackson JG, Xiong S, Terzian T, Quintas-Cardama A, Bankson JA, El-Naggar AK, Lozano G. Restoring expression of wild-type p53 suppresses tumor growth but does not cause tumor regression in mice with a p53 missense mutation. *J Clin Invest*. 2011;121(3):893-904. doi: 10.1172/JCI44504. PubMed PMID: 21285512; PMCID: PMC3049366.

93. Schneider CA, Rasband WS, Eliceiri KW. NIH Image to ImageJ: 25 years of image analysis. *Nat Methods*. 2012;9(7):671-5. PubMed PMID: 22930834.

94. Subramanian A, Tamayo P, Mootha VK, Mukherjee S, Ebert BL, Gillette MA, Paulovich A, Pomeroy SL, Golub TR, Lander ES, Mesirov JP. Gene set enrichment analysis: a knowledge-based approach for interpreting genome-wide expression profiles. *Proc Natl Acad Sci U S A*. 2005;102(43):15545-50. doi: 10.1073/pnas.0506580102. PubMed PMID: 16199517; PMCID: PMC1239896.
95. Festjens N, Vanden Berghe T, Cornelis S, Vandenabeele P. RIP1, a kinase on the crossroads of a cell's decision to live or die. *Cell Death Differ*. 2007;14(3):400-10. doi: 10.1038/sj.cdd.4402085. PubMed PMID: 17301840.
96. Muller M, Scaffidi CA, Galle PR, Stremmel W, Krammer PH. The role of p53 and the CD95 (APO-1/Fas) death system in chemotherapy-induced apoptosis. *Eur Cytokine Netw*. 1998;9(4):685-6. PubMed PMID: 9889415.
97. Muller M, Strand S, Hug H, Heinemann EM, Walczak H, Hofmann WJ, Stremmel W, Krammer PH, Galle PR. Drug-induced apoptosis in hepatoma cells is mediated by the CD95 (APO-1/Fas) receptor/ligand system and involves activation of wild-type p53. *J Clin Invest*. 1997;99(3):403-13. doi: 10.1172/JCI119174. PubMed PMID: 9022073; PMCID: PMC507813.
98. Szondy Z, Reichert U, Fesus L. Retinoic acids regulate apoptosis of T lymphocytes through an interplay between RAR and RXR receptors. *Cell Death Differ*. 1998;5(1):4-10. doi: 10.1038/sj.cdd.4400313. PubMed PMID: 10200440.
99. Beard JA, Tenga A, Chen T. The interplay of NR4A receptors and the oncogene-tumor suppressor networks in cancer. *Cell Signal*. 2015;27(2):257-66. doi: 10.1016/j.cellsig.2014.11.009. PubMed PMID: 25446259; PMCID: PMC4276441.

100. Moll UM, Marchenko N, Zhang XK. p53 and Nur77/TR3 - transcription factors that directly target mitochondria for cell death induction. *Oncogene*. 2006;25(34):4725-43. doi: 10.1038/sj.onc.1209601. PubMed PMID: 16892086.
101. Nikolettou V, Markaki M, Palikaras K, Tavernarakis N. Crosstalk between apoptosis, necrosis and autophagy. *Biochim Biophys Acta*. 2013;1833(12):3448-59. doi: 10.1016/j.bbamcr.2013.06.001. PubMed PMID: 23770045.
102. Li XS, Rishi AK, Shao ZM, Dawson MI, Jong L, Shroot B, Reichert U, Ordonez J, Fontana JA. Posttranscriptional regulation of p21WAF1/CIP1 expression in human breast carcinoma cells. *Cancer Res*. 1996;56(21):5055-62. PubMed PMID: 8895764.
103. Tanaka T, Suh KS, Lo AM, De Luca LM. p21WAF1/CIP1 is a common transcriptional target of retinoid receptors: pleiotropic regulatory mechanism through retinoic acid receptor (RAR)/retinoid X receptor (RXR) heterodimer and RXR/RXR homodimer. *J Biol Chem*. 2007;282(41):29987-97. doi: 10.1074/jbc.M701700200. PubMed PMID: 17656367.
104. Holmes WF, Dawson MI, Soprano RD, Soprano KJ. Induction of apoptosis in ovarian carcinoma cells by AHPN/CD437 is mediated by retinoic acid receptors. *J Cell Physiol*. 2000;185(1):61-7. doi: 10.1002/1097-4652(200010)185:1<61::AID-JCP5>3.0.CO;2-0. PubMed PMID: 10942519.
105. Kim HJ, Lotan R. Identification of protein modulation by the synthetic retinoid CD437 in lung carcinoma cells using high throughput immunoblotting. *Int J Oncol*. 2005;26(2):483-91. PubMed PMID: 15645134.
106. Oridate N, Higuchi M, Suzuki S, Shroot B, Hong WK, Lotan R. Rapid induction of apoptosis in human C33A cervical carcinoma cells by the synthetic retinoid 6-[3-(1-adamantyl)hydroxyphenyl]-2-naphthalene carboxylic acid (CD437). *Int J Cancer*. 1997;70(4):484-7. PubMed PMID: 9033662.

107. Sun SY, Yue P, Wu GS, El-Deiry WS, Shroot B, Hong WK, Lotan R. Implication of p53 in growth arrest and apoptosis induced by the synthetic retinoid CD437 in human lung cancer cells. *Cancer Res.* 1999;59(12):2829-33. PubMed PMID: 10383141.
108. Lamkin TJ, Chin V, Varvayanis S, Smith JL, Sramkoski RM, Jacobberger JW, Yen A. Retinoic acid-induced CD38 expression in HL-60 myeloblastic leukemia cells regulates cell differentiation or viability depending on expression levels. *J Cell Biochem.* 2006;97(6):1328-38. doi: 10.1002/jcb.20745. PubMed PMID: 16329108.
109. Rhinn M, Dolle P. Retinoic acid signalling during development. *Development.* 2012;139(5):843-58. doi: 10.1242/dev.065938. PubMed PMID: 22318625.
110. Jinadasa R, Balmus G, Gerwitz L, Roden J, Weiss R, Duhamel G. Derivation of thymic lymphoma T-cell lines from *Atm(-/-)* and *p53(-/-)* mice. *J Vis Exp.* 2011(50). doi: 10.3791/2598. PubMed PMID: 21490582; PMCID: PMC3169248.
111. Yin W, Raffelsberger W, Gronemeyer H. Retinoic acid determines life span of leukemic cells by inducing antagonistic apoptosis-regulatory programs. *Int J Biochem Cell Biol.* 2005;37(8):1696-708. doi: 10.1016/j.biocel.2005.03.003. PubMed PMID: 15869897.
112. Wajant H, Pfizenmaier K, Scheurich P. Tumor necrosis factor signaling. *Cell Death Differ.* 2003;10(1):45-65. doi: 10.1038/sj.cdd.4401189. PubMed PMID: 12655295.
113. Jin F, Liu X, Zhou Z, Yue P, Lotan R, Khuri FR, Chung LW, Sun SY. Activation of nuclear factor-kappaB contributes to induction of death receptors and apoptosis by the synthetic retinoid CD437 in DU145 human prostate cancer cells. *Cancer Res.* 2005;65(14):6354-63. doi: 10.1158/0008-5472.CAN-04-4061. PubMed PMID: 16024638.
114. Duffy MJ, Synnott NC, Crown J. Mutant p53 as a target for cancer treatment. *Eur J Cancer.* 2017;83:258-65. doi: 10.1016/j.ejca.2017.06.023. PubMed PMID: 28756138.

115. Gonda TJ, Ramsay RG. Directly targeting transcriptional dysregulation in cancer. *Nat Rev Cancer*. 2015;15(11):686-94. doi: 10.1038/nrc4018. PubMed PMID: 26493648.
116. Aryee DN, Niedan S, Ban J, Schwentner R, Muehlbacher K, Kauer M, Kofler R, Kovar H. Variability in functional p53 reactivation by PRIMA-1(Met)/APR-246 in Ewing sarcoma. *Br J Cancer*. 2013;109(10):2696-704. doi: 10.1038/bjc.2013.635. PubMed PMID: 24129240; PMCID: PMC3833220.
117. Mohell N, Alfredsson J, Fransson A, Uustalu M, Bystrom S, Gullbo J, Hallberg A, Bykov VJ, Bjorklund U, Wiman KG. APR-246 overcomes resistance to cisplatin and doxorubicin in ovarian cancer cells. *Cell Death Dis*. 2015;6:e1794. doi: 10.1038/cddis.2015.143. PubMed PMID: 26086967; PMCID: PMC4669826.
118. Navin N, Kendall J, Troge J, Andrews P, Rodgers L, McIndoo J, Cook K, Stepansky A, Levy D, Esposito D, Muthuswamy L, Krasnitz A, McCombie WR, Hicks J, Wigler M. Tumour evolution inferred by single-cell sequencing. *Nature*. 2011;472(7341):90-4. doi: 10.1038/nature09807. PubMed PMID: 21399628; PMCID: PMC4504184.
119. Navin NE. Delineating cancer evolution with single-cell sequencing. *Sci Transl Med*. 2015;7(296):296fs29. doi: 10.1126/scitranslmed.aac8319. PubMed PMID: 26180099; PMCID: PMC4785805.
120. Wang Y, Navin NE. Advances and applications of single-cell sequencing technologies. *Mol Cell*. 2015;58(4):598-609. doi: 10.1016/j.molcel.2015.05.005. PubMed PMID: 26000845; PMCID: PMC4441954.
121. Langdon SP, Rabiasz GJ, Ritchie AA, Reichert U, Buchan P, Miller WR, Smyth JF. Growth-inhibitory effects of the synthetic retinoid CD437 against ovarian carcinoma models in vitro and in vivo. *Cancer Chemother Pharmacol*. 1998;42(5):429-32. doi: 10.1007/s002800050841. PubMed PMID: 9771960.

VITA

Connie Larsson was born in Houston, TX in 1984 to Chanh and Lars Larsson. After graduating from North Shore Senior High School in 2002, she attended the University of Houston-Downtown and participated in research to investigate the impact of urbanization on turtle migration in the Houston watershed under the mentorship of Dr. Aaron Krochmal. She also did field work at Sam Houston State University's Center for Biological Field Studies, a 250-acre biological field station, where she investigated resource partitioning in a riparian environment between two sympatric species of snakes, *Agkistrodon piscivorus*, a pit viper, and *Nerodia erythrogaster*, a non-venomous water snake. After graduating *Cum Laude* with a Bachelor's of Science in Microbiology with a minor in chemistry, she obtained a full-time teaching position in the subjects of chemistry and physics at the same high school from where she graduated. In 2010 she entered The University of Texas MD Anderson Cancer Center UTHealth Graduate School of Biomedical Sciences where she joined the laboratory of Dr. Gigi Lozano in the fall of 2011.